AD-A008 947

TREATMENT OF SYNTHETIC URINOUS WASTEWATER USING COMBINED REVERSE OSMOSIS, IMMOBILIZED UREASE, AND ION EXCHANGE SYSTEMS

Burton Davidson, et al

Rutgers - The State University

Prepared for:

Army Mobility Equipment Research and Development Center

September 1974

DISCLAIMER NOTICE

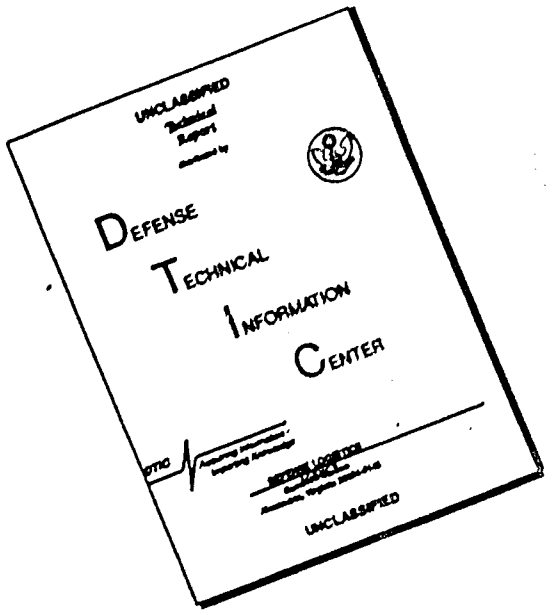

THIS DOCUMENT IS BEST QUALITY AVAILABLE. THE COPY FURNISHED TO DTIC CONTAINED A SIGNIFICANT NUMBER OF PAGES WHICH DO NOT REPRODUCE LEGIBLY.

TREATMENT OF SYNTHETIC URINOUS WASTEWATER USING COMBINED REVERSE OSMOSIS, IMMOBILIZED UREASE, AND ION EXCHANGE SYSTEMS

Contract No. DAAK02-73-C-0094

Final Report

Submitted to

Vincent J. Ciccone
Lt. Colonel, MSC, PE, Ph.D.
Sanitary Sciences Division
Military Technology Department
U.S. Army Mobility Equipment Research
and Development Center
Fort Belvoir, Virginia 22060

By

Dr. Burton Davidson, Professor
Dr. Wolf Vieth, Professor and Chairman
Dr. Shaw Wang, Assistant Research Professor
Mr. Robert Gilmore, Jr., Research Intern

Department of Chemical and Biochemical Engineering
College of Engineering
Rutgers University
New Brunswick, New Jersey 08903

ABSTRACT

A collagen-urease membrane complex of relatively stable enzymatic activity was successfully produced (and replicated numerous times) in our laboratory. In order to evaluate the potential use of this complex for the treatment of urinous wastewater, a biocatalytic reactor module of a novel spiral wound configuration was constructed and integrated into a prototype system containing reverse osmosis and ion exchange processes. The unit that was designed and constructed was sized so as to be capable of generating sufficient process data that could be used in the estimation of the system design parameters. These system design parameters could then be used to extrapolate the unit to other sizes for operation under larger feed flow rate conditions. This work was accomplished by using a synthetic urinous feed solution containing sodium chloride and urea as the major contaminants.

The performance of the biocatalytic reactor module was simulated using a transport model consisting of factors which account for simultaneous mass transfer and biochemical reaction. The model was based upon the assumptions of steady-state, plug-flow, and Michaelis-Menten kinetics. From this model, the apparent Michaelis-Menten kinetic parameters were estimated using actual experimental data as the input to a direct search, parameter optimization scheme. These estimated parameters--K_m = 0.0104 moles/liter

and V_{max} = 0.000665 moles/liter-minute--were then used to compare computer simulated curves to the actual performance data of the biocatalytic reactor module under a variety of reactor feed flow rates and urea concentrations.

As an indication of the overall urea removal efficiency of the unit (i.e., rejection by reverse osmosis plus removal via enzymatic hydrolysis of urea to ammonia), typical results of an operation run made after approximately 150 reactor liquid volume replacements (continuous single-pass operation) using a 0.01 M urea concentration at a reactor feed flow rate of 75 cc/min (approximately 25 gallons per day) and under conditions of neutral pH and room temperature are:

Urea rejection by reverse osmosis = 21.3%

Urea conversion in biocatalytic reactor = 71.0%

Overall urea removal based on initial system feed urea concentration = 85.3%

The work of characterizing the process performance of the system, although complete in some respects, requires further investigation in several other important areas. The temperature and pH dependency of the biocatalytic reactor module is one area which requires additional, in depth, work. The further characterization of the system performance over a wider range of reactor feed flow rates and contaminant concentrations is also necessary for the extrapolation of the design of the unit to sizes appropriate for other applications. A final point would be

the continuous operation of the prototype system for long periods of time (e.g., up to 100 consecutive hours) without intermittent storage of the biocatalytic reactor module. This type of operation would assist in the further evaluation of the stability of the biocatalytic reactor under controlled conditions.

PREFACE

Several quarterly progress reports have been issued to MERDC (Sanitary Sciences Division, Military Technology Department, Mobility Equipment Research and Development Center, Fort Belvoir, Virginia, Contract No. DAAK02-73-C-0094) concerning the initial phases of the project (i.e., "Development of Reactor Modules Containing Collagen-Urease Complex Membranes for the Purification of Urinous Wastewater"). In brief, these reports have dealt with:

1. November 1, 1972-January 31, 1973: Materials Research and Development
2. February 1, 1973-May 31, 1973: Choice of Prototype System Configuration
3. June 1, 1973-September 30, 1973: Prototype System Construction and Operation

The results of the research accomplished during this eleven-month period were presented in a paper entitled "Treatment of Urinous Wastewater Using a Dual-Functional Reverse Osmosis, Membrane-Enzyme System" at the Sixty-Sixth Annual Meeting of the American Institute of Chemical Engineers, November 15, 1973, in Philadelphia, Pennsylvania. This paper is also to be published in an A.I.Ch.E. Symposium Series entitled "Water--1973."

As a direct result of the above work, a contract extension was granted to further investigate and characterize the biocatalytic reactor module for use in a prototype urinous wastewater treatment unit. This report, therefore, is a culmination of the work performed during the extended period of the investigation.

ACKNOWLEDGMENTS

The author wishes to express his deep gratitude to Professor Burton Davidson for the advice, encouragement, and inspiration given throughout the course of this investigation. Professors W. R. Vieth and R. C. Ahlert are also thanked for their excellent guidance in many various matters.

Thanks are also due to Mr. Nicholas Bosko for his help in the construction of the prototype system, to Mr. Feng-Chi Hsieh and Mr. David King for their computer programming expertise, and to Mr. K. Venkatasubramanian and Mr. B. Sharma for many stimulating discussions.

The financial support of the Sanitary Sciences Division, Military Technology Department, Mobility Equipment Research and Development Center under Contract No. DAAK02-73-C-0094 is gratefully acknowledged.

TABLE OF CONTENTS

TABLE OF CONTENTS (continued)

TABLE OF CONTENTS (continued)

NOMENCLATURE

C_a = Reactor product ammonia concentration (moles/liter)

C_b = Concentration of specific reaction component in the bulk liquid phase (moles/liter)

C_{b_o} = Inlet bulk concentration of specific reaction component (moles/liter)

C_{is} = Concentration of specific reaction component inside the membrane (moles/liter)

C_{sf} = Feed salt concentration (moles/liter)

C_{sp} = Permeate salt concentration (moles/liter)

C_{ss} = Concentration of specific reaction component at the membrane surface (moles/liter)

C_{uf} = Feed urea concentration (moles/liter)

C_{up} = Permeate urea concentration (moles/liter)

D_e = Effective diffusion coefficient of specific reaction component (cm^2/min)

D_p = Characteristic particle diameter (cm)

E_o = Total enzyme concentration (moles/liter)

G = Superficial mass velocity based on total cross-sectional area (gm/cm^2-sec)

h_s = Partition coefficient for membrane (dimensionless)

j_d = Colburn's mass transfer factor (dimensionless)

J = Optimization objective function (dimensionless)

k_m = Coefficient of interfacial mass transfer (cm/min)

k_1 = Reaction velocity constant--reaction for formation of substrate-enzyme complex, equation (4-2) (liter/mole-min)

k_{-1} = Reaction velocity constant--reaction for dissociation of substrate-enzyme complex, equation (4-2) (min^{-1})

k_2 = Reaction velocity constant--reaction for formation of products, equation (4-2) (min^{-1})

K_m = Michaelis-Menten constant (moles/liter)

N'_{sh} = $k_m r_o/D_e$ (dimensionless) (Modified Sherwood Number)

P = Product concentration (moles/liter)

r = Distance in membrane (cm)

r_o = Half-thickness of membrane (cm)

$\overline{Re}$ = $D_p \bar{u} \rho_f / \mu_f (1-\bar{\epsilon})$ (dimensionless) (Modified Reynold's Number)

S = Substrate concentration (moles/liter)

t = Time (min)

u = Reactor fluid velocity based on the apparent cross-sectional area (cm/min)

$\bar{u}$ = Reactor fluid velocity based on total cross-sectional area (cm/sec)

v = Rate of enzymatic reaction (moles/liter-min)

V_{max} = Maximum reaction velocity (moles/liter-min)

X = r/r_o (dimensionless)

X_{e_1} = Particular experimental conversion (dimensionless)

X_{m_1} = Particular model conversion (dimensionless)

Y = C_{is}/C_{b_o} (dimensionless)

Y_f = C_b/C_{b_o} (dimensionless)

z = Axial distance in reactor (cm)

Z = $D_e z/r_o^2 u$ (dimensionless)

Greek Letters

α = K_m/C_{b_o} (dimensionless)

β = $r_o^2 V_{max}/D_e K_m$ (dimensionless)

ε = Fraction of fluid in the reactor based on total volume (dimensionless)

$\bar{\varepsilon}$ = Fraction of spacing material based on total volume of solids (dimensionless)

ε' = Fraction of catalytically active particles based on Total volume of solids (dimensionless)

ϕ = $\sqrt{r_o^2 V_{max}/D_e K_m}$ (dimensionless)

ρ_f = Fluid density (gm/cc)

μ_f = Fluid viscosity (gm/cm-sec)

CONSTANTS

The parameters listed below were assumed to have the constant values shown throughout this investigation.

Symbol	Physical meaning	Value	Units
D	Diffusion coefficient for urea through water	6.0×10^{-4}	cm^2/min
D_e	Effective diffusion coefficient for urea through collagen membrane	3.0×10^{-4}	cm^2/min
Dia.	Diameter of reactor	10.6	cm
h_s	Partition coefficient for collagen membrane	1.00	-
L	Length of reactor	32.5	cm
r_o	Half-thickness of collagen membrane	0.0203	cm
ε	Fraction of fluid in the reactor based on total volume	0.46	-
$\bar{\varepsilon}$	Fraction of spacing material based on total volume of solids	0.50	-
ε'	Fraction of catalytically active particles based on total volume of solids	0.50	-
ρ_f	Fluid density	1.00	gm/cc
μ_f	Fluid viscosity	0.010	gm/cm-sec
T	Temperature	19-22	°C
pH	Negative logarithm of hydrogen ion concentration	5.6-6.5	-

LIST OF FIGURES

LIST OF FIGURES (continued)

LIST OF FIGURES (continued)

LIST OF TABLES

1. INTRODUCTION AND OBJECTIVES

> Stillsuit: Body-enclosing garment invented on Arrakis. Its fabric is a micro-sandwich performing functions of heat dissipation and filter for bodily wastes. Reclaimed moisture is made available by tubes from catchpockets.
> Frank Herbert (Dune)

The novelty of a system for the re-processing of human wastes, particularly urinous wastewater, has become, in recent times, a needed practicality with the increased demand for sources of potable water in semi-isolated areas. The removal of urea and dissolved inorganic salts, the two major polluting factors in human urine, would provide a valuable and recoverable chemical intermediate, urea or ammonia, and would also produce from the separation process a source of potable water.

Current advances indicate that three processes could be combined or used individually as a solution to this separation problem. Reverse osmosis, as a single pass operation, is capable of physically removing dissolved contaminants. The 95% removal of inorganic salts is acceptable from a purity standpoint, but present technology indicates that the removal of urea is limited to approximately 45% (Lonsdale et al., 1969; Davidson et al., 1974). The construction of a two-stage process consisting of an ion exchange column for urea removal by adsorption followed by

a reverse osmosis vessel for salt removal (or vice versa) is yet another possibility. However, the 300:1 resin capacity ratio (based on milliequivalents adsorbed per gram of dry resin) for ammonia versus urea (Salemme et al., 1971) makes the size of the required resin bed in this two-stage system economically and physically unreasonable.

Work performed in our laboratory has developed a unique and third alternative to the separation problem. A biocatalytic reactor module containing a collagen-urease complex membrane is placed as a second stage between a reverse osmosis module and an ion exchange column. The reverse osmosis module removes the dissolved inorganic salts and a certain percentage of the urea. The collagen-urease membrane complex enzymatically catalyzes the hydrolysis of urea to ammonia and carbon dioxide gases. Ammonia gas is then removed by a suitable ion exchange resin (e.g., Dowex 50W-X8).

The overall objective of this investigation is the development of a pilot-plant sized, prototype unit for the purification of a synthetic urinous wastewater feed containing urea and sodium chloride as the polluting constituents. The system is to be composed of, principally, a reverse osmosis module, a biocatalytic reactor module, and an ion exchange column. To accomplish this overall objective, several secondary objectives were accomplished in a stepwise manner. These secondary objectives are:

1. The development of an active and stable collagen-urease membrane complex for the enzymatic hydrolysis of urea.

2. The design and construction of an efficient biocatalytic reactor module to contain the collagen-urease membrane complex.

3. The complete engineering specification and construction of a prototype waste treatment system with the inclusion of reverse osmosis, biocatalytic reactor, and ion exchange processes.

4. The characterization of the biocatalytic reactor module performance over a feasible range of substrate flow rates and concentrations using synthetic urine as the characteristic feed solution.

5. The development of a mathematical model based upon the assumptions of steady-state, plug-flow, and Michaelis-Menten kinetics. The model will also include a description of the inter- and intra-phase mass transfer resistances.

6. The use of the above mathematical model in a direct search, parameter optimization scheme to obtain the "best set" of kinetic parameters for the Michaelis-Menten model which most accurately describe the performance of the biocatalytic reactor module.

The objectives of this investigation serve to satisfy certain specific objectives of the Sanitary Sciences Division, Military Technology Department, U.S. Army

Mobility Equipment Research and Development Center under Contract No. DAAK02-73-C-0094.

2. LITERATURE REVIEW

2.1 Methods of Immobilization of Enzymes

While the development of new and novel means of tethering a free enzyme molecule to a solid surface has indeed been explored to great extents, four basic categories of enzyme immobilization still exist (Goldman et al., 1971; Katchalski et al., 1971; Carbonell and Kostin, 1972; Vieth and Venkatasubramanian, 1973, 1974a, b, c). These categories may be characterized as shown below.

1. Adsorption at a Solid Surface:

This is perhaps the simplest of all the immobilization methods since it only involves exposing the enzyme solution to the desired solid material under generally mild conditions. However, the method is generally considered to be ineffective because the nonspecific adsorption of the enzyme may lead to partial or total denaturation. Furthermore, continuous desorption of the enzyme during usage often occurs. Ionic bonding has been used to immobilize enzymes on DEAE-Cellulose, DEAE-Sephadex, and CM-Cellulose. On an industrial scale, Tosa et al. (1967, 1969a, b) have shown the application of fungal amino acylase attached to DEAE-Cellulose and DEAE-Sephadex by this method for the

continuous resolution of racemic mixtures of N-acetyl amino acids. Suzuki et al. (1966) reported the immobilization of invertase on DEAE-Cellulose while glucoamylase bound to the same carrier has been studied (Bachler et al., 1970; Gruesbeck and Rase, 1972). Adsorption of several different enzymes on glass beads, charcoal particles, bentonite, etc., has also been described in the literature (Goldman et al., 1971).

2. Physical Entrapment of Enzyme in a Gel:

The use of synthetic polyacrylamide type gels and starch gels has been investigated as a means of immobilizing various enzymes. Physical entrapment denotes the inability of the enzyme specie to pass the physical barriers provided by the polymeric gel, while substrate and product pass freely throughout the cross-linked gel matrix. Enzymes successfully immobilized on a polyacrylamide gel include glucose oxidase (Hicks and Updike, 1966), phosphoglycerate mutase (Bernfield et al., 1969), aldolase (Bernfield et al., 1968), fugal cells (Mosbach and Larsson, 1970), fungal spores (Johnson and Ciegler, 1969), etc. The use of semi-permeable nylon or collodion membranes shaped into microcapsules has been examined using several enzymes (Chang, 1964, 1966; Chang et al., 1966). Among the major disadvantages of this type of immobilization are the large diffusional barriers to the transport of substrate and product and the continuous leaching of enzyme from the gel matrix. Recently, Mogensen and Vieth (1973) presented

a theoretical analysis of the diffusional resistances in microencapsulated enzyme systems.

3. Cross-Linking by Means of Bifunctional Reagents:

The treatment of an enzyme solution in the presence of a solid support material with a bifunctional reagent has been explored as a means of tethering the enzyme molecule to the support through intermolecular cross-links. Some of the reagents which have been employed are glutaraldehyde (Haynes and Walsh, 1969; Jensen and Olson, 1969; Ogata et al., 1968), bisdiazobenzidine-2-2'-disulfonic acid (Goldman et al., 1965; Silman and Katchalski, 1966), diphenyl-4-4'-dithiocyanate-2-2'-disulfonic acid (Manecke and Günzel, 1967; Manecke et al., 1972). A technique of adsorbing the enzyme on to a solid surface followed by intermolecular cross-linking has recently been discussed by Goldman et al. (1965, 1968a, b, 1971). In addition, Hough and Lyons (1972) reported on the successful attachment of aminoglucosidase to yeast cell walls using a modification of the chelating agent (transition metal salts) procedure of Barker et al. (1971).

4. Covalent Binding of Enzymes:

Without doubt the most widely studied method of enzyme immobilization, the covalent linkage of an enzyme to a carrier, is accomplished through functional groups on the enzyme which are not essential to its catalytic activity. Studies of this method of immobilization include the coupling of the α-, and ε-, amino groups on enzymes to

carboxylic polymers via the corresponding azides (Hornby et al., 1966; Wharton et al., 1968a, b), the activation of the polymer carboxyls by carbodiimides (Weliky et al., 1969), the activation of cellulose by cyanuric chloride or similar agents (Kay and Crook, 1967; Kay et al., 1968; Wilson and Lilly, 1968; Kay and Lilly, 1970), activated sephadex or sepharose through treatment with cyanogen bromide (Axén et al., 1967, 1969, 1970; Porath et al., 1967; Seki et al., 1970), etc. Each of these methods has been employed successfully as a method for immobilizing various enzymes (Vieth and Venkatasubbamanian, 1974a).

Those enzymes containing tyrosine residues have been coupled to various carriers via azo bonds, using the polydiazonium salts derived from carriers such as p-aminobenzyl cellulose, m-aminobenzyloxymethyl ether of cellulose, p-amino-DL-phenylalanine copolymer, etc. (Bar-Eli and Katchalski, 1963; Silman et al., 1966; Goldman et al., 1968b). The use of inorganic carriers such as porous glass have also been successfully documented (Weetall, 1969; Weetall and Baum, 1970; Weetall and Hersh, 1969).

Although immobilization of enzymes through the method of covalent binding or intermolecular cross-linking eliminates some of the difficulties encountered with other means of immobilization, great care must be taken to avoid extremes of temperature and pH which might harm the catalytic activity of the enzyme. The possibility of chemical modification of the enzyme structure must also be explored

when implementing these methods of immobilization.

From the wealth of the literature available, the choice of a carrier substance can be seen to be painstakingly slow and tedious. The number of factors which exercise an influence upon the enzyme in its immobilized state can be enormous as well as being difficult to resolve into separate contributing components. Newer and more novel methods of immobilization include enclosing the enzyme solution inside a liquid membrane (Shrier, 1972), immobilizing the enzyme on hollow fibers (Rony, 1972), and immobilization on the inside surface of polymeric tubes such as nylon (Sundaram and Hornby, 1970).

Research efforts in our laboratory have been directed toward the development of collagen as a support material. Approximately twenty different enzymes have been successfully immobilized thus far (Vieth et al., 1972; Wang and Vieth, 1973; Bernath and Vieth, 1974). The immobilization of enzymes on collagen is accomplished through the formation of a network of noncovalent bonds between collagen and the enzyme. To date, three different procedures have been developed for production of the collagen-enzyme complexes.

1. Membrane Impregnation:

In membrane impregnation (Vieth et al., 1973) a collagen membrane is swollen in acid or alkali at that pH which is the optimum for the enzyme to be immobilized. The swollen membrane is then impregnated in an aqueous solution

of the desired enzyme where concentration and pH gradients bring about the penetration of enzyme into the membrane.

2. Macromolecular Complexation:

The complexation process involves the addition of enzyme to a collagen dispersion at the desired pH. The dispersion and enzyme are then comixed to obtain a homogeneous mixture before the membrane is cast.

3. Electrocodeposition:

The process of electrocodeposition (Vieth et al., 1973) involves the application of the phenomenon of electrophoresis, the migration of amphoteric polyelectrolytes (e.g., proteins) in an electrical field at pH values different from their isoelectric points. This can be accomplished through the application of an electric field across the collagen dispersion-enzyme mixture. The mixture can thus be deposited on a drum revolving in the dispersion.

The choice of collagen as a carrier involved extensive work concerned with the various physical properties of this material. A discussion of the structure and physical properties of collagen is presented next to elucidate the reasons for choosing it as a carrier material.

2.2 Structure and Properties of Collagen

The protein, collagen, is found widely as a structural component in biological systems in the form of connective tissues such as bone, cartilage, skin, and tendon.

As a protein, collagen contains some nineteen

L-amino acids and is strikingly unique in that it contains a high percentage of glycine (33.5 mole %) and two of the more rarely occurring amino acids, hydroxyproline and hydroxylysine (Butler et al., 1967). In addition, the total absence of the amino acid tryptophan is unique and advantageous in the determination of the enzyme content of certain collagen-enzyme complexes.

The extreme hydrophilicity of collagen can be attributed to the presence of significant amounts of the hydroxy-forms of proline and lysine. Collagen has been shown to absorb up to 500% of its own weight of water at acid pH, over 100% at neutral pH, and approximately 400% at alkaline pH (Bowers and Kenten, 1948). This is the exact phenomenon which has made the immobilization of enzymes by impregnation (Vieth et al., 1973) a viable process.

A highly rod-like particle of a molecular weight of about 300,000 (Boedtker and Doty, 1956) has been postulated to contain a triple helical polypeptide chain as the basic molecular unit of collagen (Gross et al., 1954; Ramachandran and Kartha, 1954; Ramachandran, 1963). This fundamental molecule is approximately 2800 Å in length and 14 Å in diameter. The work of Hodge and Petruska (1963) indicated the collagen macromolecule is packed in a fibril in such a fashion that there is approximately a 9% overlap head-to-tail in linear polymers and an approximate quarter-stagger of adjacent macromolecules. This structural effect causes the appearance of "holes" in the fibrillar structure of

collagen. The regular sequencing of these holes and the swelling of the collagen matrix makes these areas extremely accessible to enzyme molecules during the immobilization process. Indeed, it is postulated that the enzyme molecule may be sequestered within these areas. The binding mechanism could thus involve multiple salt linkages, hydrogen bonds, and van der Waals interactions.

The advantages of collagen as a supportive carrier of an immobilized enzyme are many and varied. However, care must be taken to consider each enzyme as a new and separate challenge to the technology of immobilization.

2.3 Urease

2.3.1 Properties of Urease as a Free Enzyme

Urea aminohydrolase (EC 3.5.1.5), nee urease, is derived in large quantities from ground meal of the jack bean plant (Canalia ensiformis). Although formerly believed specific in its activity only towards urea, recent studies (Fishbein, 1965, 1969) have shown that hydroxyurea and dihydroxyurea are also hydrolyzed by urease.

The first enzyme to be isolated in crystalline form (Sumner, 1926), urease has been well characterized in relation to its general physical properties. The first measurements of the molecular weight of urease were obtained from sedimentation velocity and diffusion data by Sumner et al. (1938). Their value of 473,000 agrees well with that of Riethel and Robbins (1967) who found it to be 489,000.

Although the amino acid composition of urease is not unique (Riethel and Robbins, 1967; Milton and Taylor, 1969), the presence of approximately 1.14 mole % of tryptophan creates an intrinsic tracer method for the enzyme content determination of the collagen-urease complex.

While no amino acid sequencing for the urease molecule has yet been proposed, certain hypotheses have been proposed concerning the nature and number of active sites contained within a urease molecule. Lynn (1967) obtained data on the apparent Michaelis-Menten kinetic constants, K_m and V_{max}, versus pH and proposed that the molecular ionization constants obtained from these data imply that there are three important amino acid ionizing groups (i.e., histidine, α-ammonium, and sulfhydryl). In a separate determination (Gorin and Chin, 1965), a titration of the sulfhydryl groups with n-ethylmaleimide indicated the presence of eight moles of active sites per mole of urease. Riethel (1971) made use of the above data but could not obtain a conclusive result because of the possibility of structural changes occurring during the titration.

While various mechanisms have been proposed for the hydrolysis of urea by urease (Bersin, 1937; Brandt, 1937; Gorin, 1958; Blakely et al., 1969), the original suggestion of an ammonium carbamate intermediate (Yamasaki, 1920; Sumner et al., 1931) has been continually reinforced. The mechanism which is suggested consists of two steps:

1. 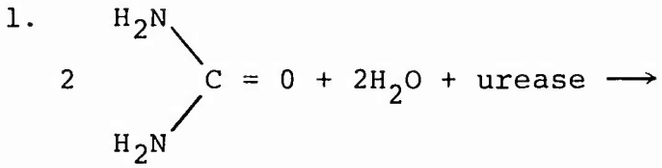

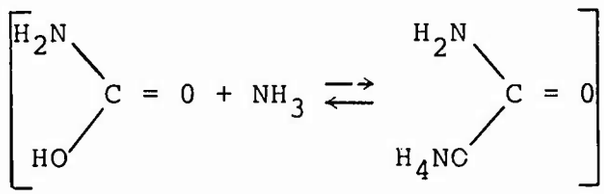

(2-1)

2. 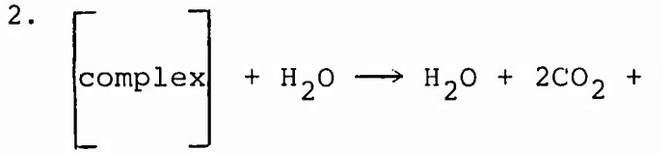

(2-2)

While the wealth of kinetic data points strongly toward this mechanism, the lack of thermodynamic equilibrium data on the intermediate formation robs one of a conclusive decision. The variation of kinetic data presented in Table 1 can be attributed primarily to variations in temperature, pH, and buffer. However, this variability also clouds the overall development of a satisfactory mechanistic picture.

The inhibition of urease by heavy metal ions such as Hg^{++}, Cu^{++}, Zn^{++}, Cd^{++}, Co^{++}, and Ni^{++} has been well documented by Katz and Cowans (1965) and Hughes et al. (1969). The presence of excess ammonia has also been shown to be inhibitory to the catalytic activity of urease (Laidler and Hoare, 1949).

2.3.2 Properties of Urease as an Immobilized Enzyme

The first form of insoluble urease was obtained by adding sodium chloride to a 30% ethanolic solution of crude

TABLE 1

MICHAELIS-MENTEN CONSTANTS OF FREE UREASE

Buffer	pH	Temperature (°C)	K_m (M)	$V_{max}\left(\frac{\text{moles}}{\text{l-sec}}\right)$	Reference
Tris-HCl	7.4	25	0.004	17.2×10^{-6}	30
Tris-HCl	7.0	38	0.00328	17.2×10^{-6}	15
Maleate	5.0	21	0.004	2.5×10^{-3}	69
Maleate	7.0	21	0.0049	6.7×10^{-3}	69
Tris-H_2SO_4	7.0	21	0.0051	8.4×10^{-3}	69
Tris-H_2SO_4	9.0	21	0.0027	1.7×10^{-3}	69
Tris-H_2SO_4	8.0	20.8	0.0040	15.5×10^{-6}	116

urease and allowing the mixture to stand at room temperature (Sumner and Graham, 1925). Purified crystalline urease was also found to be susceptible to this form of insolubilization (Sumner, 1948). Further developments in the methods of immobilizing urease are presented in Table 2 (Melrose, 1971).

Langmuir and Schaefer (1938, 1939) used a plate treated with barium stearate or barium stearate-thorium silicate to adsorb monolayers of urease from the surface of a pan of water. Indicator oil was used to restrain the monolayer to a certain size while the adsorption process was performed. Definite activities were observed by placing the plates in a 0.1% solution of urea. The activities, however, were found to be short-lived because of probable desorption of the surface layers of the carrier material.

The preparation of microcapsules with walls of semi-permeable membrane has also been investigated for the immobilization of urease (Chang, 1964; Chang et al., 1966). Results show that the encapsulated enzyme does not leak out during storage and can act effectively on urea added to the external aqueous medium. The microencapsulated urease retained in vitro and in vivo enzymatic activity throughout extended usage and was shown to raise blood ammonia to hepatic-coma levels when injected in small intraperitoneal doses. It is believed that certain therapeutic uses of this type of system do exist especially for replacement of an enzyme lost in a genetic accident.

TABLE 2

METHODS OF IMMOBILIZATION OF UREASE

Immobilizing method	Activity	Retention of activity	Reference
A. Adsorption on:			
1. Barium stearate	5%	-	65,66
2. Barium stearate-thorium silicate	5%	-	
B. Inclusion in a polyacrylamide gel	Active	100%/21 days/25°C	44
C. Inclusion in nylon microcapsules	Active	-	22,24
D. Reaction with:			
1. Poly(p-diazo-DL-phenylalanine-leucine)	78%	60%/5 months/4°C	82
2. Poly(p-diazo-DL-phenylalanine-glycine)	6%	-	
3. Poly(p-diazo-DL-phenylalanine-L-alanine)	42%	-	
E. Reaction with a diazoarysilyl derivative of glass	Active	100%/30 days use	120
F. Impregnation on collagen	Active	25%	115,117

Another water-insoluble derivative of urease was prepared by covalently binding the enzyme to an insoluble copolymer (Riesel and Katchalski, 1964). The enzyme, pretreated with p-chloromercuribenzoate, was covalently bound to the diazotized copolymer of p-amino-DL-phenylalanine and L-leucine. Approximately 65% of the original enzymatic activity was retained after five months of storage at 4°C. Porous glass beads were used in still another covalent binding procedure (Weetall and Hersh, 1969) utilizing an amino-functional silane coupling agent. An enzymatically active complex resulted which showed no apparent leakage of enzyme throughout a 30-day period of use.

The successful fabrication of a urea transducer for rapid, continuous determination of urea was accomplished by immobilization of urease through physical entrapment in a starch gel and in a polyacrylamide gel (Guilbault and Das, 1970; Guilbault and Montalvo, 1970). The urease-polyacrylamide complex was placed around a cation electrode sensitive to the presence of ammonium ions. The unit was then covered with a cellophane film for protection. A potential is registered as the electrode senses the ammonium ions produced from the hydrolysis of the urea by the immobilized urease. To date, an electrode has been produced which can be used continuously for 3 weeks at 25°C

The use of collagen has also been explored as a possible carrier matrix for urease (Vieth et al., 1972). The collagen-urease complex was produced through the method

of impregnation. A modular biocatalytic reactor was fabricated from the complex membrane. The enzymatic activity of the reactor module remained stable at 25% of its initial value for a period of operation of approximately 2 weeks.

While the use of immobilized urease is a viable possibility for the removal of urea from urinous wastewater, many other polluting constituents must also be removed. The total system thus becomes multi-phase with the inclusion of some separation process for the removal of dissolved salts and solids (Davidson et al., 1974).

2.4 Reverse Osmosis

In the past decade, much research has been performed concerning the use of reverse osmosis and its associated processes in the purification of polluted or unpotable water. However, the larger part of this research has occurred in the area of reverse osmosis treatment of saline and brackish waters. While brackish water (approximately 1.5% sodium chloride) has been treated relatively successfully, a practical as well as economical means of treating saline water (approximately 3.0-3.5% sodium chloride) has yet to be developed.

Although some research has been concentrated in the development of different types of membranes (Jadwin et al., 1970), much development has occurred in the shape and configuration of existing membrane types (Lacey, 1972). The first type developed at the very start of such research was

the plate and frame module where the membrane is placed on a porous support plate and pressure is applied from above. The permeate passes through the membrane and porous plate and is collected below. A second development was the spiral wound module where the membrane is wound around a center support in the form of a spiral (see Section 3.4.1). This type of configuration gave a larger membrane surface area for the same usage of space for unit construction.

Further development of the spiral wound module led to the tubular module. Here, a single layer of membrane is supported by a hollow porous column. The feed solution is passed through the inside of the support column and the permeate is collected outside the module. The helical module is a direct descendent of the tubular configuration. In the helical design, the same tubular membrane is wound into a helix and placed in a container to give a more compact unit. The unique advantage of this form of reverse osmosis module is its comparatively small size for an equal amount of membrane surface area as compared with other types of modules.

A new and more novel development is the "Permasep" permeator. In this module, the membrane is spun into hollow fibers (100 to 200 microns in diameter) and these are then enclosed in a supporting cylinder. Since such fibers need no supporting structure to withstand high pressures, they may be bundled in such a module to increase the available membrane surface area while keeping the size of the

unit at a minimum.

Since the advent of the reverse osmosis procedure for the purification of water containing dissolved salts and suspended solids, considerable work has been done to further characterize the physical properties which govern the performance of the membranes employed in this process (Reid and Breton, 1959; Sourirajan, 1970). However, the removal of most ions must still be performed by another physical or chemical separation process. A discussion of this process, ion exchange, follows.

2.5 Ion Exchange

The ion exchange resin has long been chosen for the removal of cations and anions from aqueous systems because of its ability to yield optimal performance in terms of cost and process efficiency. Since the performance of each resin is relative only to the system in which it is employed, much experimental work was required to produce the proper design equations for the system under consideration.

Two principal techniques of contacting solutions with ion exchange resins exist--the batch method and the column method (Applebaum, 1968; Dorfner, 1972).

1. Batch Reactor:

In the batch reactor method, the ion exchange resin is introduced into the reactor in conjunction with the ion containing solution, the two species are mixed, and time is

allowed for an equilibrium to be established. The solution is then removed by filtration and the resin is prepared for repetition of the process. The controlling factor of the extent of exchange is the selectivity of the resin under equilibrium conditions. Thus, unless the selectivity of the resin is strongly centered toward the desired ions in the solution, only a relatively small part of the total capacity of the resin will be utilized.

2. Column or Vertical Reactor:

The operation of a column reactor may be considered as a large number of batch operations in series. While the extent to which the exchange takes place in each one of these small batch operations is limited by the appropriate selectivity coefficient of the resin, the overall effect may be much more favorable. The column reactor may also be subdivided into several modes of operations. The resin bed may be fixed or moving while the feed solution and regenerant solution flow past the resin in the same relative direction or in opposite directions.

The majority of ion exchange units in operation to date employ the column or vertical reactor configuration. A specified amount of resin is supported on a bed of graded gravel of some other filter base and the column may be operated by passing all solutions in a downward direction (down-flow operation) or in an upward direction (up-flow operation). By far, the preferred mode of operation is the down-flow use of a vertical reactor. Down-flow operation

gives a maximum of resin-solution contact and a minimum of mechanical problems. The solutions must, of course, be essentially free of insoluble materials as the ion exchange bed acts as a very effective filter. An abundance of insoluble species in the solution to be treated could cause an accumulation of these materials on top of the resin bed. This accumulation, in turn, may cause a rapid increase in the pressure drop across the reactor and/or channeling through the resin bed. The up-flow operation of a vertical reactor is disadvantageous because of the possibility of fluidizing the resin bed. In this fluidized state, the efficiency of contact becomes poor, thus decreasing the total efficiency of the reactor.

Resin selection may be based primarily on the physical data supplied by individual manufacturers. Ion exchange resins come in several varieties in direct relation to their selectivity for various ions, strength, thermal stability, type of regenerant required, porosity, and chemical and physical stability (Kunin and Meyers, 1950). The capacity of an ion exchange resin, i.e., the ability of the resin to effect an exchange of ions, is perhaps the most important property to be specified. Usually measured in terms of the number of milliequivalents (1 meq = 0.001 gram-moles) of ions which can be exchanged per gram of dry resin, the resin capacity may be used for the stoichiometric calculation of the amount of resin required for a particular application. An accurate determination of the capacity

is of the essence, since it is the basis of the important design parameters of an ion exchange system.

While each of the preceding processes--ion exchange, reverse osmosis, and hydrolysis of urea by a collagen-urease complex membrane--could partially treat a urinous feed solution, only combinations of these three processes could effect the large purification desired to produce potable or drinkable water from such a reactor input. The following discussion concerns itself with certain possibilities in the combination of these processes for such a treatment operation.

2.6 Prototype System Applications

2.6.1 Wastewater Treatment and Reuse

For the purpose of treating urinous wastewater, the processes of reverse osmosis and ion exchange may be combined in a prototype unit containing a biocatalytic reactor module. For simplicity, the three processes may be placed in series where the reverse osmosis system would remove 95 to 98% of the dissolved salts and a certain percentage of the urea, the collagen-urease membrane complex contained within the biocatalytic reactor module would effect the enzymatic hydrolysis of urea to ammonia and carbon dioxide, and the ion exchange column would remove the dissolved ammonia. In addition, if the spiral wound configuration of the reverse osmosis module is utilized, the possibility of producing a module containing both reverse osmosis and

collagen-urease complex membranes becomes readily apparent (Davidson et al., 1973). A prototype system of this type (containing the reverse osmosis, biocatalytic reactor, and ion exchange processes in series) has been developed and tested in our laboratory (Davidson et al., 1974). Its use in the urinous wastewater treatment area and other modes of the enzyme engineering field are being explored at this time.

2.6.2 Hemodialysis and Dialysate Purification

The availability of some type of hemodialysis to only 1,800 of the approximately 10,000 patients in the United States (statistics presented at the Second Annual Contractor's Conference of the Artificial Kidney Program of the National Institute of Arthritis and Metabolic Diseases, January 22-24, 1969) may be attributed in part to the unavailability of a relatively inexpensive and convenient modular configuration of the hemodialysis membrane. Also, the volume of dialyzing fluid required for each dialysis seriously impairs the ability to decrease the size of the hemodialysis mechanism to convenient dimensions. Thus, to increase this availability, recent work has been concentrated in the area of developing new dialysis membranes to replace and improve upon the physical characteristics of the more common cellophane and cuprophane. The possibility of using collagen membranes for hemodialysis has been explored extensively (Nishihara et al., 1969; Kon et al., 1970).

Commercially available sausage casing in a tubular form, which consists mostly of collagen, was used by Kon et al. (1970) in their exploratory work. While the clearance rate of waste metabolites was found to be better than either of the two previously used membranes, the mechanical strength of the collagen was considerably less than the other two materials. This made necessary the use of a double screen support for the tubular collagen membrane. Nishihara et al. (1969) fabricated collagen membranes from a preparation of calf skin for their particular studies. The larger thickness of these membranes proved detrimental to any increase in the metabolite clearance rate, but a membrane of superior mechanical strength was obtained by this method. In a more recent study (Stenzel et al., 1971), tubular collagen membranes were fabricated and cross-linked by ultraviolet irradiation. The membranes obtained had a high mechanical strength and a waste metabolite clearance rate comparable to that of cellophane or cuprophane.

Efforts to increase the removal of waste metabolites from the dialysate bath has led to the incorporation of urease (Gordon et al., 1969, 1971) into a hemodialysis unit. The enzyme acts to hydrolyze urea, the primary waste metabolite, to ammonia and carbon dioxide which are more amenable to removal by conventional adsorption processes. Now, the use of the collagen-urease membrane complex, as a result of the research of this and prior investigations

(Vieth et al., 1972; Wang and Vieth, 1973), may also be proposed as an effective treatment step in the purification of spent dialysate fluid. Collagen acts as a molecular filter since it is impermeable to macromolecules such as hemoglobin and albumin (Nishihara et al., 1969). Its matrix structure may also be used as a support for the enzyme, urease, which can again effect the enzymatic hydrolysis of urea to ammonia and carbon dioxide. A further expansion of this system to remove the dissolved ammonia would be the addition of an ion exchange column. This prototype process would provide for the complete reuse of the dialysate bath, thus decreasing its size proportionately. In addition, the low cost of the collagen membrane could also increase the eventual availability of such a hemodialysis unit to many more patients.

3. MATERIALS AND METHODS

3.1 Preparation of Collagen Dispersion and Collagen Membranes

The work of this investigation was carried out using collagen prepared from a 50:50 solution of methanol and water which is 1.0% solids by weight. This method of preparation from calf tendon or cowhide is described in U.S. Patent No. 2,920,000 (Hochstadt et al., 1960).

The collagen from cowhide is obtained as a by-product of the meat packing industry from the U.S. Department of Agriculture, Agricultural Research Service, Philadelphia, Pennsylvania. The steps in preparing the collagen dispersion are as follows:

1. Four liters of glass distilled water are acidified to pH 3.0 by the addition of lactic acid.

2. The collagen is dried as much as possible to remove most of the excess water. Sixty grams of this dried collagen is added to the distilled water.

3. This mixture is completely homogenized in a commercial Waring blender at low speed. This is done for at least eight one-minute treatments. The dispersion must be cooled in an ice bath between treatments to prevent the temperature from rising above 25°C and causing denaturation of the collagen.

4. The pH of this dispersion is checked since it has been noted that collagen, upon dispersion, tends to make the mixture more alkaline. Lactic acid is added to lower the dispersion pH to 3.0.

5. The dispersion is deaerated in a vacuum of 25 inches of mercury for about 2 hours, or until all air bubbles are removed and a dispersion of smooth consistency is obtained.

Collagen membranes of various thicknesses may be prepared on a Mylar supporting sheet by the use of a Gardner knife. Since large sheets of membrane of constant thickness were desired, the dispersion was placed on the Mylar sheet in front of the Gardner knife as it was drawn across the Mylar sheet at a uniform speed by a motor. The cast dispersion and Gardner knife were both contained by an aluminum frame placed on the Mylar support sheet. The membrane, after being allowed to dry for 3 to 4 days, was found to be about 1.0% of the thickness of the wet dispersion. After drying, the membrane may be peeled off the Mylar sheet, and is ready for the immobilization procedure.

3.2 Immobilization of Urease on Collagen Membrane

Jack bean urease was obtained from Sigma Chemical Company, St. Louis, Missouri. This preparation, known as Type III urease powder, claimed to have a specific activity of between 1,500 and 3,000 units per gram. One unit of urease activity is defined as that amount of enzyme which

will produce one milligram of ammonia nitrogen from urea in 5 minutes at 30°C and pH 7.0.

The collagen membranes which were used in the construction of the biocatalytic module ranged in thickness from 0.0051 cm to 0.0076 cm.

Two procedures for immobilizing the membranes by the impregnation method were employed because of the size of the collagen membranes. In both cases, the membrane was first swollen for 2 hours in 0.1 M Tris buffer adjusted to pH 9.0 with lactic acid. The swollen membrane was then soaked for 96 hours in 0.1 M Tris buffer adjusted to pH 8.5 with lactic acid containing 20 mg/ml of urease. This was stored at 4°C for the complete impregnation period. The membrane was finally placed on a Mylar sheet and allowed to dry completely. The difference between the two procedures occurred in the handling of the membrane in each of the steps discussed above. In the first method, the long sheets of membrane were layered into a pan containing each of the particular solutions. Because of the fear of the lack of contacting which might occur between the folds of the membrane, this method was abandoned in favor of a second procedure. In this alternative method, the membranes were wound into their final reactor configuration (see Section 3.4.2). Because of the spacing material used in the winding, nearly 100% contacting of the solutions with the membrane could be assumed. The reactor was simply used as a storage vessel and container for the membrane and

solution during each step of the impregnation procedure. All of the collagen-urease complex membranes used in this investigation were prepared according to this second procedure.

3.3 Enzymatic Activity Assay

The production of ammonia during urea hydrolysis was followed by the use of a Beckman No. 39137 cationic electrode in conjunction with a standard Beckman reference electrode and a Beckman Expandomatic pH meter. Katz and Cowans (1965) give a detailed account of this method. A standard calibration curve was prepared using standard ammonium chloride solutions ranging in concentration from 0.1 M to 0.0001 M (Figure 1). (Note: Because of the physical properties of the cationic electrode, the calibration curve developed was found to shift without changing slope. This necessitates the reading of a standard 0.1 M ammonium chloride solution each day to obtain a new intercept for the calibration curve. This behavior was found to be typical of all the electrodes employed in this investigation.)

Reactions employing both free and immobilized urease were conducted at 25±1°C in 0.1 M Tris buffer adjusted to pH 7.0 with hydrochloric acid. For the evaluation of the free urease preparation, a measured quantity of enzyme was dissolved in a solution containing an excess concentration of urea, i.e., much larger than K_m. The electrodes were placed in the reaction mixture and the

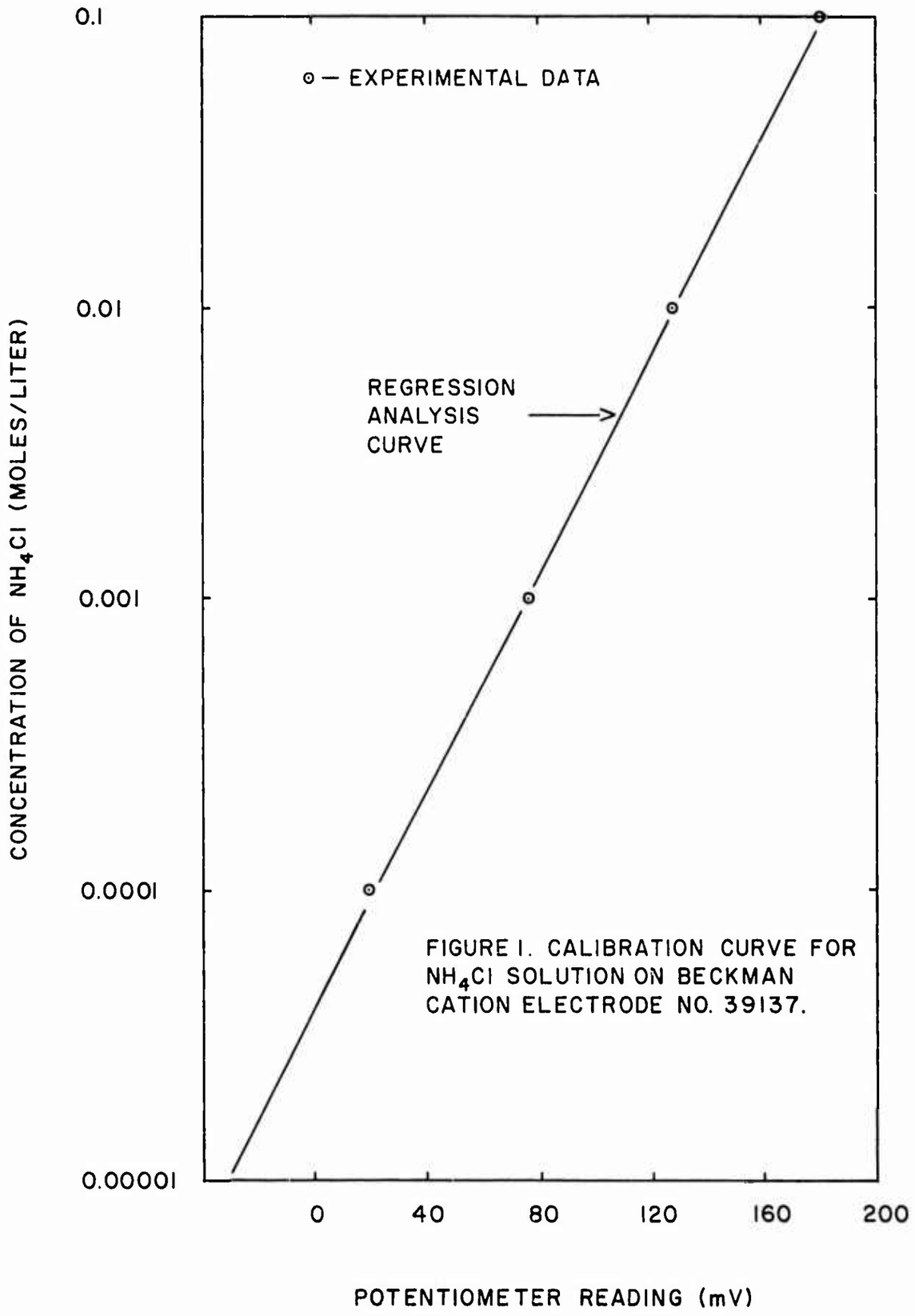

FIGURE 1. CALIBRATION CURVE FOR NH_4Cl SOLUTION ON BECKMAN CATION ELECTRODE NO. 39137.

potential was recorded over the course of the reaction for 15 minutes. The changes in ammonia concentration corresponding to the observed changes in potential could then be read off the calibration curve. In a like manner, the activity of the collagen-urease complex could be determined by repeating the above procedure with a known weight of the immobilized enzyme. This gives a quantitative measurement of the enzymatic activity per gram of the collagen-urease membrane complex. Additional reactions may be done (Zwiebel, 1972) to obtain estimations of the apparent Michaelis-Menten kinetic parameters, K_m and V_{max}.

3.4 Use of Collagen-Urease Complex Membrane for the Hydrolysis of Urea

3.4.1 Equipment Specifications

Several pieces of specialized equipment were purchased for the construction of the prototype system. Throughout, metallic parts contacting the fluids are specified type 316 stainless steel while plexiglass was chosen for use in the biocatalytic reactor module and ion exchange column.

1. High Pressure Diaphragm Pump:

The pump chosen for use was a controlled volume diaphragm pump for normal corrosive or toxic chemicals and light slurries with viscosities up to 40 centipoises. The pump is capable of pumping 25 gallons per hour at 1,500 psig. Repetitive accuracy of the metered discharge volume is maintained within a plus or minus 1.0% range at constant

conditions of pressure, temperature, and pump capacity adjustment setting.

A plunger, reciprocating at a fixed stroke, displaces a fixed volume of hydraulic fluid which actuates a flexible, chemically inert Teflon diaphragm to create the pumping action. Double ball check values are used on the suction and discharge to insure consistent metering accuracy. Capacity control is established by adjusting the volume of hydraulic fluid which bypasses the diaphragm cavity. Metering with such repetitive accuracy is possible only if the volume of the hydraulic oil in the displacement chamber is maintained constant for each stroke. This is accomplished by mechanically opening the displacement chamber to the oil reservoir for a short period at the end of every suction stroke and the beginning of each pressure stroke. During this period air or vapor is bled from the system, lost oil is replenished, and allowances are made for the expansion or contraction of the oil due to temperature change.

2. Accumulator:

The desire to have a constant flow of fluid at a constant pressure makes the accumulator one of the most important parts of this prototype system. In a sense, the accumulator acts as a shock absorber to smooth out the steady rise and fall of pressure and fluid flow created by the diaphragm pump.

The accumulator consists simply of a high pressure

container which is divided into two compartments by a rubber diaphragm. On one side of this flexible wall, nitrogen gas is introduced at a relatively high pressure (normally 25% of the system operating pressure). The fluid passing through the system is allowed to pass into and out of the other compartment of the accumulator. As the pressure in the system increases on a particular stroke of the pump, the pressurized diaphragm deflects within the accumulator to stop the pressure in the entire system from rising. On the opposite stroke, the diaphragm pushes fluid out of the accumulator as the pump pressure decreases. This, then, gives a smooth flow of liquid through the system with only small fluctuations in the system pressure.

3. Pressure Vessel Assembly and Spiral Wound Reverse Osmosis Module:

The choice of the spiral wound configuration was made primarily because of its size as compared with other modules having the same membrane surface area. The spiral wound module (Figure 2) consists basically of two sheets of membrane separated by a porous support material. This material both supports the membrane against the operating pressure and provides a flow path for the product water. An "envelope" is created by sealing around three sides with a waterproof cement to prevent contamination of the product water by the feed or retentate streams. The fourth edge is sealed to a hollow plastic tube which has perforations inside the edge seal area so that the product water can be

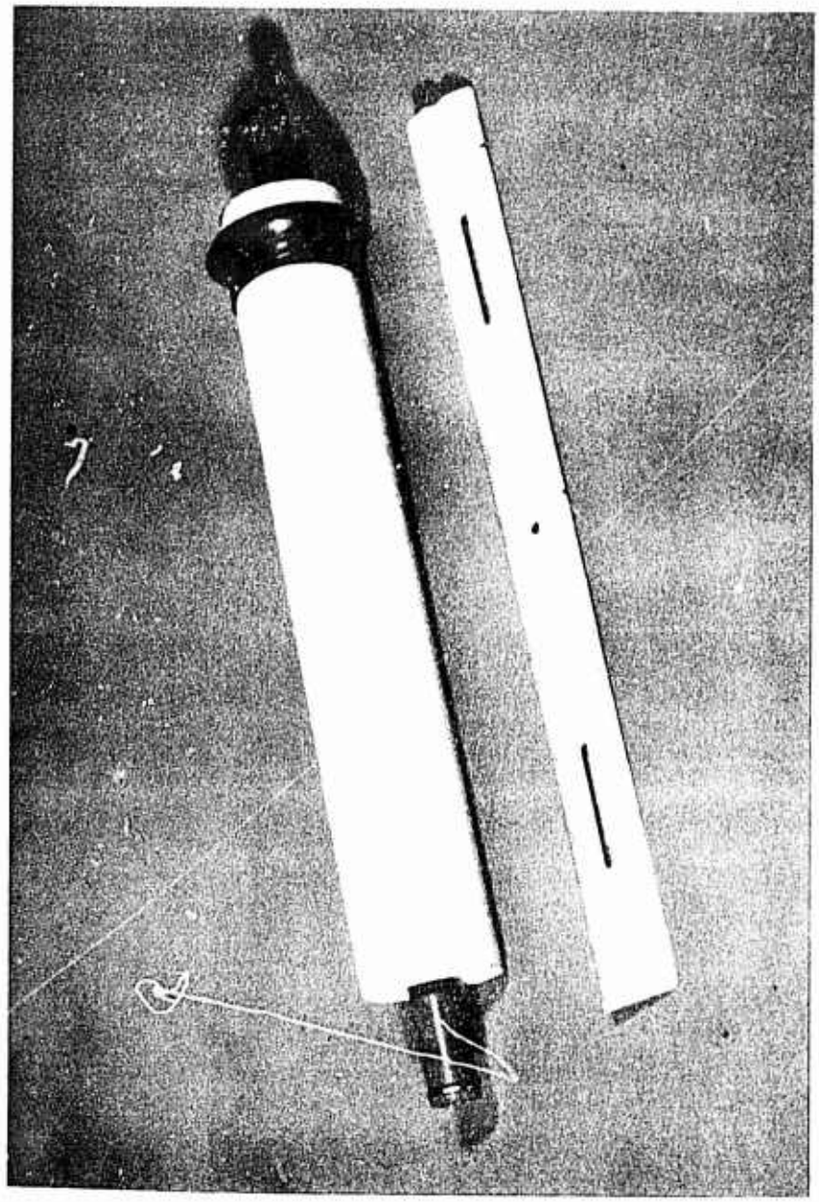

FIGURE 2. SPIRAL WOUND REVERSE OSMOSIS MODULE.

removed from the porous support material. This long "envelope" is rolled up about the central tube in the form of a spiral, along with a mesh spacer which separates the facing membrane surfaces and promotes turbulence of the feedwater as it passes through the module. The spiral wound module is placed inside any of a number of commercially available pressure vessels for use in a variety of systems.

During operation (Figure 3), the feedwater enters the upstream end of the module and flows axially through the module. Some purified water flows through the membrane surface, where it travels down the porous backing material to the central tube. The retentate (slightly more concentrated in salt than the feed because of the removal of purified water) exits from the module at the bottom. The peripheral seal ensures that all of the flow passes through the module and none bypasses it. The retentate exits the pressure vessel, while the product from the module is collected in the central tube. The product then flows down through the central tube and exits the pressure vessel through a special fitting in the end cap.

Two additional modules were prepared for use in this system. The modules contained both the reverse osmosis membrane and a collagen-urease complex membrane first in a co-spiral wound and second in a bi-spiral wound configuration (Davidson et al., 1973). The purpose of these modules was to integrate the reverse osmosis and biocatalytic modules into one element in the prototype system.

FIGURE 3. SCHEMATIC CROSS-SECTIONAL VIEW OF SPIRAL WOUND REVERSE OSMOSIS MODULE AND PRESSURE VESSEL ASSEMBLY.

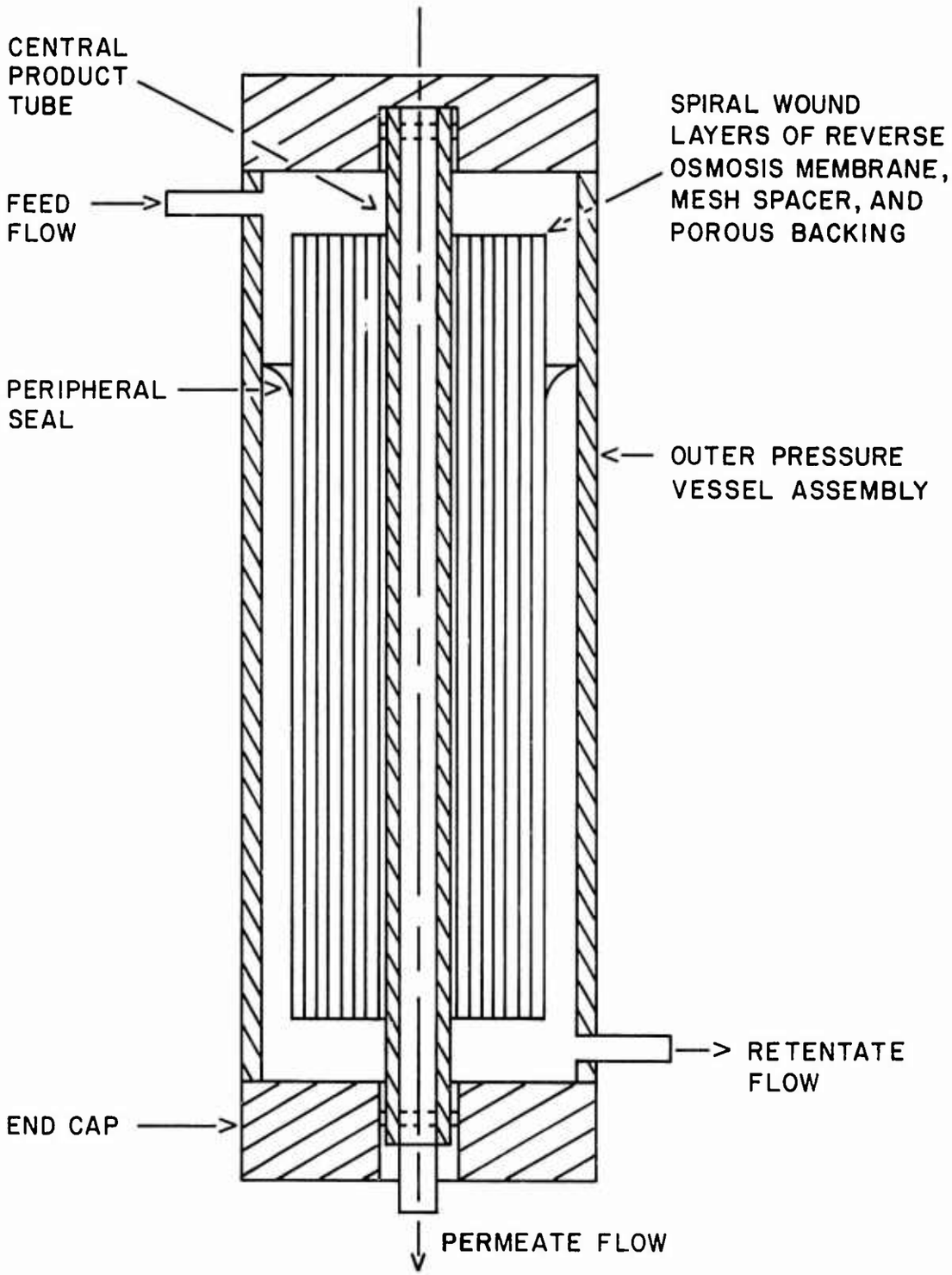

The spiral wound reverse osmosis module has now been in successful operation for more than one year in the system constructed in our laboratory.

4. Pressure Indicators:

The accurate indication of the pressure applied to the reverse osmosis module was necessary to make repetitive determinations of the system performance under constant conditions. These two gauges were chosen for their stainless steel and Teflon construction and their consistency of measurement in the pressure range from 500 to 1,500 psig.

5. Flow Indicator:

The choice of an accurate in line flow indicator was also important for the operation of the prototype system under constant conditions. The unique feature of this rotameter is that it has a permanent magnet in the float. This is magnetically coupled to the indicator assembly which translates vertical float movement into horizontal pointer movement indicating the flow rate on a properly calibrated scale. A calibration curve (Figure 4) was obtained by operating the rotameter over a range of flow rates and measuring the throughput of the system with a graduated cylinder.

6. Mixers:

The mixers were obtained to insure the homogeneity of the solution being fed to the system. They were operated continuously during the operation of the prototype system.

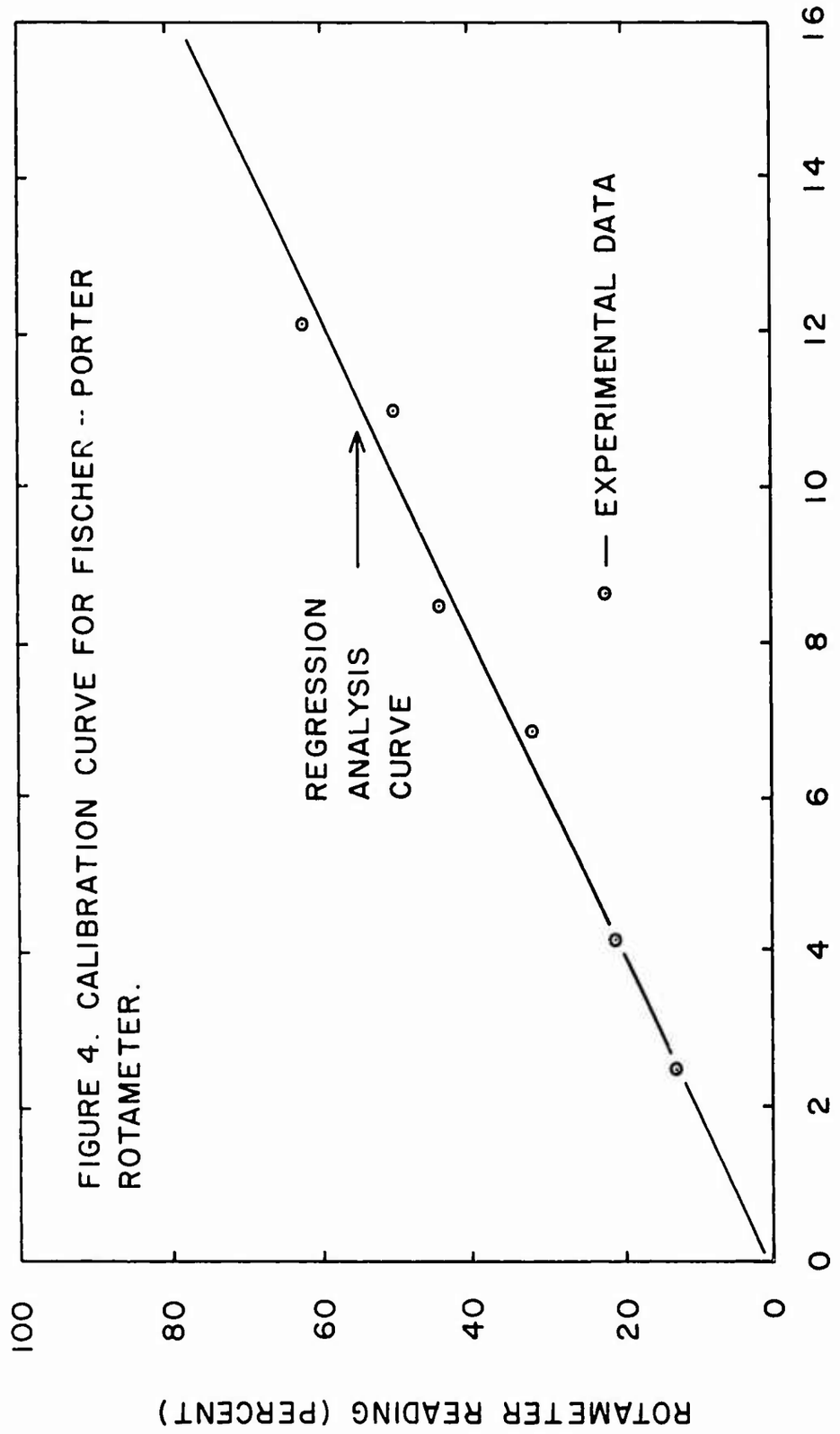

FIGURE 4. CALIBRATION CURVE FOR FISCHER -- PORTER ROTAMETER.

7. In addition to the above larger pieces of equipment, two stainless steel storage drums (25-gallon capacity) and many smaller parts (e.g., valves, fittings, piping, etc.) all specified to be of type 316 stainless steel and capable of withstanding 3,000 psig were secured for completion of this system.

3.4.2 Biocatalytic Reactor Module

For the purposes of this investigation a novel adaptation of the spiral wound biocatalytic reactor module was designed, developed, and constructed in our laboratory. The first consideration was, of course, the size of the reactor to be constructed since a large amount of the collagen-urease membrane complex was needed for the system operation. A second point was to develop a way to insure that a minimum amount of bypassing and channeling occurred in the reactor during all phases of operation. Third, and finally, a modification in the reactor was to be made to obtain conditions as close to as what might be assumed to be plug-flow as possible (see Section 4.4.1).

To these ends, the reactor (Figures 5 and 6; Table 3) was produced. Since no pressure was to be applied to the module, plexiglass was deemed the most logical material to be used in its construction. Its easy machinability and transparent character made plexiglass a good selection for this type of low pressure reactor.

The shell of the reactor (1) was constructed from

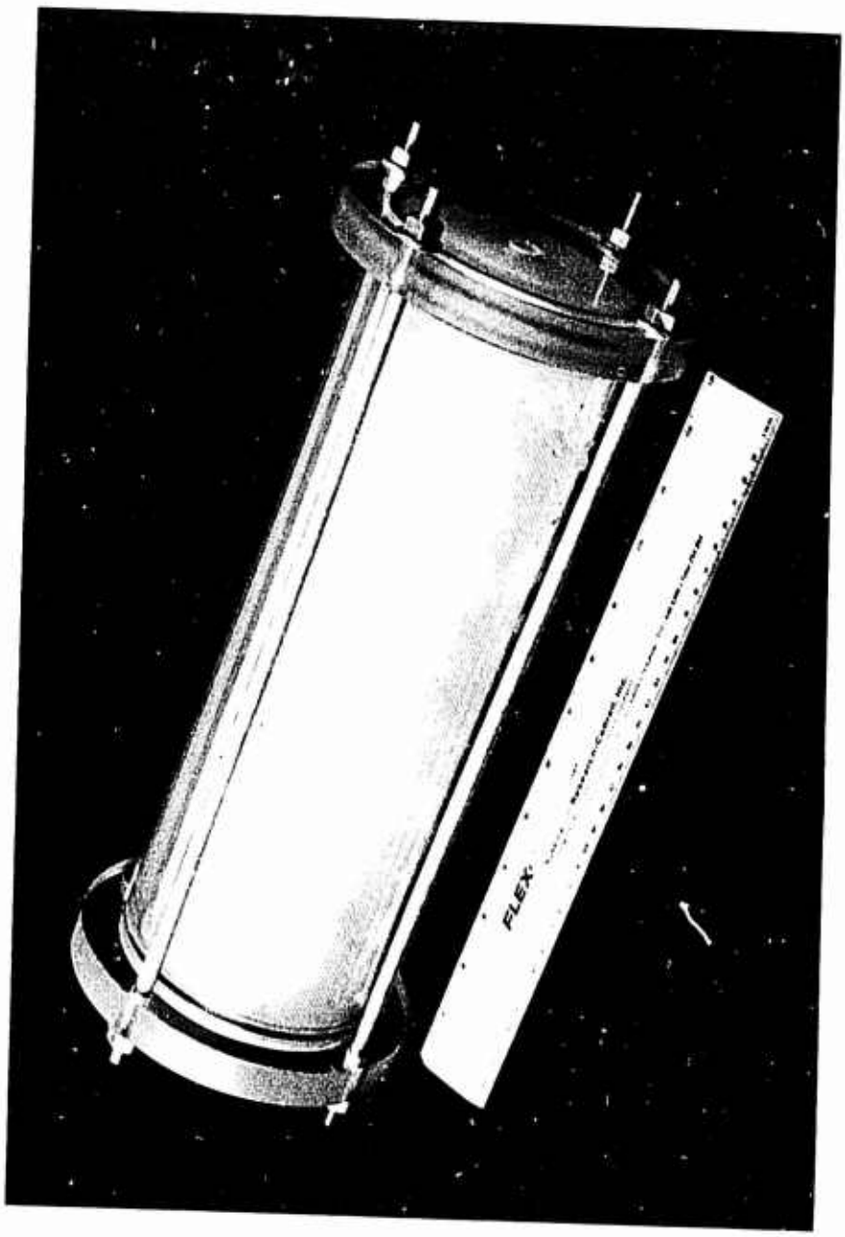

FIGURE 5. SPIRAL WOUND BIOCATALYTIC REACTOR MODULE.

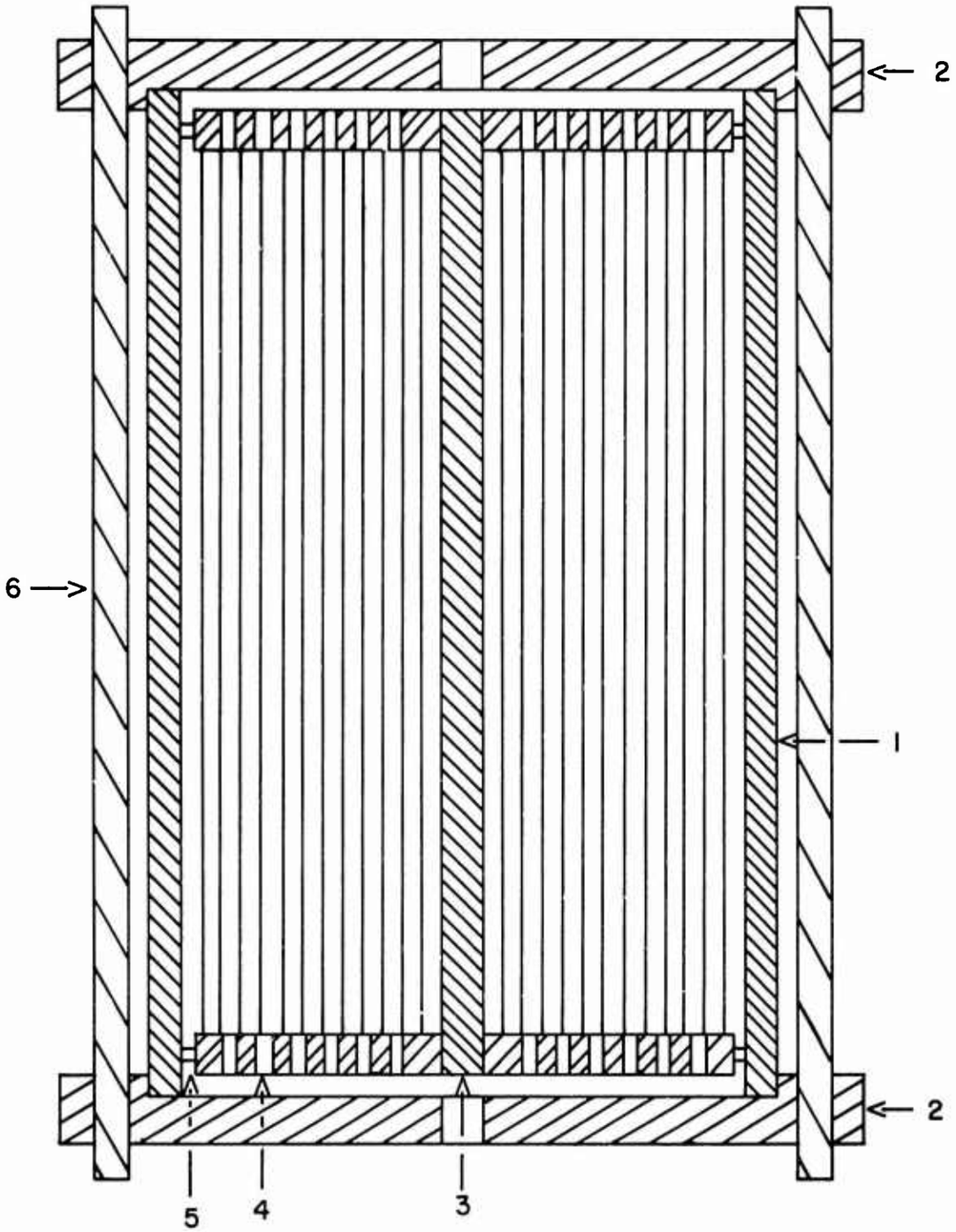

FIGURE 6. SCHEMATIC CROSS-SECTIONAL VIEW OF SPIRAL WOUND BIOCATALYTIC REACTOR MODULE.

TABLE 3

SPECIFICATIONS FOR BIOCATALYTIC REACTOR MODULE

Part No.	Part name	Material and dimensions
1	Reactor shell	Plexiglass tube: Inside diameter = 10.6 cm Outside diameter = 12.2 cm Length = 34 cm
2	End cap	Plexiglass sheet: Thickness = 1.8 cm Diameter = 15.5 cm
3	Center rod	Aluminum: Diameter = 0.9 cm Length = 32.5 cm (threaded at both ends)
4	Flow distribution disk	Plexiglass sheet: Thickness = 0.9 cm Diameter = 10.5 cm
5	O-Ring seal	Viton rubber: Thickness = 0.3 cm Diameter = 10.2 cm
6	Tie rods	Aluminum: Diameter = 0.8 cm Length = 39.3 cm (threaded on both ends)

plexiglass tubing and the end caps (2) from 1.8 cm thick plexiglass sheet. Each end cap was machined to fit snugly around the reactor shell with a groove provided for an 0-ring to insure a watertight seal around each end of the reactor. The center rod (3) of aluminum was threaded onto two flow distribution disks (4) which were force fitted inside the reactor shell by means of a second 0-ring seal (5). This inner core was constructed in such a manner so as to make it possible to wind the collagen-urease membrane complex and Vexar mesh spacer around it much like a spool or cartridge. The modular capability of the reactor was thus preserved, making it possible to replace the inner cartridge at any time.

The configuration of holes in the flow distribution disks (Figure 7) was obtained from an empirical relation of the amount of liquid supplied by each hole in order to maintain a constant fluid velocity across any cross section of the reactor. This relation leads, by simple intuition, to the fact that more holes must appear in the disk as one moves further from the central axis of the reactor.

The biocatalytic reactor module was prepared for operation in the following manner:

1. The immobilized collagen membrane was soaked in distilled water to make it more pliable and easier to handle.

2. The membrane was then placed on a single sheet of Vexar mesh spacer (0.0625 cm thick).

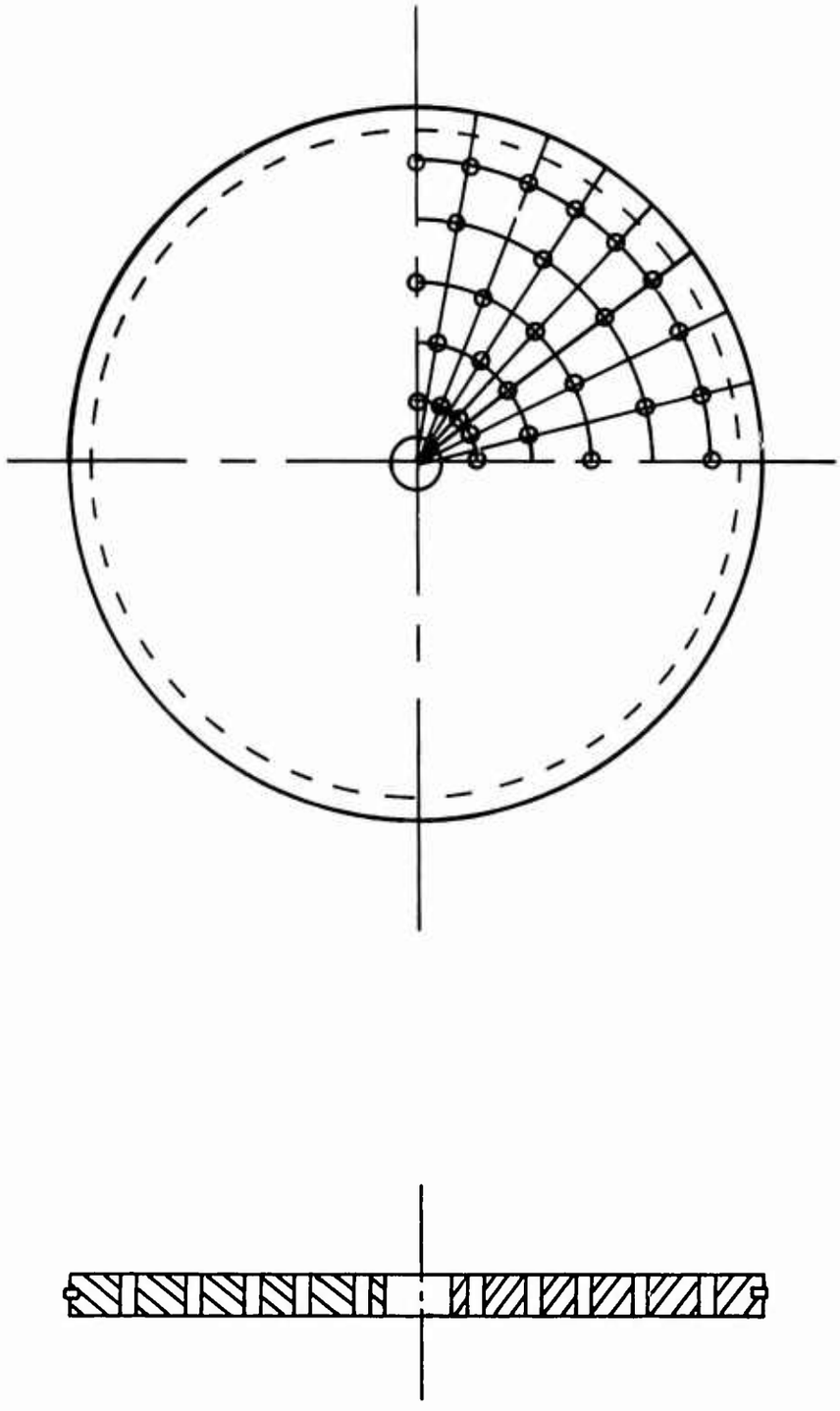

FIGURE 7. SCHEMATIC CROSS - SECTIONAL VIEW OF FLOW DISTRIBUTION DISKS FOR BIOCATALYTIC REACTOR MODULE.

3. This double layer was wound around the center support as previously described to obtain a cartridge of the same diameter as the flow distribution disks (Figure 8).

4. The inner cartridge was then inserted into the reactor shell (Figure 9) and the end caps were placed on the reactor.

In order to hold the end caps securely and insure a proper liquid seal inside the reactor, four aluminum tie rods (6) were positioned around the outside of the reactor.

This adaptation of the spiral wound module has performed remarkably well under a variety of flow conditions. Additional work will expand this reactor to a larger size or possibly to a multiple module system.

3.4.3 Ion Exchange Column

For simplicity of construction, the ion exchange column (Figure 10) was constructed in the same manner as the shell for the biocatalytic reactor module. However, several experiments were needed to produce the proper parameters from which the size of the column could be obtained.

Because of the toxicity of ammonia, an ion exchange resin had to be chosen which would reduce the ammonia concentration to below 0.2 ppm. From various manufacturers' data, a strongly acid exchange resin, Dowex 50W-X8, was chosen as the most likely candidate for this task.

As has been stated, resin capacity is measured by

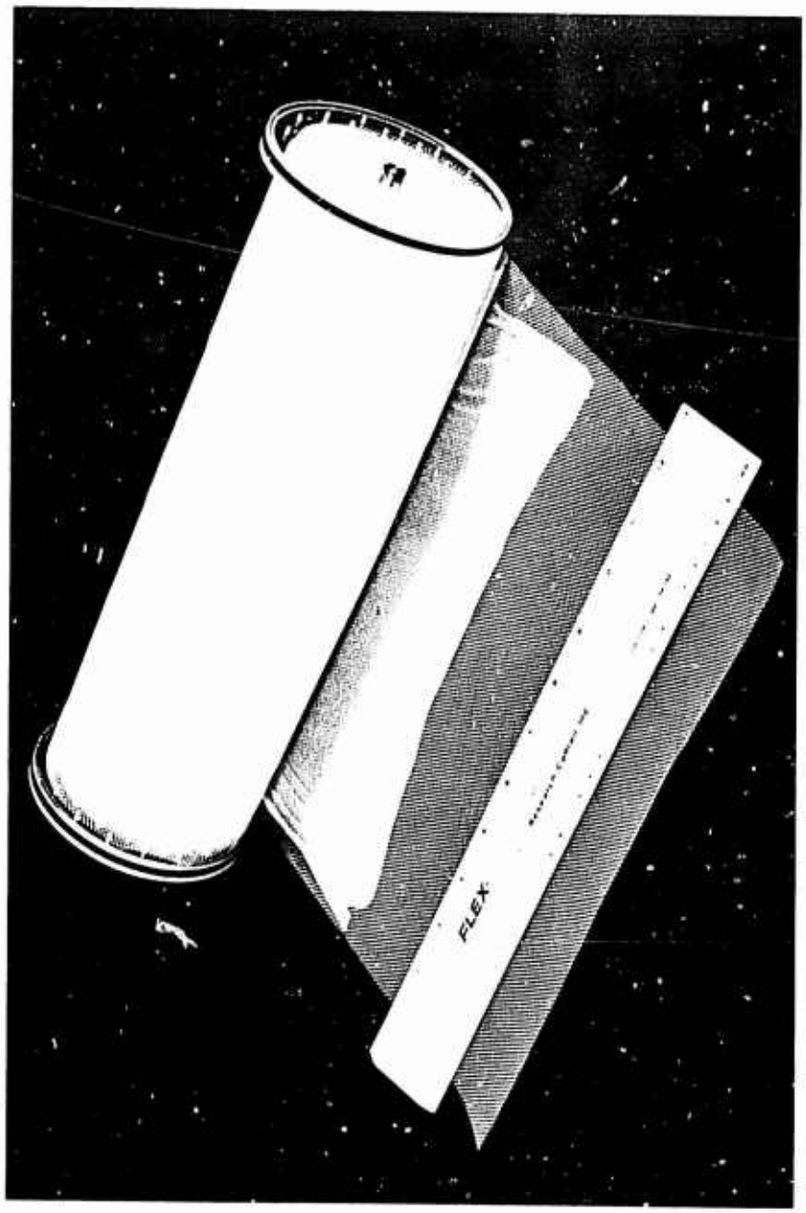

FIGURE 8. SPIRAL WOUND BIOCATALYTIC MODULE WITHOUT REACTOR SHELL.

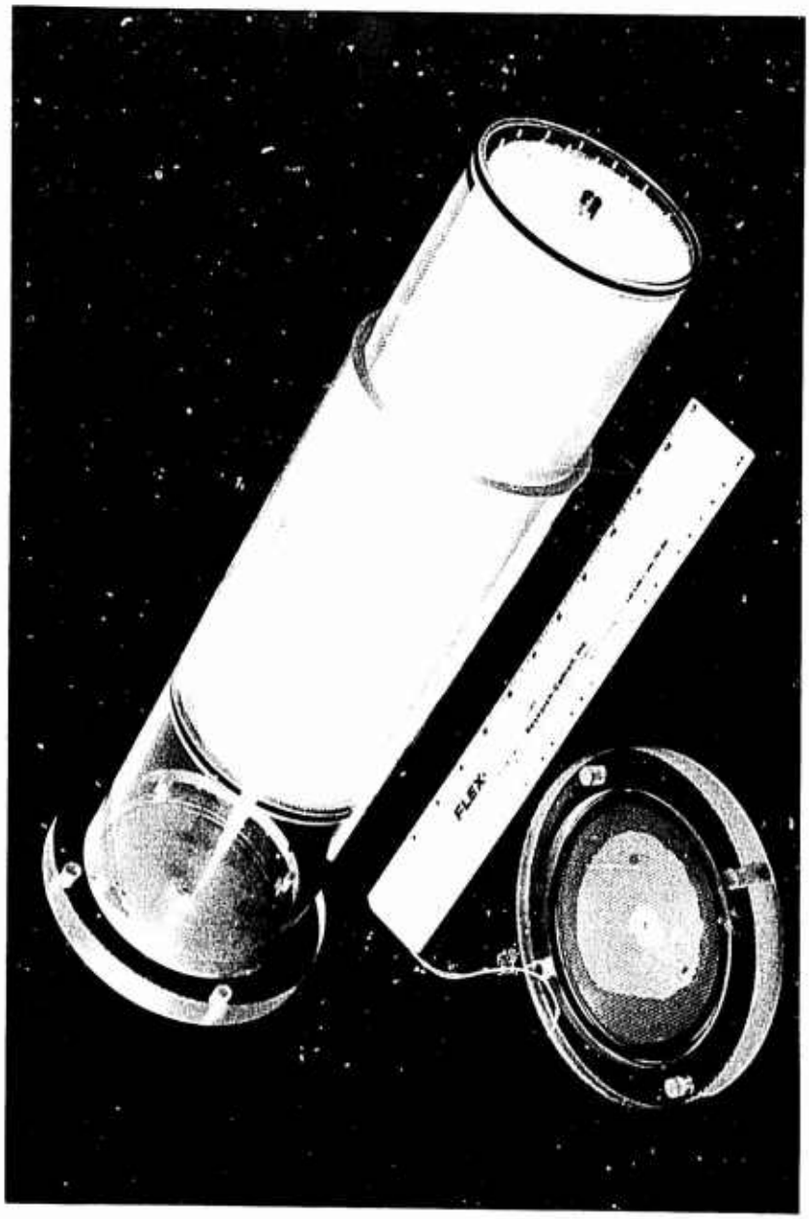

FIGURE 9. INSERTION OF SPIRAL WOUND BIOCATALYTIC MODULE INTO THE REACTOR SHELL.

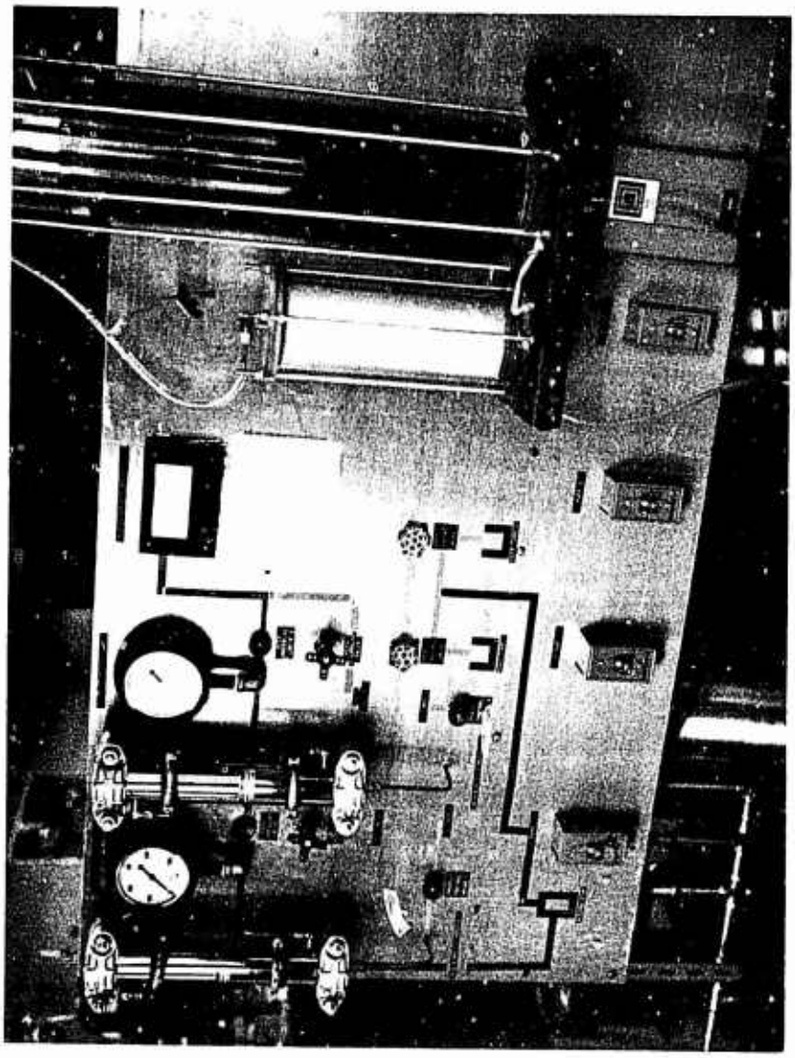

FIGURE 10. ION EXCHANGE COLUMN AND PROTOTYPE SYSTEM.

the number of milliequivalents (meq) of ions which can be exchanged per gram of dry resin. This is determined by titration of the resin with a standard solution of the ion to be exchanged. The capacity of Dowex 50W-X8 resin was found to be 4.08 meq per gram of dry resin.

To translate this capacity into more meaningful terms, calculations were made to determine the volume of product which could be processed per gram of dry resin before regeneration is required. This was calculated as a function of the feed urea concentration assuming 100% urea conversion in the biocatalytic reactor module. The range of 4.5 to 200 ppm of urea was considered and the results are plotted in Figure 11. A concentration of 4.5 ppm of urea represents 152 cc of urine per 180 gallons of dilution water, while 200 ppm of urea represents 152 cc of urine per 3.5 gallons of dilution water. The processing capacity of the resin is thus seen to vary from 27.2 to 0.6 liters per gram of dry resin over this concentration range.

Considering the most concentrated urea feed, and hence the lowest processing capacity of the resin, with a 50-gallon per day flow of product, only 333 grams of resin would be exhausted per day. Thus, if a 30-day period of operation is desired before regeneration is necessary, 20,000 grams or about 22 pounds of resin would be required for the exchange column. For continuous operation, two ion exchange columns could be used. One column could be off-line and regenerating while the other is on-line and in

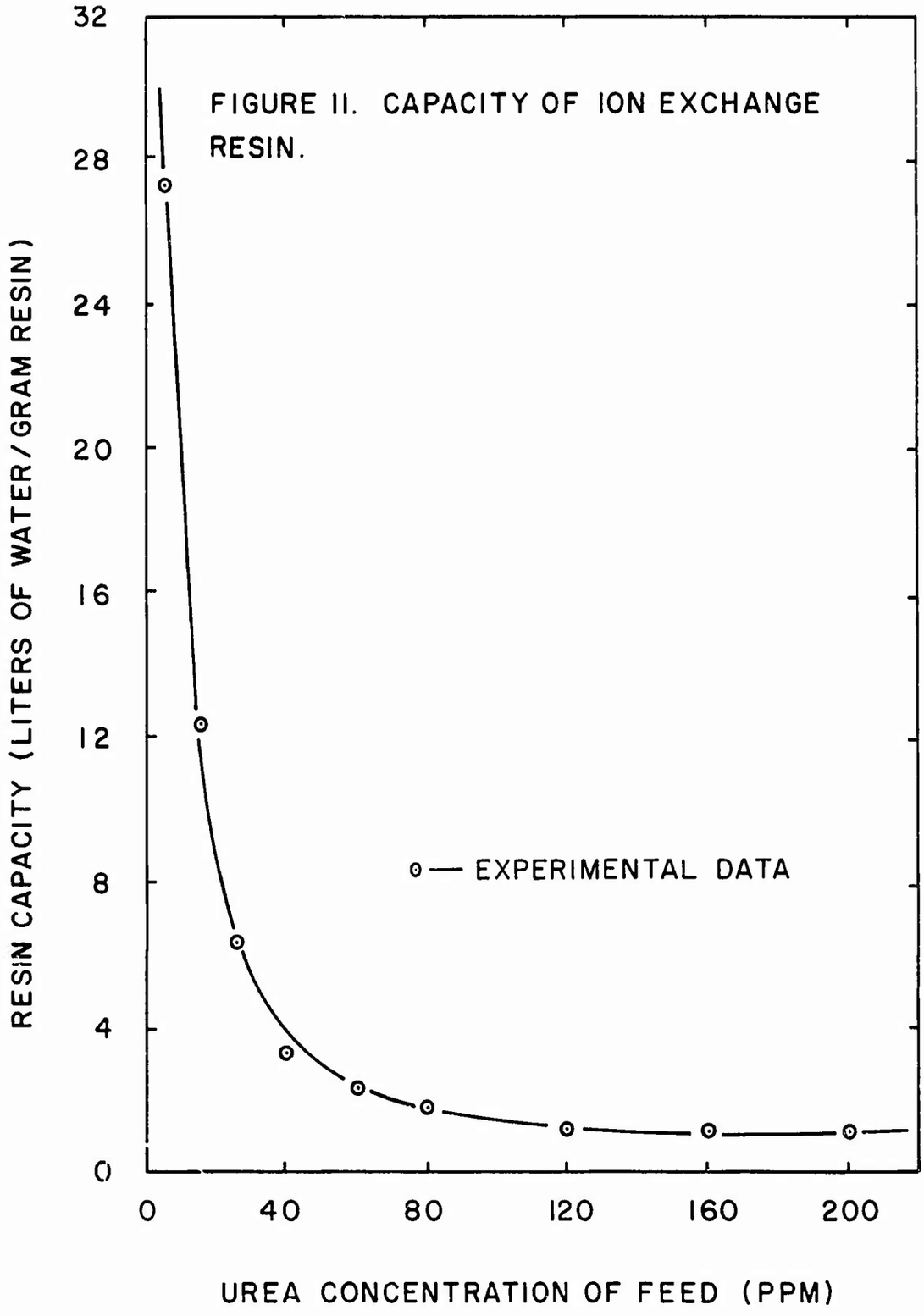

FIGURE II. CAPACITY OF ION EXCHANGE RESIN.

active use.

For the purposes of our prototype system, only one ion exchange column of 10-day capacity was deemed necessary. Since the system was operated only for 5 to 8 hours at a time, sufficient time was available for the regenerating procedure. The regenerating procedure followed was a simple washing of the resin bed with two resin bed volumes of 2.0 N HNO_3. This was followed by several washings (5-8 bed volumes) with distilled water to remove the regenerating solution.

3.4.4 Modes of System Operation

The system, in its operational form, may be described simply by a process flow diagram (Figure 12):

1. The feed is pumped from a storage drum to the first of two reverse osmosis modules (RO-1 and RO-2). The feed flow rate may be controlled by the capacity adjustments on the pump or by a feed control valve (V-1).

2. By closing a back-pressure valve (V-2), part of the feed solution is forced to permeate the reverse osmosis membrane in the first module. This becomes the feed stream for the second reverse osmosis module.

3. A second back-pressure valve (V-3) causes a portion of this stream to permeate the reverse osmosis membrane in the second module and pass on to the biocatalytic reactor module.

4. Pressure in the reverse osmosis modules is

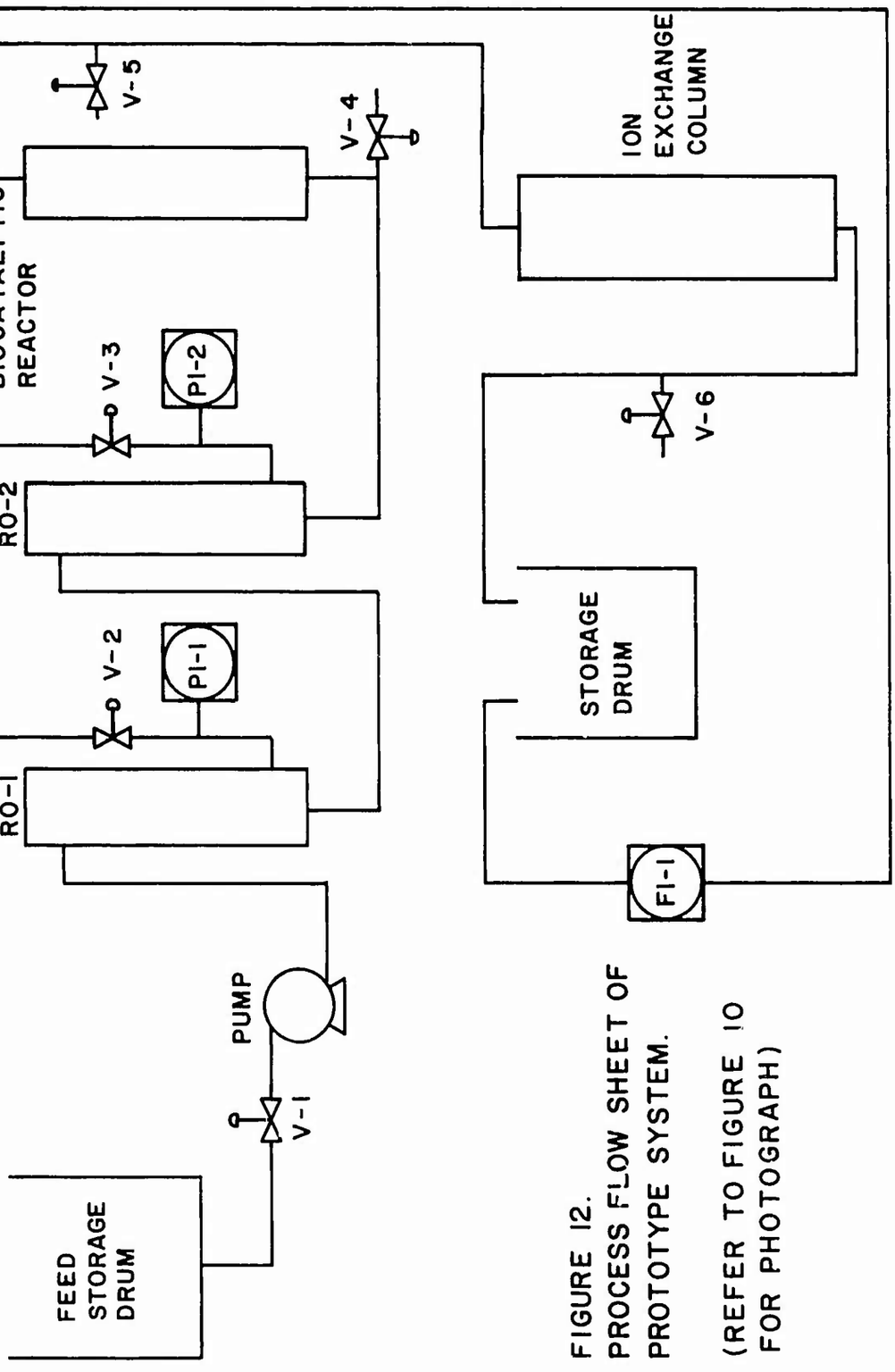

FIGURE 12.
PROCESS FLOW SHEET OF PROTOTYPE SYSTEM.

(REFER TO FIGURE 10 FOR PHOTOGRAPH)

indicated on pressure indicators (PI-1 and PI-2). In addition, both retentate streams from the modules join, pass through a flow indicator (FI-1), and empty into a storage drum.

5. The permeate from the second reverse osmosis module passes vertically upward through the biocatalytic reactor module contacting the collagen-urease membrane complex. Two valves (V-4 and V-5) are provided for sampling of the streams before and after the biocatalytic reactor module.

6. The product from the biocatalytic reactor module is passed vertically downward through the ion exchange column and finally into a storage drum. Again, a value (V-6) is provided for sampling of the final product stream.

The system, as described, may now be operated at various conditions of temperature, pressure, and feed flow rate. In addition, various types of operation of the system are possible. The system may be operated in a once-through continuous manner or any number of recycle options may be adopted.

Straightforward, single-pass continuous operation has been the primary mode of operation of the prototype system to date. The feed solution is pumped through the system and the output is simply discarded. While it is not the most efficient method of operation, the continuous flow method does show the limitations of the processing ability of the prototype system in a simple and

unencumbered manner.

The use of recycle is possible at several points in this prototype system. The combined retentate streams from the two reverse osmosis modules may be partially recycled to the feed tank to obtain larger amounts of permeate water from the same initial input. A second recycle loop could be provided around the biocatalytic reactor module. Partial recycle of the product stream from the reactor could effect a larger amount of the desired conversion of the urea in the reactor feed. Still a third recycle loop could be imposed around the ion exchange column and biocatalytic reactor module to insure that no product (ammonia) inhibition of the immobilized urease occurs.

The possibilities of operational configurations are, of course, endless. For initial characterization and testing of the system, the once-through continuous mode of operation was chosen for its simplicity and ease of analysis.

3.4.5 Analysis of System Performance

Several different steps and procedures were involved in order to obtain a complete analysis of each of the flow paths in the system. These analytical procedures are outlined below:

1. Analysis of Feed, Retentate, and Pre-Biocatalytic Reactor Module Streams:

A. Salt and/or Cation Concentration:

The concentration of salt and other cations in these streams is determined by use of a Beckman No. 39137 cationic electrode in conjunction with a standard Beckman reference electrode and a Beckman Expandomatic pH meter. A standard calibration curve was prepared using standard sodium chloride solutions ranging in concentration from 0.1 M to 0.0001 M (Figure 13).

B. Urea Concentration:

The urea concentration of the stream cannot be measured directly but must be obtained by measuring the amount of ammonia produced by 100% hydrolysis of the urea present by the addition of free urease to each sample. The procedure is outlined below:

(1) Obtain a 30 cc sample of the stream to be tested for urea concentration.

(2) Insert the Orion ammonia probe into the sample and begin agitation with a small magnetic stirring bar.

(3) Add 2.0 cc of enzyme solution containing 10 mg/cc of urease and allow the reaction to go to completion.

(4) Because of the existence of a pH dependent equilibrium between ammonium ion and dissolved ammonia gas (Figure 14), 1 cc of 10 M NaOH is added to insure the liberation of all of the ammonia gas.

The ammonia concentration is obtained by using an Orion ammonia gas electrode (No. 95-10) in conjunction with a Beckman Expandomatic pH meter. A standard

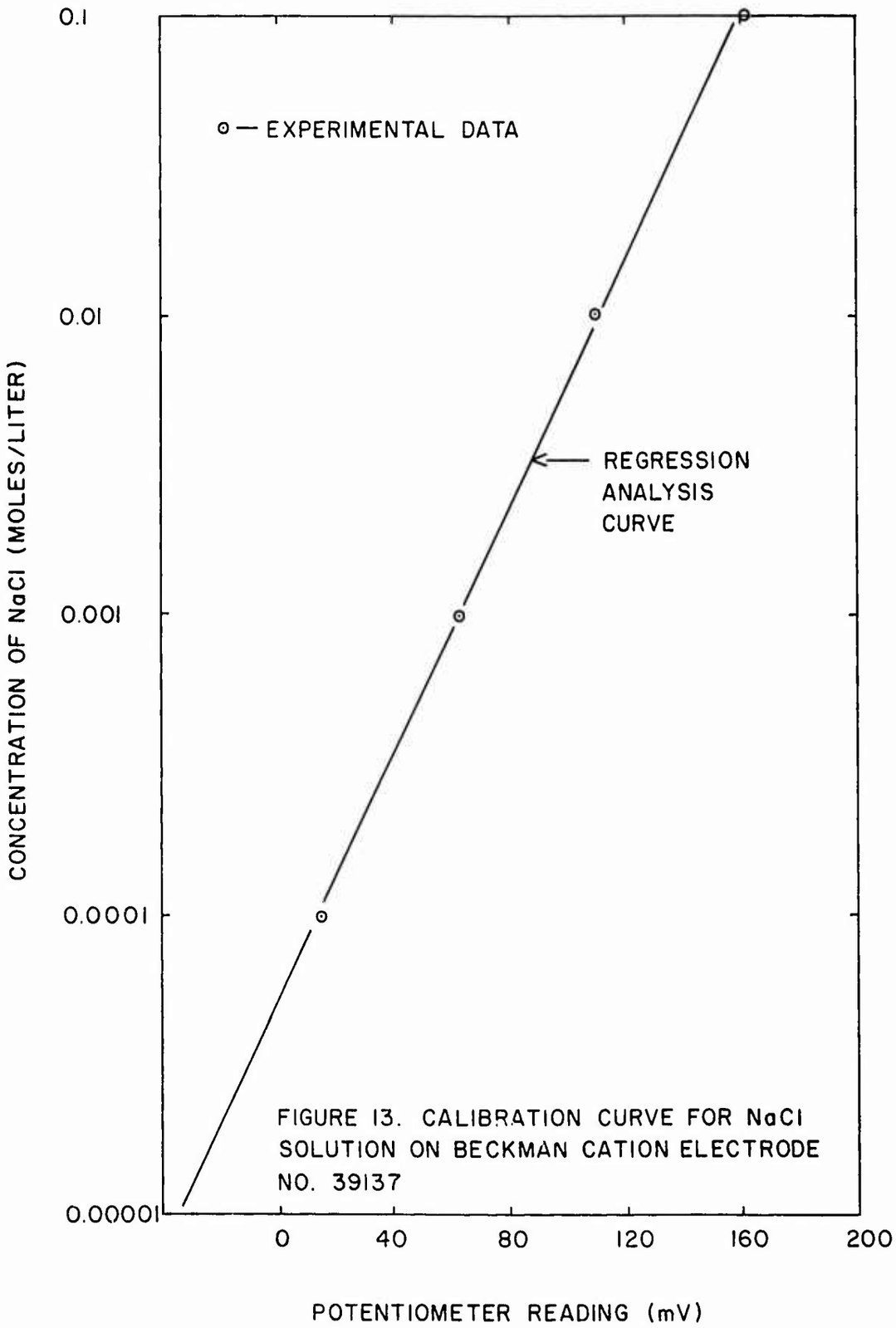

FIGURE 13. CALIBRATION CURVE FOR NaCl SOLUTION ON BECKMAN CATION ELECTRODE NO. 39137

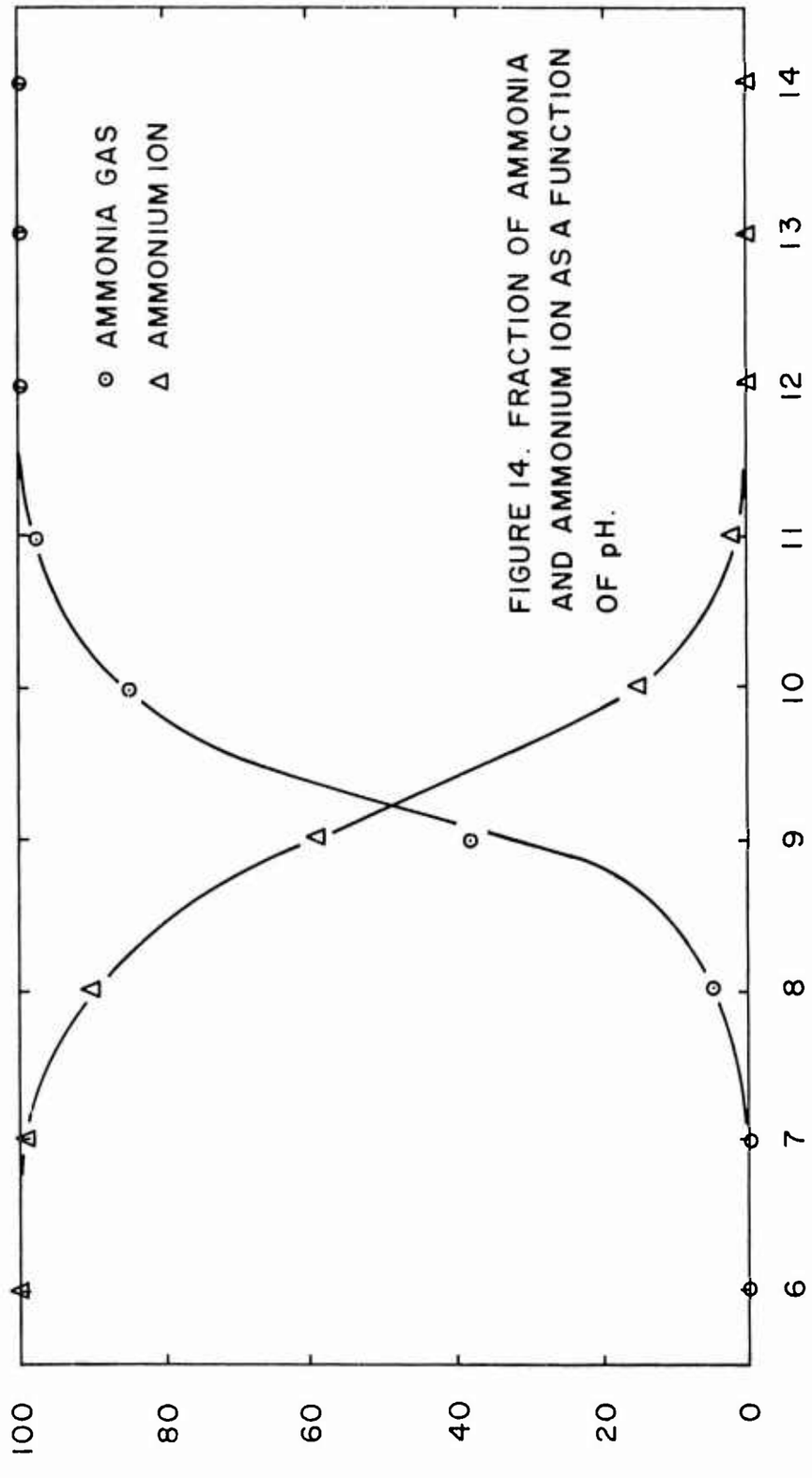

FIGURE 14. FRACTION OF AMMONIA AND AMMONIUM ION AS A FUNCTION OF pH.

calibration curve is prepared by the addition of 1 cc of 10 M NaOH to standard ammonium chloride solutions ranging in concentration from 0.1 M to 0.0001 M (Figure 15). Knowledge of the stoichiometry of the hydrolysis reaction then gives the actual urea concentration by a simple halving of the ammonia concentration.

2. Analysis of Post-Biocatalytic Reactor Module and Final Product Streams:

A. Ammonia Concentration:

The presence of cations other than ammonium ions in these two streams makes the use of a standard Beckman cationic electrode impossible (see Section 3.4). The alternative method is to again use the Orion ammonia gas electrode. The procedure is outlined below:

(1) Obtain a 30 cc sample of the stream to be tested for ammonia concentration.

(2) Insert the Orion ammonia probe into the sample and begin agitation with a small magnetic stirring bar.

(3) Add 1 cc of 10 M NaOH to drive the pH dependent equilibrium to the ammonia gas specie. Again, the ammonia gas concentration is exactly twice that of the comparable urea concentration.

The performance of the system by components and the overall prototype system performance may be obtained through the use of several equations. These system performance parameters may be defined as:

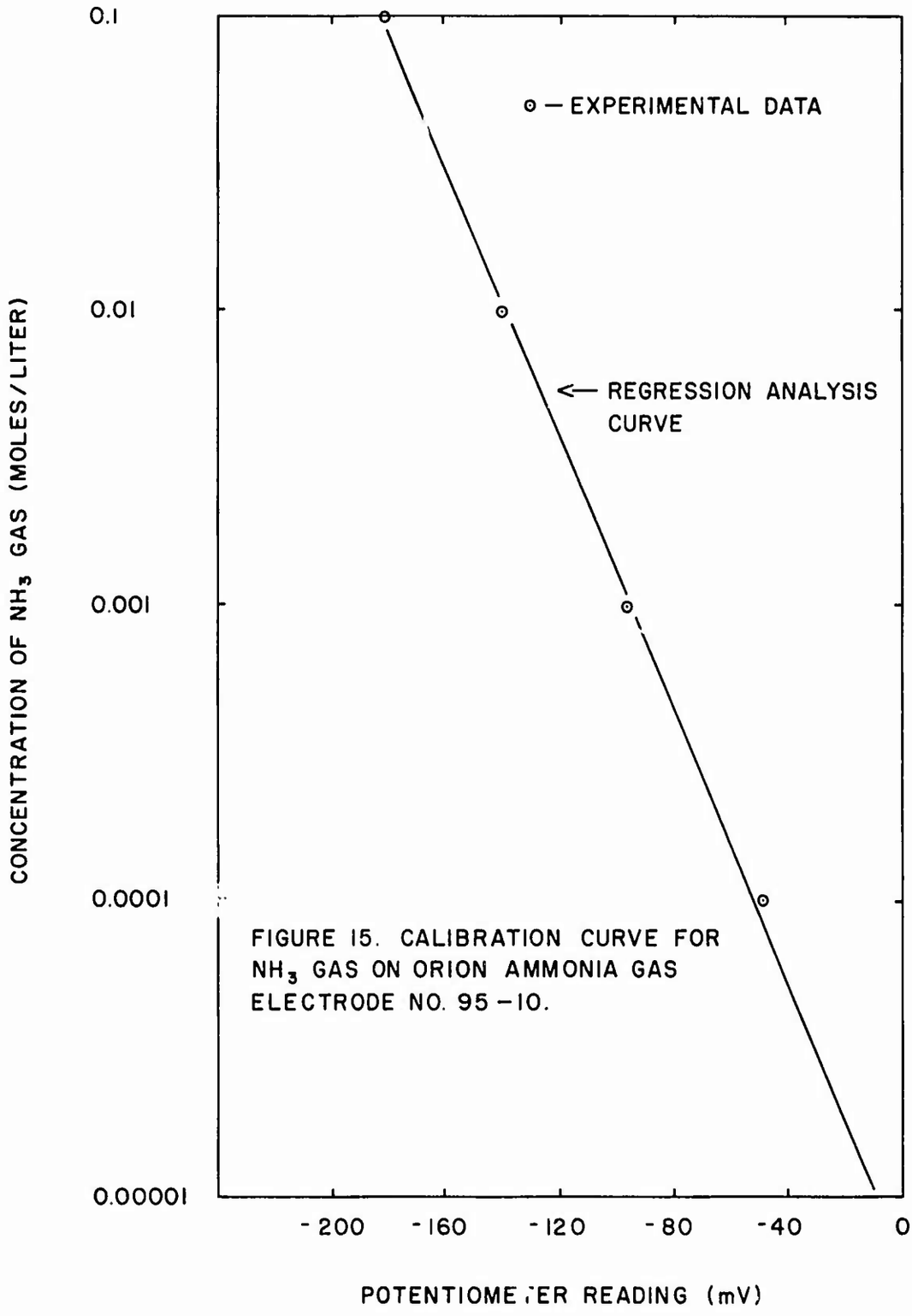

FIGURE 15. CALIBRATION CURVE FOR NH_3 GAS ON ORION AMMONIA GAS ELECTRODE NO. 95-10.

$$\text{Percent salt rejection} = \frac{C_{sf}-C_{sp}}{C_{sf}} \times 100 \qquad (3\text{-}1)$$

$$\text{Percent urea rejection} = \frac{C_{uf}-C_{up}}{C_{uf}} \times 100 \qquad (3\text{-}2)$$

$$\text{Percent reactor urea conversion} = \frac{C_a}{2C_{up}} \times 100 \qquad (3\text{-}3)$$

$$\text{Percent urea conversion based on feed} = \frac{C_a}{2C_{uf}} \times 100 \qquad (3\text{-}4)$$

$$\text{Overall urea removal} = \frac{2C_{uf}-2C_{up}+C_a}{2C_{uf}} \times 100 \qquad (3\text{-}5)$$

where: C_{sf} = feed salt concentration (moles/liter)

C_{sp} = permeate salt concentration (mole/liter)

C_{uf} = feed urea concentration (moles/liter)

C_{up} = permeate urea concentration (mole/liter)

C_a = reactor product ammonia concentration (moles/liter)

The characterization of these performance parameters can then be used to determine the true feasibility of the prototype system.

3.5 Assay of Enzyme Content of Collagen-Urease Complex Membranes

One of the most important factors to be identified in this system was the stability of the collagen-urease complex. In order to obtain an accurate idea as to how much enzyme was washed from the system and how much was still intact on the membrane, a suitable assay procedure had to be chosen to determine the amount of enzyme present on a particular specimen of membrane.

The method of Spies and Chambers, as described by Blackburn (1968), for the quantitative analysis of the amino acid tryptophan was chosen for the lack of tryptophan in collagen which provides a direct calibration to the enzyme content of the membrane. The procedure is based on a spectrophotometric analysis of the formation of a blue product. The steps in this method are outlined below:

1. Dissolve 30 mg of p-dimethylaminobenzaldehyde in 9 cc of 21.4 N H_2SO_4.

2. Dissolve a sample of membrane containing from 5 to 120 µg of tryptophan in 1 cc of 1 N NaOH.

3. Mix the two solutions while cooling in an ice bath to prevent the temperature from rising above 25°C.

4. Store the mixture in the dark for 90 minutes.

5. Add 0.1 cc of freshly prepared 0.04% sodium nitrite to develop the blue color.

6. Store the mixture in the dark for 30 minutes.

7. Read the absorbance at 595 mµ against a blank obtained in the same manner, but omitting the p-dimethylaminobenzaldehyde reagent.

A Bausch and Lomb Spectronic 20 Colorimeter was used for the absorbance readings. A calibration curve for urease (Figure 16) was obtained in the same manner as described above by using 1 cc samples of a known concentration of enzyme solution. From such a calibration curve, the urease content of various membrane samples may be easily obtained.

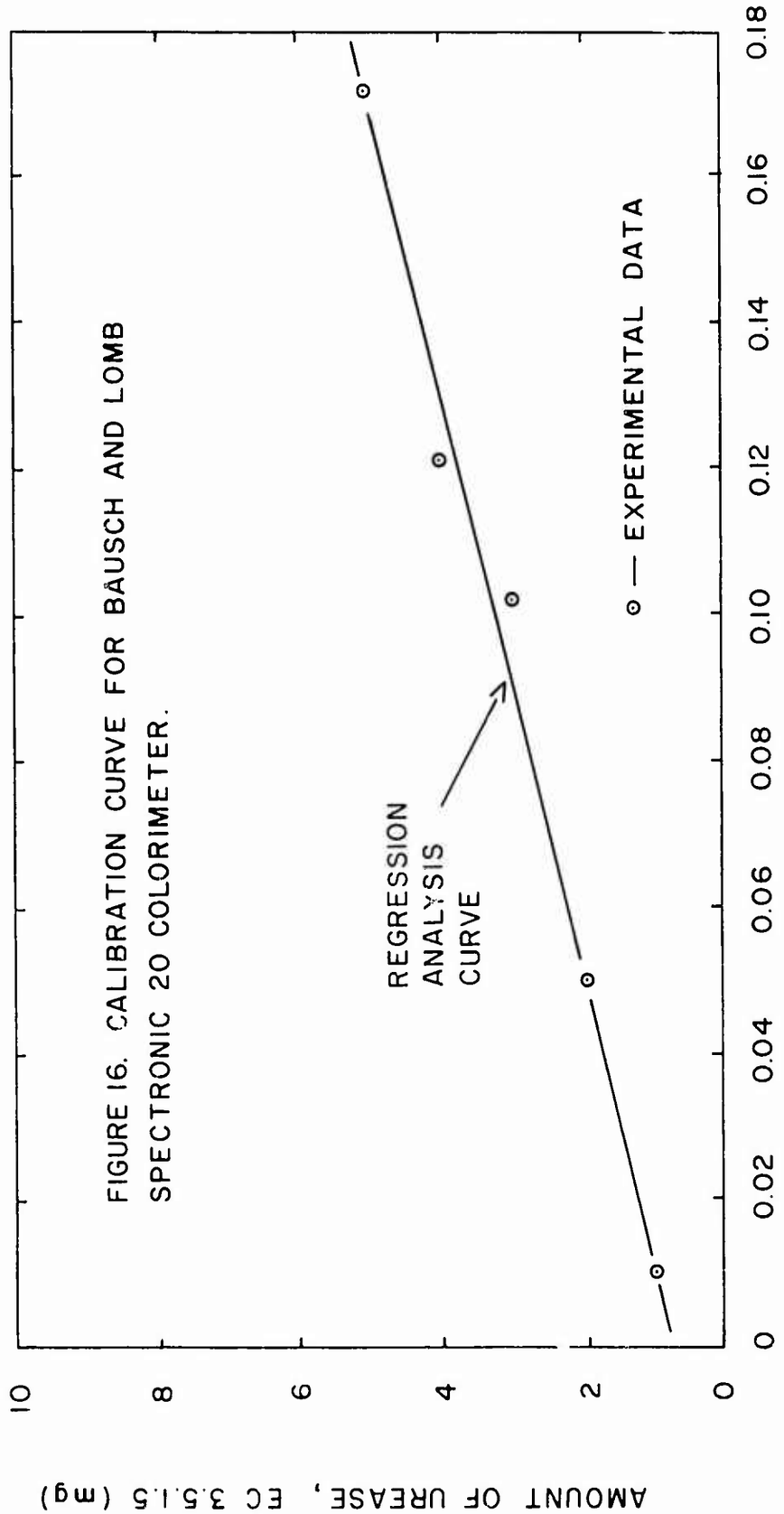

FIGURE 16. CALIBRATION CURVE FOR BAUSCH AND LOMB SPECTRONIC 20 COLORIMETER.

4. RESULTS AND DISCUSSION

While a multitudinous amount of raw data has been obtained during the 12-month operation of this prototype system, the characterization of the performance of the biocatalytic reactor module under a variety of conditions is perhaps the single, most important purpose of this investigation. To that end, a short discussion of the performance of the spiral wound reverse osmosis module and ion exchange resin column is first presented for the sake of completeness. Following this discussion, the performance of the biocatalytic reactor module will be evaluated and a numerical modeling method developed.

4.1 Reverse Osmosis Module Performance

Extensive preliminary work was performed in order to characterize the salt and urea rejecting capabilities of the spiral wound reverse osmosis module. While the salt rejecting characteristics of the module are well documented by the manufacturer, the performance of the module was unknown in relation to a urea and salt feed solution. Figures 17 and 18 show the desired result. From these figures, an optimum pressure for both urea and salt rejection may be obtained for this particular system. This, of course, is a valuable point of concern since operation beyond this

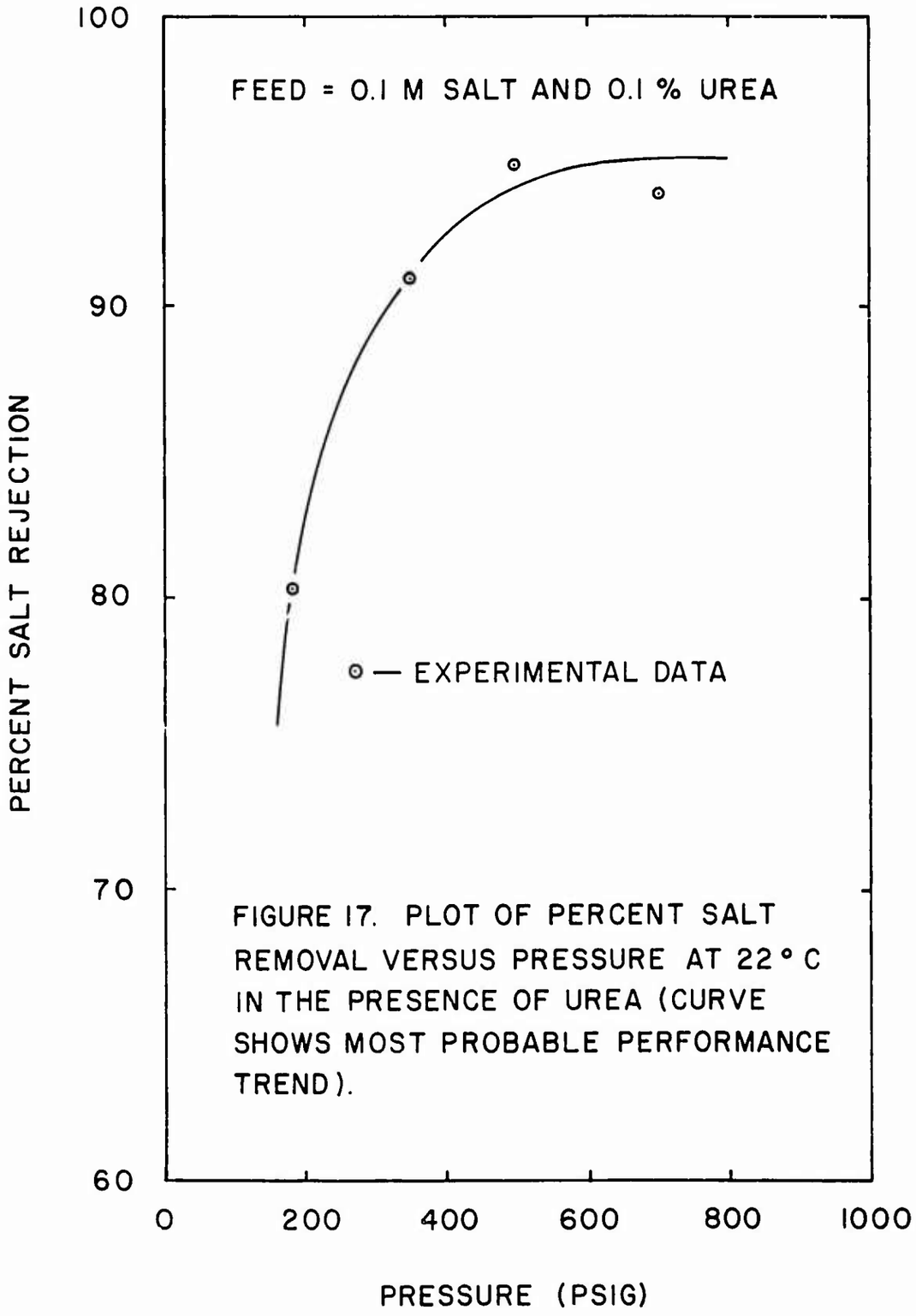

FIGURE 17. PLOT OF PERCENT SALT REMOVAL VERSUS PRESSURE AT 22° C IN THE PRESENCE OF UREA (CURVE SHOWS MOST PROBABLE PERFORMANCE TREND).

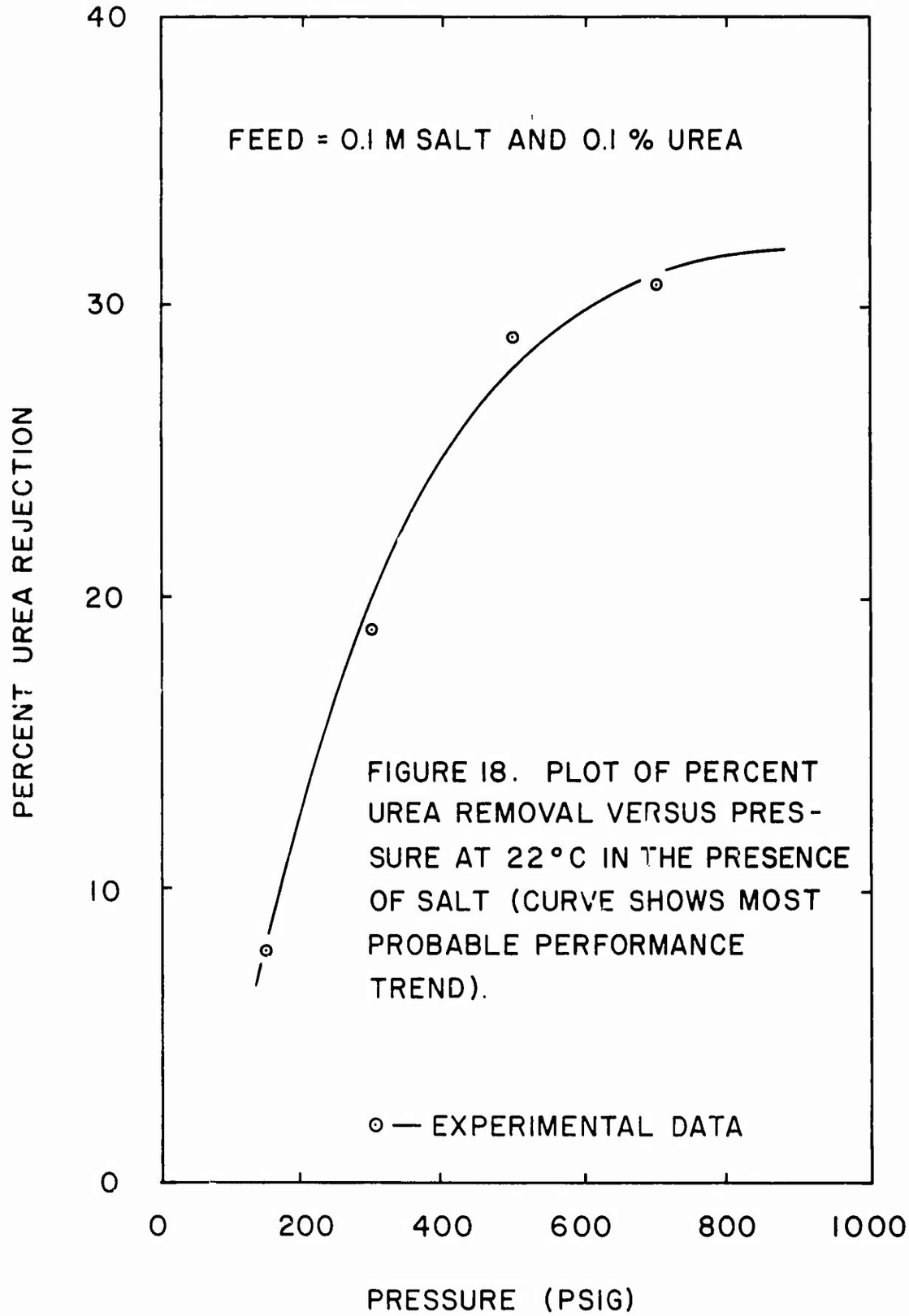

FIGURE 18. PLOT OF PERCENT UREA REMOVAL VERSUS PRESSURE AT 22°C IN THE PRESENCE OF SALT (CURVE SHOWS MOST PROBABLE PERFORMANCE TREND).

pressure optimum would cause an unnecessary consumption of power and below this point the desired salt and urea removal in this component of the system would not be obtained.

4.2 Ion Exchange Column Performance

The successful removal of dissolved ammonia gas from the product stream of the biocatalytic reactor module is mandatory if such a product stream is desired for use as potable water. The design parameters described previously for the ion exchange resin column were used to size a column which would give 100% removal of ammonia from a 0.1% urea reactor feed (assuming complete conversion in the biocatalytic reactor module) for a period of 2 weeks of continuous operation at a projected flow rate of 25 gallons per day. The performance of the ion exchange column over 100 hours of intermittent operation at a variety of flow rates and ammonia gas concentrations is shown in Figure 19. The presence of a variety of cations as well as urea in the stream being fed to this column is the reason for its failure to span the projected 2-week operating period. The deterioration of the adsorbing capacity of the resin is rapid once the total capacity of the bed is exceeded. Of course, the possibilities of size for such a column are numerous and must be explored extensively to insure adequate removal without oversizing the reactor.

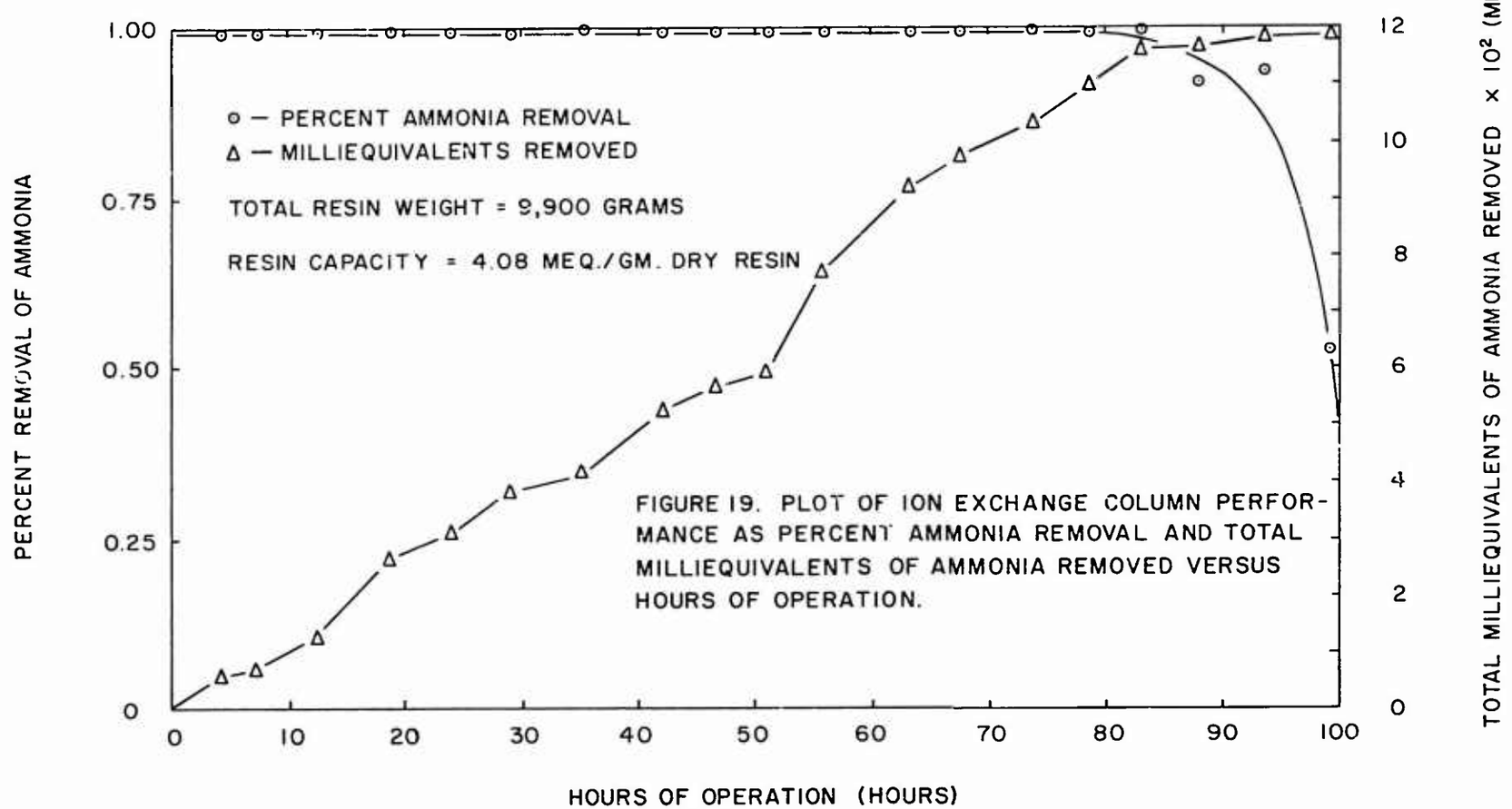

FIGURE 19. PLOT OF ION EXCHANGE COLUMN PERFORMANCE AS PERCENT AMMONIA REMOVAL AND TOTAL MILLIEQUIVALENTS OF AMMONIA REMOVED VERSUS HOURS OF OPERATION.

4.3 Stability and Reusability of Collagen-Urease Membrane Complex

These are without doubt the most important factors which control the economic feasibility of any system involving a biocatalytic reactor module. The cost of raw materials, particularly enzymes, and man-hours required for the preparation of the membrane complex must be outweighed by an increased stability of the immobilized enzyme and an ability of the membrane complex to endure alternating periods of operation and storage without losing mechanical strength.

The stability and reusability of the biocatalytic reactor module may be portrayed in a variety of ways. Previously (Davidson et al., 1973), the stability of a packed bed of collagen-urease membrane complex chips was analyzed via the calculation of an apparent first-order reaction rate constant. For the purposes of obtaining some idea of the stability of the collagen-urease membrane complex in the spiral wound configuration, a different approach was taken to elucidate the steady-state operation of such a reactor. Figure 20 shows the steady-state reactor urea conversion as a function of the number of liquid reactor volume replacements. Each point is shown with its corresponding reactor feed urea concentration (moles/liter) and feed flow rate (cc/min). While the variability of these two factors plays an integral role in the steady-state conversion obtained from the reactor, the conversion is

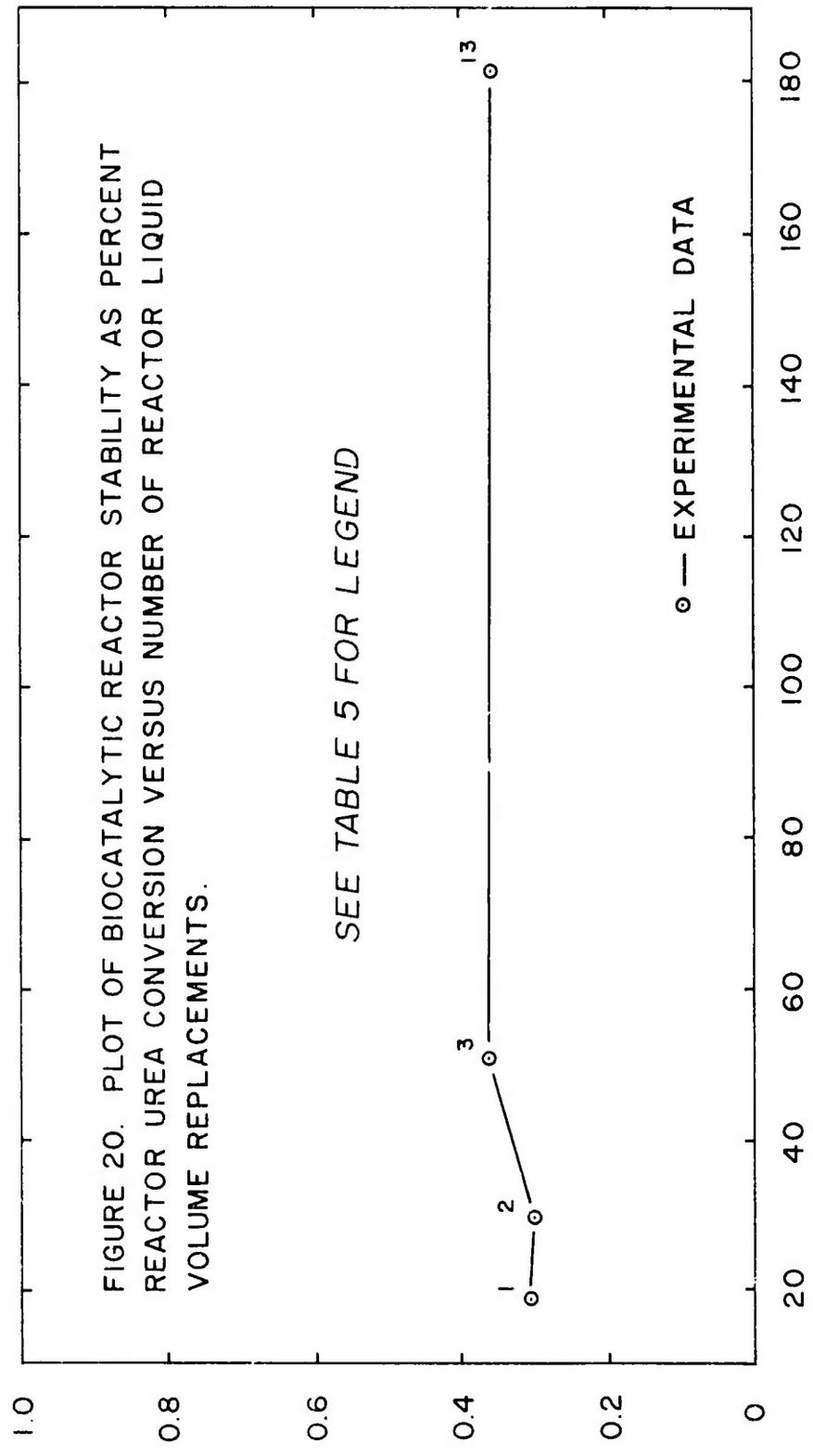
FIGURE 20. PLOT OF BIOCATALYTIC REACTOR STABILITY AS PERCENT REACTOR UREA CONVERSION VERSUS NUMBER OF REACTOR LIQUID VOLUME REPLACEMENTS.
SEE TABLE 5 FOR LEGEND
o — EXPERIMENTAL DATA
X (REACTOR UREA CONVERSION)
1.0
0.8
0.6
0.4
0.2
0
20
40
60
80
100
120
140
160
180
NUMBER OF REACTOR LIQUID VOLUME REPLACEMENTS
1
2
3
13

remarkably constant over a relatively wide range of reactor liquid volume replacements. (During the time period portrayed as liquid volume replacements [approximately 4 weeks], the reactor was operated at a variety of feed flows and urea concentrations. Between each of these runs, the reactor was stored under aerobic conditions in a refrigerator at 4°C.)

In order to determine if any enzyme was being desorbed from the membrane complex, the reactor module was washed in situ with several liquid volume replacements of glass distilled water. After each washing, the spent distilled water was assayed for enzymatic activity. This washing procedure brings about the initially stable enzymatic activity of the biocatalytic reactor module. The module was then placed on-line in the prototype system.

After approximately 5 weeks of operation (250 reactor liquid volume replacements), the reactor module was placed in storage for 10 days in the manner described previously. At the end of this storage period, the module was again placed on-line and analyzed for steady-state urea conversion. The conversion at this time was found to be less than 25% of the conversion shown previously by the biocatalytic reactor module. In order to understand what had actually occurred during the operation and storage period, a tryptophan analysis was performed to determine the amount of urease present on a piece of used membrane complex from the module as compared with that present on

an unused piece of membrane complex stored under similar conditions. The results of this analysis are shown in Table 4. Two important points may be noted from consideration of these data. The first is that, on the average, the amount of urease present on any two pieces of membrane complex (used and unused) differs by an amount which would not be expected to contribute such a large drop in reactor urea conversion. The decrease in enzyme content is apparently due to the desorption of loosely held enzyme from sublayers near the surface of the membrane. However, care must be taken in correlating these data to enzyme stability. While the tryptophan analysis is indeed indicative of the amount of urease present, the analysis in no way reveals what percentage of the total enzyme content is actually active. In addition, the fact that urease has been characterized as an enzyme with a multiple sub-unit structure (Sumner, 1926) may also contribute to the inherent variability of such an analytical procedure. If the active sub-units of such an enzyme molecule contain a low percentage of tryptophan as compared with other portions of the molecule, loss of these active sub-units would show a decrease in enzymatic activity (urea conversion) without a comparative loss of tryptophan. Thus, the analysis would show a high enzyme loading rate but a low enzymatic activity.

The second point to explain the sudden decrease in conversion appears from consideration of protein denaturation. Previous work with ovalbumin-urea systems (Frensdorff

TABLE 4

ENZYME CONTENT OF COLLAGEN-UREASE COMPLEX MEMBRANES

Sample characteristics	mg of enzyme/gm of catalyst
Used	97.2
Used	120.5
Used	111.6
Used	106.8
Unused	115.3
Unused	111.9
Unused	157.2
Unused	170.3

et al., 1953; Simpson and Kauzmann, 1953) shows that at urea concentrations greater than 4.37 M, an irreversible denaturation of the protein occurs. While the biocatalytic reactor module was not operated using urea concentrations in this range, the microenvironmental concentration during transient periods might have approached these levels. In addition, Weetall and Hersh (1969) have shown that urea inhibits the enzymatic hydrolysis reaction at concentrations above 0.34 M for urease immobilized on porous glass beads. While both of these possibilities exist, none can fully explain the loss in enzymatic activity of the biocatalytic reactor module. Indeed, the activity loss may be due primarily to the steady denaturation of the enzyme which occurs in any of the proposed immobilized enzyme systems.

4.4 Effect of Substrate Flow Rate and Concentration Upon Biocatalytic Reactor Performance

In addition to stability and reusability, the economic feasibility of such a prototype system is also dependent upon the effective range of operation of the system with respect to the flow rate and urea concentration of the feed solution. In order to characterize these factors, the biocatalytic reactor module was operated at three different feed flow rates while simultaneously varying the feed urea concentration.

The analysis of these data may be made by two

uniquely different methods. Since some type of assumption as to the character of the flow through the reactor must be made, the most logical choice would be that of plug-flow operation. The incorporation of flow distribution disks into the reactor module and the operation of the reactor in a vertical, upward flow position aid extensively in justifying this assumption. Now a meaningful analysis of the experimental data may be obtained. Figure 21 shows the reactor urea conversion as a function of residence time as a family of curves on a single set of axes. The data show a straightforward result that, as residence time in the reactor increases (decreasing reactor feed flow rate), the conversion of urea in the reactor also increases. The conversion is also seen to be dependent upon the feed urea concentration. An increase in urea concentration causes a decrease in the urea conversion for the same reactor residence time. A second point which must be elucidated, however, is the evaluation of the effect of mass transfer on the conversion. As can be seen, the combination of a high urea concentration and a low feed flow rate gives the same apparent conversion as that of a high feed flow rate. These, in turn, are both considerably lower than the apparent conversion obtained at an intermediate feed flow rate and a comparable feed urea concentration. This factor may now be explored as the second method of analysis.

By showing reactor urea conversion as a function of the total weight of catalyst in the reactor divided by the

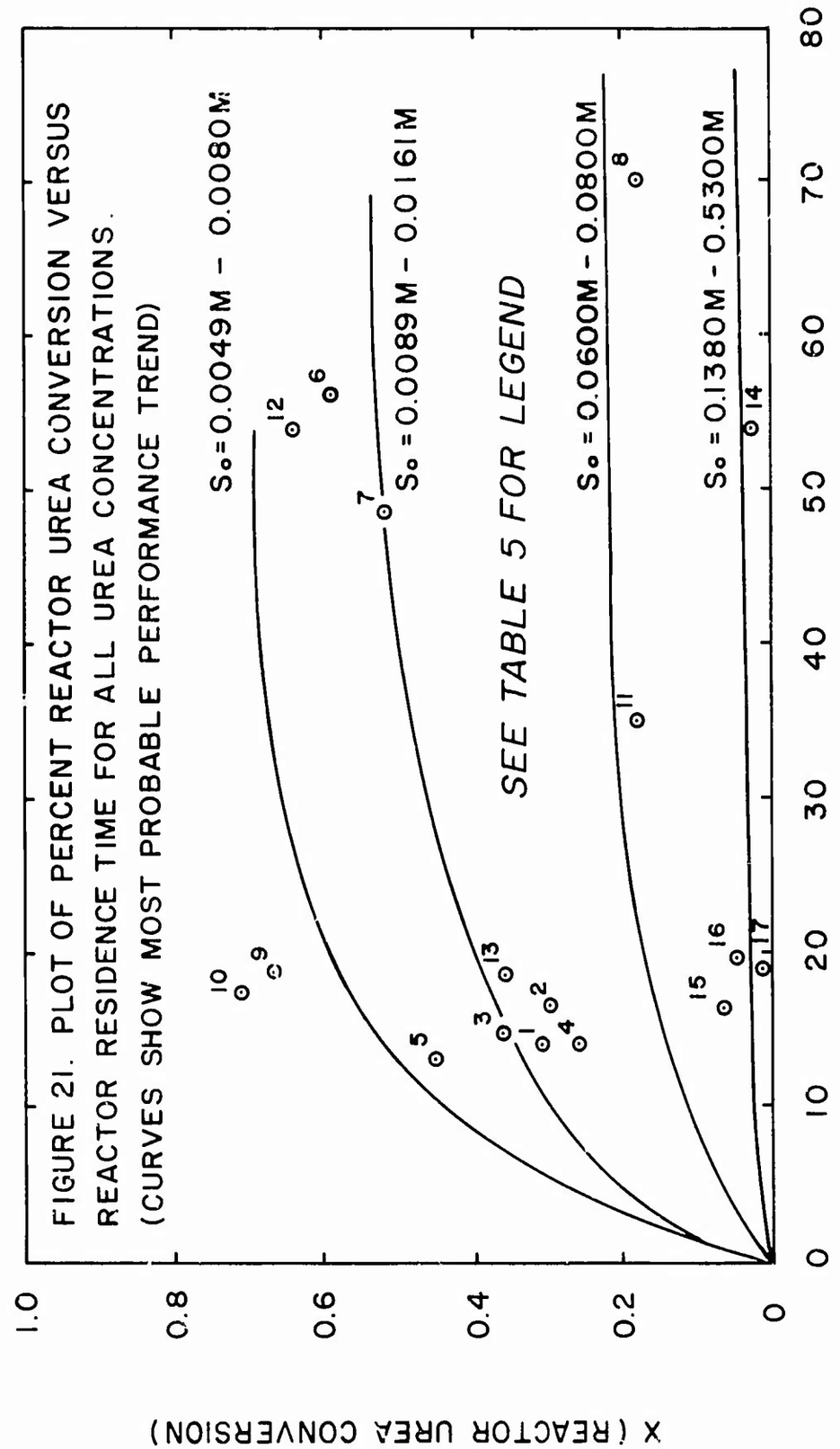
FIGURE 21. PLOT OF PERCENT REACTOR UREA CONVERSION VERSUS REACTOR RESIDENCE TIME FOR ALL UREA CONCENTRATIONS. (CURVES SHOW MOST PROBABLE PERFORMANCE TREND)
So=0.0049M - 0.0080M
So = 0.0089 M - 0.0161M
So = 0.0600M - 0.0800M
So = 0.1380M - 0.5300M
SEE TABLE 5 FOR LEGEND
X (REACTOR UREA CONVERSION)
REACTOR RESIDENCE TIME (MINUTES)
0
0.2
0.4
0.6
0.8
1.0
10
20
30
40
50
60
70
80

TABLE 5

LEGEND FOR BIOCATALYTIC REACTOR PERFORMANCE

Point No.	Urea concentration (moles/liter)	Flow rate (cc/min)
1	0.0145	100
2	0.0089	84
3	0.0114	95
4	0.0600	100
5	0.0080	108
6	0.0130	25
7	0.0051	29
8	0.0766	20
9	0.0071	76
10	0.0049	80
11	0.1380	40
12	0.0161	26
13	0.0114	76
14	0.2070	26
15	0.0800	86
16	0.1815	72
17	0.5300	74

feed flow rate in moles per minute (W/F), the effects of mass transfer at a variety of conditions may be evaluated. One must first take note of the fact that the mass transfer resistance is a function of the fluid velocity through the reactor which is intrinsically related to the feed flow rate. The method of analysis involves obtaining values for the reactor urea conversion as a function of W/F at different reactor fluid velocities while maintaining the W/F ratio constant. This may be accomplished in two ways. First, the amount of catalyst may be changed as the fluid velocity changes thereby keeping the ratio constant. This method was not amenable to the system under consideration as it would have involved changing the weight of catalyst by removing a certain amount of the collagen-urease membrane complex. This, in turn, would also cause a change in the desired flow configuration through the reactor. The second choice was to realize that the feed flow rate is the product of the fluid velocity (cc/min) and the feed urea concentration (moles/cc). Thus, by changing both of these parameters proportionate amounts in opposite directions, the feed flow rate would remain constant making the W/F ratio a constant as well. In this manner, a range of data was obtained (Figure 22). Each data point is identified by its feed urea concentration (moles/liter) and reactor feed flow rate (cc/min). The remarkable similarity of the data indicates that no difference exists in the effect of mass transfer over this range of fluid velocities. This is not

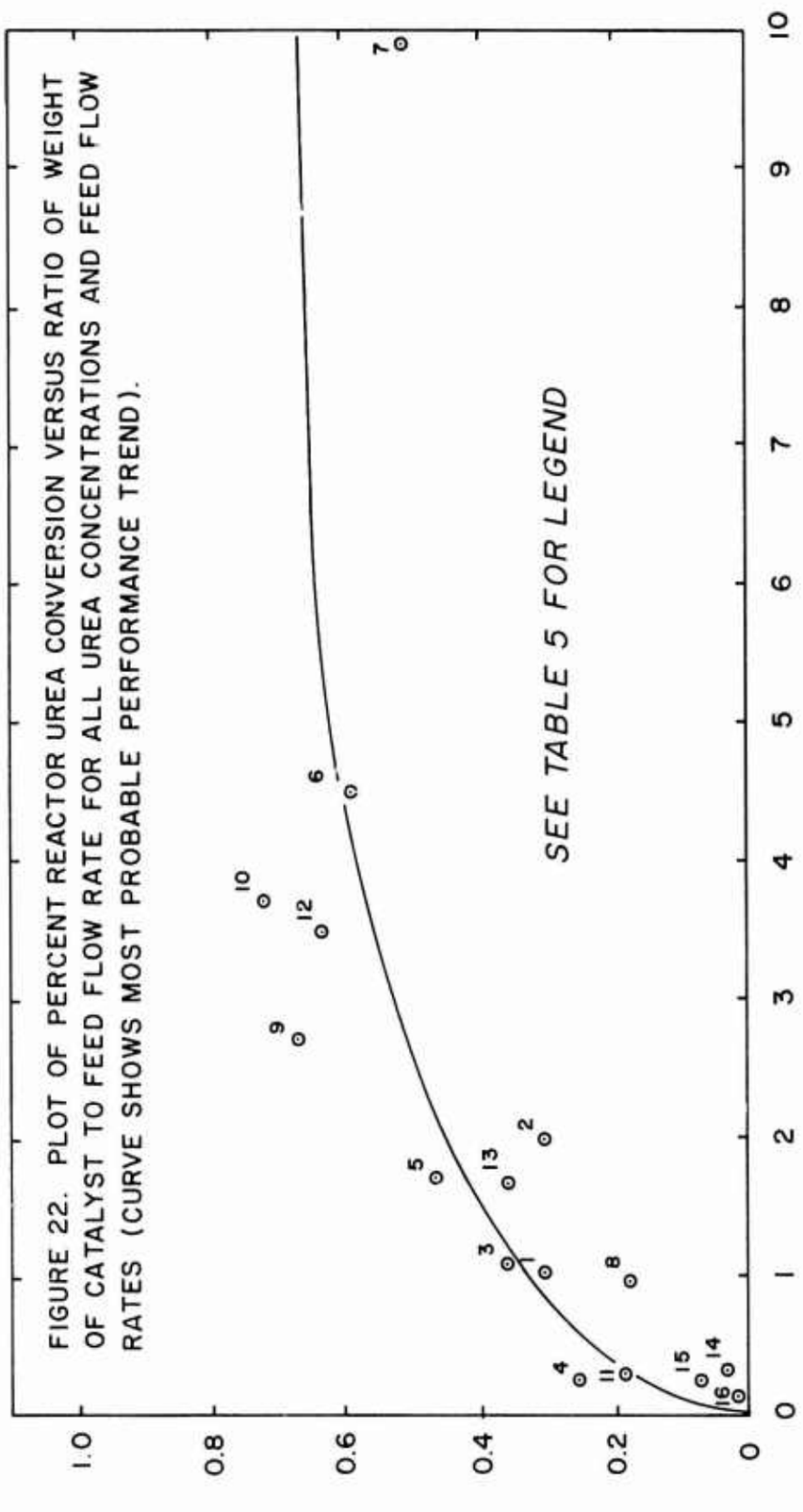
FIGURE 22. PLOT OF PERCENT REACTOR UREA CONVERSION VERSUS RATIO OF WEIGHT OF CATALYST TO FEED FLOW RATE FOR ALL UREA CONCENTRATIONS AND FEED FLOW RATES (CURVE SHOWS MOST PROBABLE PERFORMANCE TREND).
SEE TABLE 5 FOR LEGEND
X (REACTOR UREA CONVERSION)
W/F × 10⁵ (GM. – CAT. – MIN./MOLE)
0
0.2
0.4
0.6
0.8
1.0
0
1
2
3
4
5
6
7
8
9
10

to say that there are no resistances to mass transfer present, but rather that they are equal in magnitude over the range of fluid velocities explored by the data. Perhaps a secondary point of interest is the fact that in the case of large mass transfer effects, an optimal reactor flow rate would exist as a direct trade off between the reduction of the mass transfer resistance by increased fluid velocities, thus increasing the apparent conversion, and the decreased reactor residence time causing a proportionate decrease in the apparent conversion. This would lead to a sub-optimization of the biocatalytic reactor performance as a function of reactor feed flow rate and urea concentration.

From an optimum performance standpoint, a low flow rate in conjunction with a low urea concentration will give the highest reactor urea conversion. However, the obvious economic controls would dictate an increase in both of these parameters in order to make the system operation more favorable.

4.5 Kinetic Behavior of Immobilized Enzyme

The kinetics of most free enzymes in solution follow the well-known Michaelis-Menten kinetic equation. This states that the velocity or rate of an enzymatic reaction, v, is:

$$v = \frac{dP}{dt} = \frac{V_{max}S}{K_m+S} \qquad (4\text{-}1)$$

where: P = product concentration (moles/liter)

S = substrate concentration (moles/liter)

K_m = Michaelis-Menten constant (moles/liter)

V_{max} = maximum reaction velocity (moles/liter-min)

t = time (min)

v = rate of enzymatic reaction (moles/liter-min)

This kinetic equation is obtained from the Michaelis-Menten model which shows an enzyme E, acting as a catalyst, combining with substrate S to give an intermediate complex, E·S. This intermediate complex then breaks down to the product(s) of the reaction and the enzyme:

$$E+S \underset{k_{-1}}{\overset{k_{+1}}{\rightleftharpoons}} E\cdot S \xrightarrow{k_2} E + \text{product} \qquad (4\text{-}2)$$

The Michaelis-Menten constant then becomes:

$$K_m = \frac{k_{-1}+k_2}{k_{+1}} \qquad (4\text{-}3)$$

In addition, when the substrate concentration is very much larger than K_m, the maximum reaction velocity may be given by:

$$V_{max} = k_2 E_o \qquad (4\text{-}4)$$

where: E_o = total enzyme concentration (moles/liter)

The two constants, K_m and V_{max}, are the two parameters most frequently used to characterize the kinetics of any particular enzyme. However, they are usually quite dependent upon pH, temperature, the type of buffering system used, and the concentrations of any activators or inhibitors of the reaction. In addition, these parameters

are also dependent on the time of reaction if the Michaelis-Menten hypothesis breaks down and a Briggs-Haldane expression has to be utilized (Shyam, 1974).

For the immobilized enzyme system, the apparent Michaelis-Menten constant and maximum reaction velocity may be obtained from exhaustive studies of initial reaction rates in a small batch reactor. Such studies result in a Lineweaver-Burke plot from which the two parameters may be obtained (Zwiebel, 1972). These two kinetic parameters, in this investigation, were obtained by employing an optimization scheme utilizing a numerical model which combined both biochemical reaction and mass transfer effects.

4.6 Model Selection and Parameter Estimation

4.6.1 Transport Model for Simultaneous Mass Transfer and Biochemical Reaction

The development of a suitable mathematical model to describe the performance of the biocatalytic reactor module may be made through the assumption of four factors:

1. The reactor is operating at steady-state and its performance will be analyzed at that point of operation.

2. The reactor consists of a packed bed operated under plug-flow, turbulent conditions. This assumption dictates that the turbulent fluid velocity is assumed constant in each channel or annulus of the reactor.

3. The kinetic behavior of the immobilized enzyme system follows the Michaelis-Menten model.

4. There is no longitudinal turbulent diffusion in

the reactor. This assumption presumes that convection is the only active transport mechanism.

Now, by considering both the inter- and intra-phase mass transfer resistances in conjunction with the enzymatic hydrolysis of the substrate, a concentration profile and the system equations may be developed.

The first step is to develop the solid phase equations, and secondly to develop the fluid phase equations. From the steady-state assumption, the rate of diffusion into the membrane of a specific reaction component, as described by Fick's Law, must be exactly equal to the rate of reaction of that component as given by Michaelis-Menten kinetics. Thus:

Solid Phase Equation

$$D_e\left[\frac{\partial^2 C_{is}}{\partial r^2}\right] = \frac{V_{max}C_{is}}{K_m+C_{is}} \tag{4-5}$$

where: D_e = effective diffusion coefficient of specific reaction component (cm^2/min)

C_{is} = concentration of specific reaction component inside membrane (moles/liter)

r = distance in membrane (cm)

The boundary conditions for this equation may be stated as:

$$\frac{\partial C_{is}}{\partial r} = 0 \ @ \ r = 0,z \tag{4-6}$$

$$\frac{\partial C_{is}}{\partial r} = \frac{k_m}{D_e}(C_b - h_s C_{ss}) \ @ \ r = r_o,z \tag{4-7}$$

where: k_m = coefficient of interfacial mass transfer (cm/min)

C_b = concentration of specific reaction component in the bulk liquid phase (moles/liter)

C_{ss} = concentration of specific reaction component at the membrane surface (moles/liter)

h_s = partition coefficient for the membrane (dimensionless)

r_o = half-thickness of membrane (cm)

z = axial distance in the reactor (cm)

Equation (4-6) expresses the assumption of symmetry or rather that there is no net flux of the reaction component at the center of the membrane. In addition, equation (4-7) expresses the fact that the flux of the reaction component at the surface of the membrane is a function of the interfacial mass transfer coefficient, k_m, the effective diffusion coefficient of the component, D_e, and the bulk concentration. The fluid phase equation now arises from a consideration of the inter-phase mass transfer occurring at the membrane surface in combination with bulk mass transfer by convection. Thus:

Fluid Phase Equation

$$-\frac{\partial}{\partial z}(uC_b) = \frac{(1-\varepsilon)k_m(C_b - h_s C_{ss}|_{r=r_o})}{\varepsilon r_o} \qquad (4\text{-}8)$$

where: u = fluid velocity based on the apparent cross-sectional area (cm/min)

ε = fraction of fluid in the reactor based on the total volume (dimensionless)

The boundary conditions for equation (4-8) may now be stated as:

$$C_b = C_{b_o} \text{ @ } z = 0,\ r_o < r \qquad (4\text{-}9)$$

where: C_{b_o} = inlet bulk concentration of specific reaction component (moles/liter)

Now, in order to facilitate the manipulation of the desired parameters in these equations, a dimensionless format for the equations is developed from the system parameters.

$$Y = \frac{C_{is}}{C_{bo}} \tag{4-10}$$

$$X = \frac{r}{r_o} \tag{4-11}$$

$$\alpha = \frac{K_m}{C_{b_o}} \tag{4-12}$$

$$\beta = \frac{r_o^2 V_{max}}{D_e K_m} \tag{4-13}$$

$$N'_{sh} = \frac{k_m r_o}{D_e} \tag{4-14}$$

The solid and fluid phase equations and their appropriate boundary conditions may now be modified to include the above dimensionless parameters.

Solid Phase Equation

$$\frac{\partial^2 Y}{\partial X^2} = \frac{\beta \alpha Y}{\alpha + Y} \tag{4-15}$$

The boundary conditions are:

$$\frac{\partial Y}{\partial X} = 0 \text{ and } 0 \leq Y \leq 1 \text{ @ } X = 0, Z \tag{4-16}$$

$$\frac{\partial Y}{\partial X} = N'_{sh}\left[Y_f - h_s Y\big|_{X=1}\right] \text{ @ } X = 1, Z \tag{4-17}$$

where:

$$Y_f = \frac{C_b}{C_{b_o}} \tag{4-18}$$

$$Z = \frac{D_e z}{r_o^2 u} \tag{4-19}$$

Fluid Phase Equation

$$-\frac{\partial Y_f}{\partial Z} = \frac{1-\varepsilon}{\varepsilon} N'_{sh}\left[Y_f - h_s Y\big|_{X=1}\right] \tag{4-20}$$

The boundary conditions are:

$$Y_f = 1 \ @ \ Z = 0, \ r_o < r \tag{4-21}$$

At this point an efficient format must be developed for the numerical solution of these equations using a suitable integration technique. The problem of solution arises from the appearance of the split-boundary value conditions of the system equations. However, before a numerical solution is attempted, a suitable correlation for the interfacial mass transfer coefficient, k_m, must be placed in the model equations.

The correlation for this interfacial mass transfer coefficient may be developed from two separate expressions for the j_d factor. The first, involving the modified Reynold's Number, has been given by Chu et al. (1953):

$$\text{for } 0 < \overline{Re} < 30; \qquad j_d = 5.7(\overline{Re})^{-0.78} \tag{4-22}$$

where:

$$\overline{Re} = \frac{D_p \bar{u} \rho_f}{\mu_f (1-\bar{\varepsilon})} \tag{4-23}$$

and: D_p = characteristic particle diameter (cm)

ρ_f = density of fluid (gm/cc)

μ_f = viscosity of fluid (gm/cm-sec)

$\bar{u}$ = fluid velocity in reactor based on total cross-sectional area (cm/sec)

$\bar{\varepsilon}$ = fraction of spacing material based on total volume of solids (dimensionless)

This may be equated to Colburn's definition of the j_d factor (Smith, 1970) and an expression for the interfacial mass transfer coefficient results:

$$\frac{k_m \rho_f}{G}\left(\frac{\mu_f}{\rho_f D_e}\right)^{0.667} = 5.7(\overline{Re})^{-0.78} \tag{4-24}$$

$$k_m = 5.7 \frac{G}{\rho_f}(Re)^{-0.78}\left(\frac{\mu_f}{\rho_f D_e}\right)^{-0.667} \tag{4-25}$$

where: G = superficial mass velocity based on total cross-sectional area (gm/cm^2-sec)

The system of equations, as developed, may now be solved numerically by a suitable integration technique provided a solution to the split-boundary conditions is produced.

4.6.2 Numerical Scheme for Solving the Two-Point Boundary Value Problem

The conventional method of solution was chosen to obtain a solution to the split-boundary value conditions. While requiring excessive computer time for convergence as opposed to other methods (Shyam, 1974), it is the simplest method of solution. The conventional method involves the

following iterative steps:

Step 1:

Equation (4-15) can be treated as an ordinary differential equation at a given spatial point Z in the reactor:

$$\frac{d^2Y}{dX^2} = \frac{\beta\alpha Y}{\alpha+Y} \tag{4-26}$$

The ordinary differential of equation (4-26) may be split into two first-order equations by substitution:

$$\frac{dY}{dX} = P \tag{4-27}$$

$$\frac{dP}{dX} = \frac{\beta\alpha Y}{\alpha+Y} \tag{4-28}$$

The boundary conditions are:

$$\frac{dY}{dX} = P = 0 \text{ and } 0 \leq Y \leq 1 \text{ @ } X = 0,Z \tag{4-29}$$

$$\frac{dY}{dX} = P = N'_{sh}\left[\bar{Y}_f - h_s Y\Big|_{X=1}\right] \text{ @ } X = 1,Z \tag{4-30}$$

Step 2:

Assume a value for P at X = 1:

$$P = \theta_i \text{ @ } X = 1,Z \tag{4-31}$$

Obtain $Y|_{X=1}$ from equation (4-30):

$$Y|_{X=1} = \left[\bar{Y}_f - \frac{\theta_i}{N'_{sh}}\right]\frac{1}{h_s} \text{ @ } X = 1,Z \tag{4-32}$$

where $Y_f|_{Z=0}$ is a known boundary condition for the first iteration and is then estimated from the fluid phase equation by integration as will be shown below. (Note that Y_f plays the role of an imbedded parameter and must be pinned down by this iteration technique.)

The variational equations are obtained as follows:

$$\frac{d}{d\theta}\left[\frac{dY}{dX}\right] = \frac{\partial P}{\partial \theta} \tag{4-33}$$

$$\frac{\partial}{\partial \theta}\left[\frac{dP}{dX}\right] = \frac{\partial}{\partial \theta}\left[\frac{\beta\alpha Y}{\alpha+Y}\right] \tag{4-34}$$

Assuming that the order of differentiation can be reversed (Seinfeld and Lapidus, 1974):

$$\frac{d}{dX}\left[\frac{\partial Y}{\partial \theta}\right] = \frac{\partial P}{\partial \theta} \tag{4-35}$$

$$\frac{d}{dX}\left[\frac{\partial P}{\partial \theta}\right] = \left[\frac{\beta\alpha^2}{(\alpha+Y)^2}\right] \frac{\partial Y}{\partial \theta} \tag{4-36}$$

The boundary conditions now are:

$$\frac{\partial Y}{\partial \theta} = 0 \ @ \ X = 1, Z \tag{4-37}$$

$$\frac{\partial P}{\partial \theta} = 1 \ @ \ X = 1, Z \tag{4-38}$$

Now a suitable integration technique is used to integrate equations (4-27), (4-28), (4-35), and (4-36) with the boundary conditions given by equations (4-31), (4-32), (4-37), and (4-38). The method chosen was the Fourth Order

Runge-Kutta Method. The integration solves the above equations to obtain a value of $P|_{X=0}$. But from equation (4-29), $P|_{X=0}$ is known. Hence a correction for $P|_{X=1}$ is provided by the following equation:

$$\theta_{i+1} = \theta_i - \frac{[P|_{X=0}(\text{computed}) - P|_{X=0}(\text{given})]}{\left[\frac{\partial P}{\partial \theta}\right]} \quad @ \; X = 1, Z \qquad (4\text{-}39)$$

or

$$\theta_{i+1} = \theta_i - \frac{[P_{X=0}(\text{computed})]}{\left[\frac{\partial P}{\partial \theta}\right]} \qquad (4\text{-}40)$$

Step 3:

Repeat Step 2 until convergence is obtained for equation (4-40), i.e., until $\theta_{i+1} = \theta_i$. Then compute $Y|_{X=1}$ and proceed to the next step.

Step 4:

Substitute the value of $Y|_{X=1}$ obtained from Step 3 into the fluid phase equation as given by equation (4-20) and integrate this equation by the Fourth Order Runge-Kutta Method to obtain $Y_f|_{Z+\Delta Z}$.

Step 5:

Repeat Steps 2, 3, and 4 until $Y_f|_{Z_f}$ is obtained.

In the above iterative procedure, actual experimental values of initial feed urea concentration and feed flow rate are provided to the integrating process which proceeds stepwise giving values of conversion at each step through the reactor. In addition, concentration profiles

of the reaction component in the membrane (Figure 23) are generated to show the absence of any mass flux at the center of the membrane as indicated by equation (4-6).

The intrinsic numerical noise produced by this method of integration was analyzed by developing an analytical solution for the system equations assuming a first-order kinetic behavior for the immobilized enzyme system. This steady-state analytical solution may be developed as shown below:

Solid Phase Equation

$$\frac{d^2Y}{dX^2} - \phi^2 Y = 0 \qquad (4\text{-}41)$$

where:

$$\phi = \sqrt{\frac{r_o V_{max}}{D_e K_m}} \qquad (4\text{-}42)$$

The boundary conditions are:

$$\frac{dY}{dX} = 0, \; Y = \text{finite} \; @ \; X = 0 \qquad (4\text{-}43)$$

$$\frac{dY}{dX} = N'_{sh}(Y_f - Y|_{X=1}) \; @ \; X = 1 \qquad (4\text{-}44)$$

The solution to this second-order differential equation may be given as:

$$Y = A_1 \cosh\phi X + A_2 \sinh\phi X \qquad (4\text{-}45)$$

Applying equation (4-43):

$$A_2 = 0 \qquad (4\text{-}46)$$

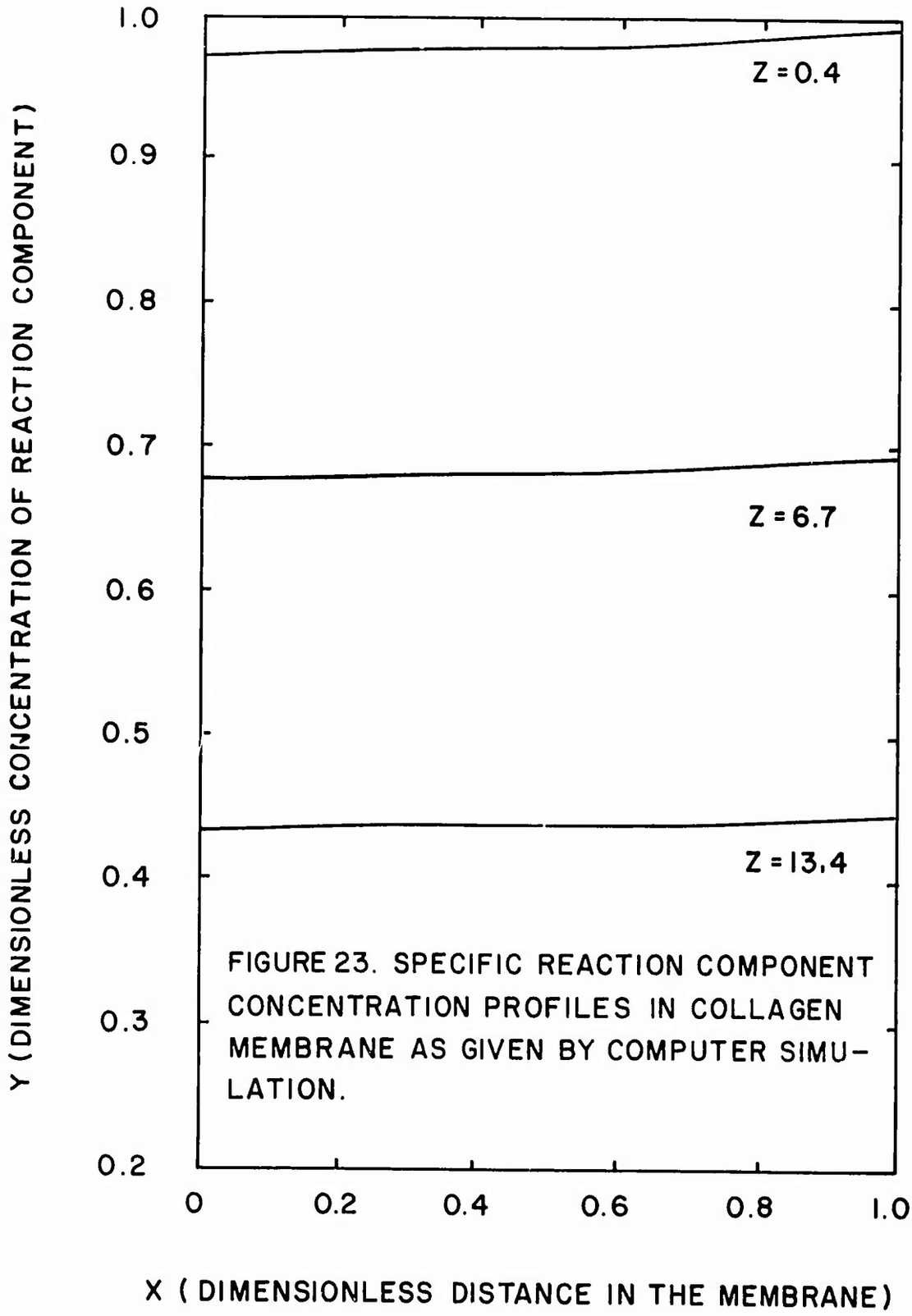

FIGURE 23. SPECIFIC REACTION COMPONENT CONCENTRATION PROFILES IN COLLAGEN MEMBRANE AS GIVEN BY COMPUTER SIMULATION.

$$\frac{dY}{dX} = A_1 \phi \sinh\phi X \tag{4-47}$$

$$Y|_{X=1} = A_1 \cosh\phi \tag{4-48}$$

$$\frac{dY}{dX}\Big|_{X=1} = A_1 \phi \sinh\phi \tag{4-49}$$

Applying equation (4-44):

$$A_1 = \frac{N'_{sh} Y_f}{\phi \sinh\phi + N'_{sh} \cosh\phi} \tag{4-50}$$

Now, by substitution of equation (4-50) into equation (4-49):

$$\frac{dY}{dX}\Big|_{X=1} = \frac{N'_{sh} Y_f}{1 + N'_{sh} \frac{\coth\phi}{\phi}} \tag{4-51}$$

Fluid Phase Equation

$$\frac{dY_f}{dZ} = -\varepsilon' \left[\frac{1-\varepsilon}{\varepsilon}\right] N'_{sh} \left[Y_f - Y|_{X=1}\right] \tag{4-52}$$

$$= -\varepsilon' \left[\frac{1-\varepsilon}{\varepsilon}\right] \frac{dY}{dX}\Big|_{X=1} \tag{4-53}$$

where: ε' = fraction of catalytically active particles based on total volume of solids (dimensionless)

The solution to this equation may be given as:

$$Y_f = Y_o e^{-B_1 Z} \tag{4-54}$$

where:

$$B_1 = \varepsilon' \left[\frac{1-\varepsilon}{\varepsilon}\right] \frac{N'_{sh}}{1 + N'_{sh} \frac{\coth\phi}{\phi}} \tag{4-55}$$

Comparison of the conversion values produced by this analytical solution and the involved numerical solution differed by a maximum of 0.000001 which indicates that the errors produced by the numerical integration are many orders of magnitude smaller than the values of the conversion over the length of the reactor.

4.6.3 Scheme for Obtaining "Best Set" of Kinetic Parameters

The mathematical model discussed previously may now be used in an attempt to obtain the "best" values of K_m and V_{max} for the biocatalytic reactor module system. While an involved computation method of parameter estimation by classical gradient search techniques (Carnahan et al., 1969; Himmelblau, 1970; Seinfeld and Lapidus, 1974) is indeed possible, the parameters may also be obtained by a convergent, direct search process in parameter space.

For the purposes of constraining the search for the "best" parameters, the Michaelis-Menten constants for the free enzyme model may be used as approximate limiting values. The Michaelis-Menten constant, K_m, for the free enzyme model becomes the lower bound in a search for that particular parameter while the V_{max} becomes the upper bound for that particular parameter. These assumptions of limiting boundary values may be made from realizing that the enzyme is most effective in its free, solubilized state. From these two limiting boundary values, a two-dimensional parameter grid is constructed by incrementing both K_m and

V_{max} over a suitable range of values. As the input to the numerical model is the same as the input to the real reactor, the outputs may be compared to obtain the parameters which best describe the kinetic behavior of the system. In this comparison, only data in which the mass transfer effects may be assumed to be a minimum should be used with confidence. The method of comparison involves the calculation of a minimization function:

$$J = \sum_{i=1}^{N} (X_{m_i} - X_{e_i})^2 \qquad (4\text{-}56)$$

where: X_{m_i} = particular model conversion

X_{e_i} = particular experimental conversion

This function is then plotted in a third dimension above the previously constructed parameter grid of K_m and V_{max} values. The "best set" of kinetic parameters will occur at the minimum value of the function J. The function is possibly polymodal, but the constraints placed on the search of parameter space make it monotonic without an extremum in this range of values. Figure 24 shows contours of constant value of the objective function J superimposed on the K_m-V_{max} parameter grid. The insensitivity of the objective function contour mapping program to the flatness of the surface drawn initially created some problems in the interpretation of the figure shown. However, an intricate search of the range showed a minimum to exist between the two contours labeled 0.115. The "best set" of

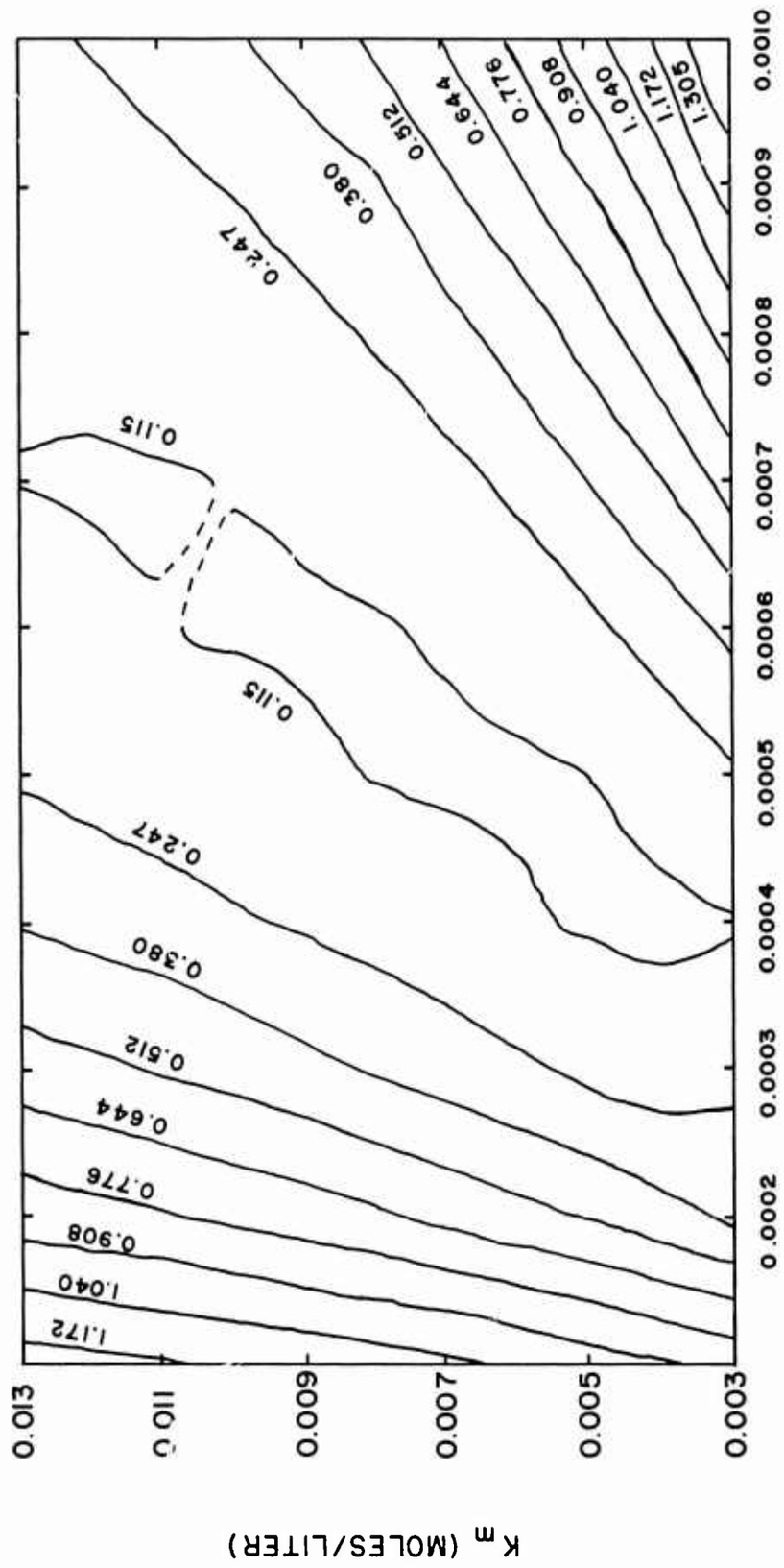

FIGURE 24. PLOT OF OBJECTIVE FUNCTION CONTOURS VERSUS K_m AND V_{max}.

kinetic parameters may thus be shown to be:

$$K_m = 0.0104 \text{ moles/liter}$$

$$V_{max} = 0.000665 \text{ moles/liter-min}$$

These values agree comparatively well with those obtained by Zwiebel (1972) from initial rate studies. Those values are:

$$K_m = 0.0121 \text{ moles/liter}$$

$$V_{max} = 0.000822 \text{ moles/liter-min}$$

This agreement is somewhat surprising since the data of Zwiebel (1972) were obtained from an unsteady-state batch reactor while the data of this investigation were obtained from a steady-state plug-flow reactor. This could quite possibly indicate that the pseudo-steady-state hypothesis is in effect and is following the proper guidelines as discussed by Shyam (1974). The "best set" of kinetic parameters may now be used to discuss the accuracy of the mathematical modeling of the biocatalytic reactor module.

4.6.4 Comparison of Experimental Data with Model Predictions

By using actual experimental data (feed flow rate and urea concentration) as input data to the numerical model and the kinetic parameters identified previously, a family of curves describing the biocatalytic reactor module performance may be obtained and overlaid against the actual experimental performance of the biocatalytic reactor module (Figure 25).

While the differences at lower reactor residence

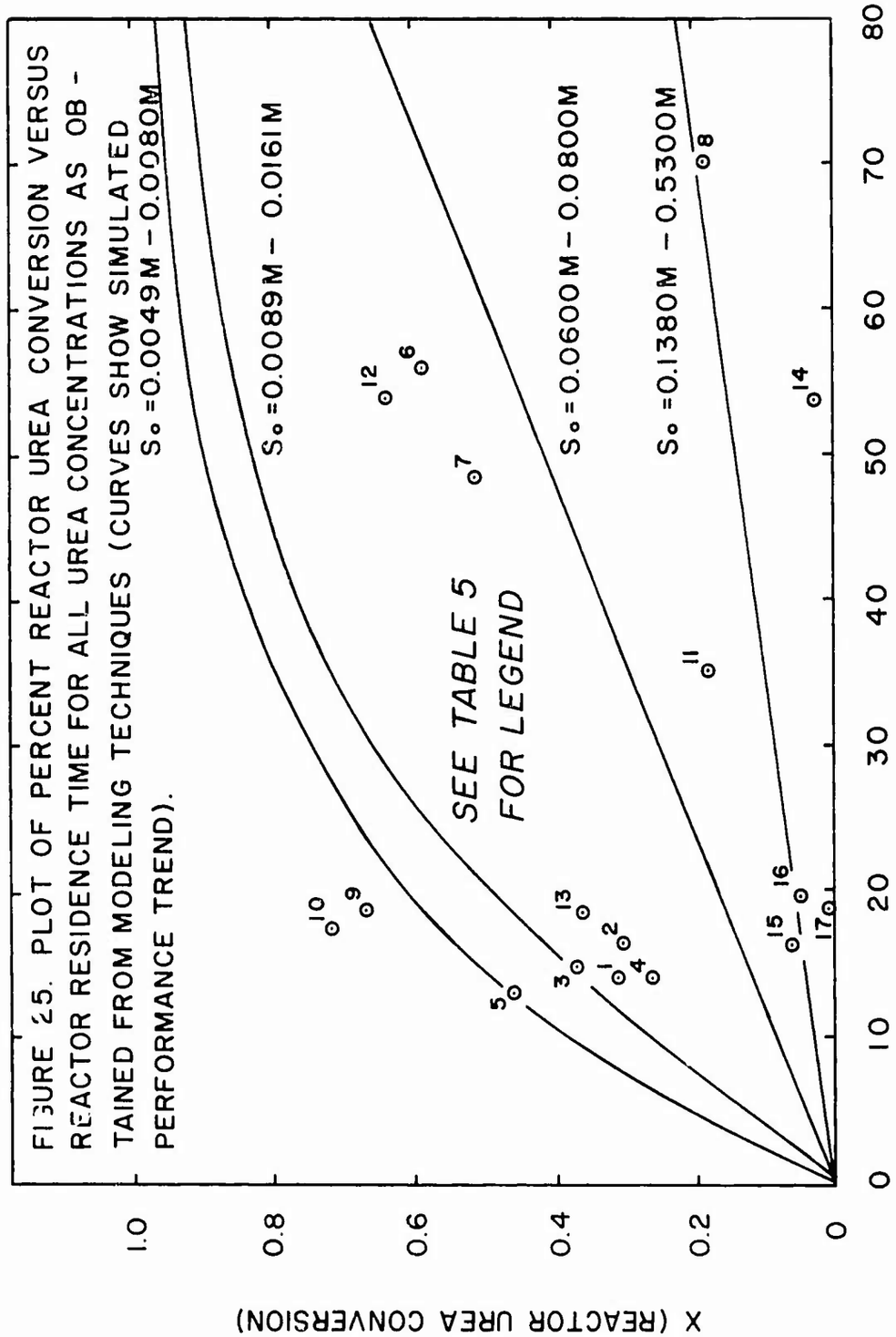
FIGURE 25. PLOT OF PERCENT REACTOR UREA CONVERSION VERSUS REACTOR RESIDENCE TIME FOR ALL UREA CONCENTRATIONS AS OBTAINED FROM MODELING TECHNIQUES (CURVES SHOW SIMULATED PERFORMANCE TREND).
So =0.0049M – 0.0080M
So =0.0089M – 0.0161M
So =0.0600M – 0.0800M
So =0.1380M – 0.5300M
SEE TABLE 5 FOR LEGEND
X (REACTOR UREA CONVERSION)
REACTOR RESIDENCE TIME (MINUTES)
0
0.2
0.4
0.6
0.8
1.0
10
20
30
40
50
60
70
80

times (high flow rates) may be attributed primarily to experimental error in the analysis procedures, there must be some physical explanation for the large differences which occur at the low flow rate points. One explanation may be obtained through consideration of a possible residence time distribution in the reactor module. The flow pattern at this low fluid velocity may give rise to a parabolic velocity profile in each channel with an overall flat velocity profile, a flat velocity profile in each channel with an overall parabolic velocity profile, or a parabolic velocity profile in each channel and in the overall profile. These profiles, rather than the desired flat plug-flow velocity profile in each channel and in the overall profile, would cause a 10 to 20% drop in conversion as compared with the conversion shown by the plug-flow model (Aris, 1969; Smith, 1970; Levenspiel, 1972). A second explanation comes from consideration of the interfacial mass transfer resistance in the liquid boundary layer at these low flow conditions. Results of sample calculations show the interfacial mass transfer coefficient to be of the same order of magnitude at each of the flow rates explored. This would seem to indicate that the correlation for the interfacial mass transfer coefficient is quite questionable in this low flow regime. Indeed, the possibility of creeping flow at these low flow rate levels (Bird et al., 1960) exists and would cause the laminar liquid boundary layer to extend completely across each annulus or channel in the

reactor. This would lead one to consider substrate or product inhibition as a third explanation for the extreme difference in conversion at the low flow levels. At the creeping flow conditions, substrate and more so product could produce an inhibitory effect upon the enzymatic activity of the biocatalytic reactor module if not removed by mass transport through the boundary layer or convective transport.

The most obvious conclusion is that none of the above explanations may be discounted and that others may indeed exist. The numerical modeling of a physical system is not always completely satisfying and can never really predict the system's behavior under all conditions.

5. CONCLUSIONS AND RECOMMENDATIONS

This investigation has portrayed the successful design, construction, and operation of a prototype system for the treatment of urinous wastewater. The rejection capability of a reverse osmosis system has been shown to be limited to removing approximately 45% of the urea in a particular feed solution. In a like manner, an ion exchange column would have to contain in excess of 6,000 pounds of the ion exchange resin to remove the contaminants from a 25-gallon per day feed stream of 0.1% urea for a 2-week operation period. However, the integration of these two processes into a prototype unit in conjunction with a biocatalytic reactor module for the enzymatic hydrolysis of urea to ammonia and carbon dioxide has decreased the size of the necessary ion exchange column by a factor of 300. In addition, the overall removal of urea has been increased to levels of 75 to 80%. This multi-system unit is thus imminently more feasible than any single stage operation from both a system size and economic viewpoint.

A complete characterization of the performance of the biocatalytic reactor module using a collagen-urease membrane complex has been developed using a synthetic urinous feed solution containing urea and sodium chloride

over a range of feed flow rates and urea concentrations. This characterization procedure has led to a study of the stability of the biocatalytic reactor module and estimation of the parameters necessary to scale the unit size for operation at higher flow rate conditions.

Work has been accomplished in an attempt to show the nature of the deactivation of the biocatalytic reactor module. A tryptophan analysis has shown that 60 to 80% of the enzyme is still intact within the carrier matrix after intermittent storage and use. This has indicated that an irreversible denaturation of the enzyme must also be occurring in order to account for the decline in enzymatic activity of the collagen-urease membrane complex.

The effects of mass transfer have been explored and have been found to be of the same order of magnitude throughout the flow regimes investigated. While the effects of such mass transfer resistances cannot be neglected, they are fairly constant across the probable operating range of such a reactor.

The transport model based on steady-state operation, plug-flow velocity profiles, and Michaelis-Menten kinetics has been developed and calibrated. By comparison of the computer simulation to actual experimental data through a direct search, parameter optimization scheme, the Michaelis-Menten constant, K_m, and the maximum reaction velocity, V_{max}, were identified and families of curves constructed to describe the theoretical operation of the biocatalytic

reactor module. In addition, the model has been used to show the possibility of a residence time distribution and/or substrate and product inhibition occurring at the lower feed flow rates.

While the feasibility of the successful operation of this system has been demonstrated, several areas require further study in order that such a biocatalytic reactor system be operated at the available optimum conditions. Some studies which could be particularly fruitful are outlined below:

1. Further studies to determine the exact binding mechanism and the binding sites of collagen and urease. This work should also include attempts to examine if active enzyme sites are used for binding and also to explore the possibility of conformational changes during the immobilization process which could also cause to inactivate the bound enzyme.

2. A more complete exploration of the techniques of immobilization should be made to produce a more active enzyme complex. This could include the method of complexation and also the use of bifunctional reagents to further bind the enzyme to the collagen matrix.

3. A variety of reactor operation modes also exist. The use of partial or total recycle to increase the possible conversion is one area of operation which must be more fully characterized.

4. A careful study of the low flow rate regime

would be invaluable in clarifying the possibilities of residence time distribution and inhibition by reaction species.

5. The continuous operation of the prototype system for extended periods of time (e.g., 100 consecutive hours or more) would also help to clarify the part that storage of the biocatalytic reactor module plays in the stability of the membrane complex.

The list of possibilities is indeed endless. Operation of the system with different specie concentrations, flow rates, temperatures, and pH must also be added to the above. All these points are necessary for the complete economic evaluation of this system.

REFERENCES

Applebaum, S. B. (1968) Demineralization by Ion Exchange, Academic Press, New York, New York.

Aris, R. (1969) Elementary Chemical Reactor Analysis, Prentice-Hall, Inc., Englewood Cliffs, New Jersey.

Axén, R., Heilbron, E., and Winter, A. (1969) Biochim. Biophys. Acta 191, 478.

Axén, R., Myrin, P. A., and Janson, J. C. (1970) Biopolymers 9, 401.

Axén, R., Porath, J., and Ernback, S. (1967) Nature 214, 1302.

Bachler, M. J., Strandberg, G. W., and Smiley, K. L. (1970) Biotech. Bioeng. 12, 85.

Bar-Eli, A., and Katchalski, E. (1963) J. Biol. Chem. 238, 1690.

Barker, S. A., Emery, A. N., and Novais, J. M. (1971) Process Biochem. 6, 11.

Bernath, F. R., and Vieth, W. R. (1974) In Immobilized Enzymes in Food and Microbial Processes, A. C. Olson and C. L. Cooney, eds., Plenum Press, New York, New York. (In press.)

Bernfield, P., Bieber, R. E., and MacDonnell, P. C. (1968) Arch. Biochem. Biophys. 127, 779.

Bernfield, P., Bieber, R. E., and Watson, D. M. (1969) Biochim. Biophys. Acta 191, 570.

Bersin, T. (1937) Kurzes Lehrbuch der Enzymologie, p. 69, Akadem, Verlagsgesellschaft, Leipzig.

Bird, R. B., Stewart, W. E., and Lightfoot, E. N. (1960) Transport Phenomena, John Wiley and Sons, Inc., New York, New York.

Blackburn, H. (1968) Amino Acid Determination, p. 193, Macel Dekker, Inc., New York, New York.

Blakely, R. L., Hinds, J. A., Kunze, H. E., Webb, E. C., and Zerner, B. (1969) Biochemistry 8, 1991.

Boedtker, H., and Doty, P. (1956) J. Am. Chem. Soc. 78, 4267.

Bowers, J. H., and Kenten, R. H. (1948) Biochem. J. 43, 369.

Brandt, W. (1937) Biochem. Z. 291, 99.

Butler, W. T., Piez, K. A., and Bornstein, P. (1967) Biochemistry 6, 3771.

Carbonell, R. G., and Kostin, M. D. (1972) A.I.Ch.E.J. 18, 1.

Carnahan, B., Luther, H. A., and Wilkes, J. O. (1969) Applied Numerical Methods, John Wiley and Sons, Inc., New York, New York.

Chang, T. M. S. (1964) Science 146, 524.

Chang, T. M. S. (1966) Trans. Am. Soc. Artif. Organs 12, 13.

Chang, T. M. S., MacIntosh, F. C., and Mason, S. G. (1966) Can. J. Physiol. Pharmacol. 44, 115.

Chu, J. C., Kalil, J., and Wetteroth, W. A. (1953) Chem. Eng. Prog. 49, 141.

Davidson, B., Vieth, W. R., Wang, S. S., and Zwiebel, S. (1973) Second Quarterly Report submitted to U.S. Army Mobility Equipment Research and Development Center, Contract No. DAAK02-73-C-0094.

Davidson, B., Vieth, W. R., Wang, S. S., Zwiebel, S., and Gilmore, Jr., R. (1974) A.I.Ch.E. Symp. Series. (In press.)

Dorfner, K. (1972) Ion Exchangers, Ann Arbor Science Publishers, Ann Arbor, Michigan.

Fishbein, W. N. (1965) J. Biol. Chem. 240, 2402.

Fishbein, W. N. (1969) J. Biol. Chem. 244, 1188.

Frensdorff, H. K., Watson, M. T., and Kauzmann, W. (1953) J. Am. Chem. Soc. 75, 5157.

Goldman, R., Goldstein, L., and Katchalski, E. (1971) In Biochemical Aspects of Reactions on Solid Supports,

G. R. Stark, ed., p. 1, Academic Press, New York, New York.

Goldman, R., and Katchalski, E. (1971) J. Theo. Biol. 32, 243.

Goldman, R., Kedem, O., and Katchalski, E. (1968b) Biochemistry 7, 4518.

Goldman, R., Silman, H. I., Caplan, S. R., Kedem, O., and Katchalski, E. (1965) Science 150, 758.

Goldman, R., Silman, H. I., Caplan, S. R., Kedem, O., and Katchalski, E. (1968a) Biochemistry 7, 486.

Gordon, A., Better, O. S., Greenbaum, M. A., Marantz, L. B., Gral, T., and Maxwell, M. H. (1971) Trans. Amer. Soc. Artif. Int. Organs 17, 253.

Gordon, A., Greenbaum, M. A., Marantz, L. B., McArthur, M. J., and Maxwell, M. H. (1969) Trans. Amer. Soc. Artif. Int. Organs 15, 347.

Gorin, G. (1958) Biochim. Biophys. Acta 34, 268.

Gorin, G., and Chin, C. C. (1965) Biochim. Biophys. Acta 99, 418.

Gross, J. J., Highberger, H., and Schmitt, F. O. (1954) Proc. Nat. Acad. Sci., U.S. 40, 679.

Gruesbeck, C., and Rase, H. (1972) IEC Prod. Rec. Dev. 11, 74.

Guilbault, G. G., and Das, J. (1970) Anal. Biochem. 33, 341.

Guilbault, G. G., and Montalvo, J. G. (1970) J. Am. Chem. Soc. 92, 2533.

Haynes, R., and Walsh, K. A. (1969) Biochem. Biophys. Res. Commun. 36, 235.

Hicks, G. P., and Updike, S. J. (1966) Anal. Chem. 38, 726.

Himmelblau, D. M. (1970) Process Analysis by Statistical Methods, John Wiley and Sons, Inc., New York, New York.

Hochstadt, H. R., Park, F., and Lieberman, E. R. (1960) U.S. Patent No. 2,920,000.

Hodge, A. J., and Petruska, J. A. (1963) In Aspects of Protein Structure, G. N. Ramachandran, ed., p. 289, Academic Press, New York, New York.

Hornby, W. E., Lilly, M. D., and Crook, E. M. (1966) Biochem. J. 98, 420.

Hough, J. S., and Lyons, T. P. (1972) Nature 235, 389.

Hughes, R. B., Katz, S. A., and Stubbins, S. E. (1969) Enzymologia 36, 332.

Jadwin, T. A., Hoffman, A. S., and Vieth, W. R. (1970) J. Appl. Poly. Sci. 14, 68.

Jensen, E. F., and Olson, A. C. (1969) Arch. Biochem. Biophys. 129, 221.

Johnson, D. E., and Ciegler, A. (1969) Arch. Biochem. Biophys. 130, 384.

Katchalski, E., Silman, I., and Goldstein, R. (1971) Adv. Enzymology 34, 445.

Katz, S. A., and Cowans, J. A. (1965) Biochim. Biophys. Acta 107, 605.

Kay, G., and Crook, E. M. (1967) Nature 216, 514.

Kay, G., and Lilly, M. D. (1970) Biochim. Biophys. Acta 198, 276.

Kay, G., Lilly, M. D., Sharp, A. K., and Wilson, R. J. H. (1968) Nature 217, 641.

Kon, T., Mrava, G. L., Weber, D. C., and Nosé, Y. (1970) J. Biomed. Mat. Res. 4, 13.

Kunin, R., and Meyers, R. J. (1950) Ion Exchange Resins, John Wiley and Sons, Inc., New York, New York.

Lacey, R. E. (1972) Chem. Eng. 79, 56.

Laidler, K. J., and Hoare, J. P. (1949) J. Am. Chem. Soc. 71, 2699.

Langmuir, I., and Schaefer, V. J. (1938) J. Am. Chem. Soc. 60, 1351.

Langmuir, I., and Schaefer, V. J. (1939) Chem. Rev. 24, 181.

Levenspiel, O. (1972) Chemical Reaction Engineering, John Wiley and Sons, Inc., New York, New York.

Lonsdale, H. K., Milstead, C. E., Cross, B. P., and Graber, F. M. (1969) OSW Report No. 14-01-0001-1717.

Lynn, K. R. (1967) Biochim. Biophys. Acta 146, 205.

Manecke, G., and Günzel, G. (1967) Naturwissenschaften 54, 647.

Manecke, G., Günzel, G., and Forster, H. J. (1972) J. Poly. Sci. (Part C) 30, 617.

Melrose, G. J. H. (1971) Rev. Pure and Appl. Chem. 21, 83.

Milton, J. M., and Taylor, I. E. P. (1969) Biochem. J. 113, 678.

Mogensen, A. O., and Vieth, W. R. (1973) Biotech. Bioeng. 15, 467.

Mosbach, K., and Larsson, P. O. (1970) Biotech. Bioeng. 12, 19.

Nishihara, T., Rubin, A. L., and Stenzel, K. H. (1969) In Biomaterials, L. Stark and G. Agarwal, eds., p. 185, Plenum Press, New York, New York.

Ogata, K., Ottensen, M., and Svendsen, I. (1968) Biochim. Biophys. Acta 159, 403.

Porath, J., Axén, R., and Ernback, S. (1967) Nature 215, 1491.

Ramachandran, G. N. (1963) Aspects of Protein Structure, Academic Press, New York, New York.

Ramachandran, L. K., and Kartha, P. (1954) Nature 174, 269.

Reid, C. E., and Breton, E. J. (1959) J. Appl. Poly Sci. 1, 26.

Riesel, E., and Katchalski, E. (1964) J. Biol. Chem. 239, 1521.

Riethel, F. J. (1971) In The Enzymes, P. D. Boyer, ed., Vol. 4, p. 20, Academic Press, New York, New York.

Riethel, F. J., and Robbins, J. E. (1967) Arch. Biochem. Biophys. 120, 158.

Rony, P. R. (1972) J. Am. Chem. Soc. 94, 8247.

Salemme, R. M., Litt, M. H., Lindau, O., and Sparks, R. E. (1971) Chem. Eng. Prog. Symp. Ser. 67, 133.

Second Annual Contractor's Conference of the Artificial Kidney Program of the National Institute of Arthritis and Metabolic Diseases, January 22-24, 1969, Proceedings, p. 15.

Seinfeld, J. H., and Lapidus, L. (1974) Mathematical Models in Chemical Engineering--Volume 3--Process Modeling, Estimation, and Identification, Prentice-Hall, Inc., Englewood Cliffs, New Jersey.

Seki, T., Jensen, T. A., Levin, Y., and Eroös, E. G. (1970) Nature 225, 864.

Shrier, A. L. (1972) Biotech. Bioeng. Symp. No. 3, 323.

Shyam, R. (1974) Ph.D. Thesis, Rutgers University, Department of Chemical and Biochemical Engineering.

Silman, I. H., Albu-Weissenberg, M., and Katchalski, E. (1966) Biopolymers 4, 441.

Silman, I. H., and Katchalski, E. (1966) Ann. Rev. Biochem. 35, 873.

Simpson, R. B., and Kauzmann, W. (1953) J. Am. Chem. Soc. 75, 5139.

Smith, J. M. (1970) Chemical Engineering Kinetics, 2nd ed., McGraw-Hill Publishing Co., New York, New York.

Sourirajan, S. (1970) Reverse Osmosis, Academic Press, New York, New York.

Stenzel, K. H., Rubin, A. L., Yamayoshi, W., Miyata, T., Suzuki, T., Sohoe, T., and Nishizawa, M. (1971) Trans. Amer. Soc. Artif. Int. Organs 17, 293.

Sumner, J. B. (1926) J. Biol. Chem. 69, 435.

Sumner, J. B. (1948) Science 108, 410.

Sumner, J. B., and Graham, V. A. (1925) Proc. Soc. Exptl. Biol. Med. 22, 504.

Sumner, J. B., Gralèn, N., and Eriksson-Quensel, I-B. (1938) J. Biol. Chem. 125, 37.

Sumner, J. B., Hand, D. B., and Holloway, R. G. (1931) J. Biol. Chem. 91, 333.

Sundaram, P. V., and Hornby, W. E. (1970) Fed. Eur. Biochem. Soc. Lett. 10, 325.

Suzuki, H., Ozawa, Y., and Maeda, H. (1966) Agr. Biol. Chem. 30, 807.

Tosa, T., Mori, T., Fuse, N., and Chibata, I. (1967) Biotech. Bioeng. 9, 603.

Tosa, T., Mori, T., Fusi, N., and Chibata, I. (1969a) Agr. Biol. Chem. 33, 1047.

Tosa, T., Mori, T., Fusi, N., and Chibata, I. (1969b) Agr. Biol. Chem. 33, 1053.

Vieth, W. R., Gilbert, S. G., Wang, S. S. Enzymatically Active Protein-Enzyme Complex Membranes, U.S. Patent Application No. 135,753, Claims Allowed, November, 1973.

Vieth, W. R., Gilbert, S. G., Wang, S. S., and Saini, R. (1973) Electrocodeposition of Enzymatically Active Protein-Enzyme Complex Membranes, U.S. Patent No. 3,758,396.

Vieth, W. R., and Venkatasubramanian, K. (1973) Chemtech 3, 677.

Vieth, W. R., and Venkatasubramanian, K. (1974a) Chemtech 4, 47.

Vieth, W. R., and Venkatasubramanian, K. (1974b) Chemtech 4, 309.

Vieth, W. R., and Venkatasubramanian, K. (1974c) Chemtech 4, 434.

Vieth, W. R., Wang, S. S., Bernath, F. R., and Mogensen, A. O. (1972) In Recent Developments in Separation Science, p. 175, Chemical Rubber Co. Press, Cleveland, Ohio.

Vieth, W. R., Wang, S. S., and Gilbert, S. G. (1972) Biotech. Bioeng. Symp. No. 3, 285.

Wall, M. C., and Laidler, K. J. (1953) Arch. Biochem. Biophys. 43, 299.

Wang, S. S., and Vieth, W. R. (1973) Biotech. Bioeng. 15, 93.

Weetall, H. H. (1969) Science 166, 615.

Weetall, H. H., and Baum, G. (1970) Biotech. Bioeng. 12, 399.

Weetall, H. H., and Hersh, L. S. (1969) Biochim. Biophys. Acta 185, 464.

Weliky, N., Brown, F. S., and Dale, E. C. (1969) Arch. Biochem. Biophys. 131, 1.

Wharton, C. W., Crook, E. M., and Brocklehurst, K. (1968a) Eur. J. Biochem. 6, 572.

Wharton, C. W., Crook, E. M., and Brocklehurst, K. (1968b) Eur. J. Biochem. 6, 575.

Wilson, R. J. H., and Lilly, M. D. (1969) Biotech. Bioeng. 11, 349.

Yamasaki, E. (1920) Sci. Repts. Tôhuku Imp. Univ. Ser. 1, 9, 97.

Zwiebel, S. R. (1972) M.S. Thesis, Rutgers University, Department of Chemical and Biochemical Engineering.

APPENDIX 1

ADDITIONAL STUDIES CONDUCTED WITH BIOCATALYTIC REACTOR MODULE

In an attempt to show some type of regenerating capacity for the biocatalytic reactor module, a re-immobilization procedure was initiated after the enzymatic activity of the module had fallen below a reasonably usable level. The technique used is outlined below:

1. The reactor module was washed continuously with glass distilled water at a high flow rate (400 cc per minute) for 4 hours. The washing system consisted of a simple recycle loop where the spent distilled water was replaced approximately every 30 minutes.

2. The reactor module was filled with a standard solution of 0.1 M Tris buffer acidified to a pH of 9.0 with lactic acid. This was allowed to stand, with occasional shaking, for 2 hours at room temperature. The Tris-lactic acid solution acts as a swelling solution allowing the collagen membrane to absorb water, thus opening up the fibrous structure.

3. The final step was to replace this swelling solution with an immobilization solution of 0.1 M Tris buffer adjusted to pH 8.5 with lactic acid and containing

20 mg/ml of urease enzyme. The reactor module was stored at 4°C for 96 hours to complete the impregnation procedure.

In order to discover the success of the re-immobilization technique, a series of data collection runs were made using a 0.1% urea solution as a standardized feed solution. The feed flow rate was also kept constant in order to maintain as great a degree of consistency between the data as possible. The stability of this reactor module is shown as reactor urea conversion versus the number of reactor liquid volume replacements in Figure 26.

There are several possible explanations for the almost constant decline in the apparent conversion obtained with the reactor module. One might simply indicate that no new enzyme was bound to the collagen membrane by the re-impregnation process because of the lack of available binding sites. However, this assumption would dictate a steady decrease in the conversion rather than the apparent short-lived plateaus. A more likely explanation is the adsorption or loose binding of new enzyme to the enzyme already bound to the collagen membrane. This would give a slow desorption of enzyme, as well as denaturation, and provide the possibility of the plateau behavior exhibited by the reactor module.

From this study, it is apparent that a simple re-immobilization process is not particularly effective in regenerating the biocatalytic reactor module and returning it to its original level of enzymatic activity and half-life

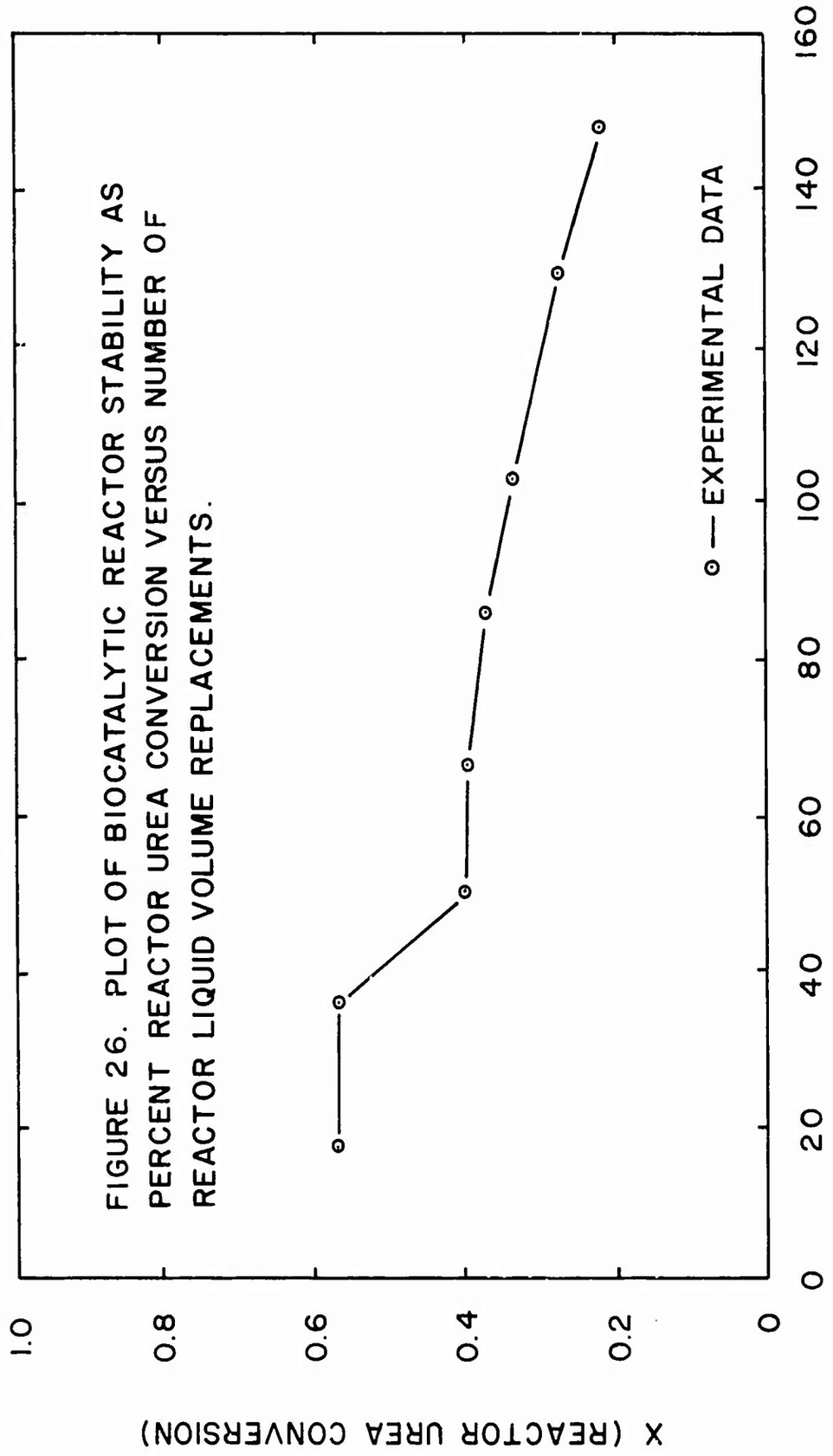

FIGURE 26. PLOT OF BIOCATALYTIC REACTOR STABILITY AS PERCENT REACTOR UREA CONVERSION VERSUS NUMBER OF REACTOR LIQUID VOLUME REPLACEMENTS.

status. While this method is attractive if short periods of operation are desired (e.g., emergency kidney assist, final urea removal, etc.), another method of regeneration must be devised which removes the denatured enzyme from the collagen membrane providing binding sites for new, active enzyme. As a possible alternative method, the addition of certain reagents to increase the number of available binding sites should also be explored in detail.

APPENDIX 2

SIMULATED SCALE-UP FOR THE BIOCATALYTIC REACTOR MODULE

The biocatalytic reactor module constructed has been used to identify the Michaelis-Menten kinetic parameters which best characterize its performance via a numerical model. These parameters may now be used to produce curves which show the reactor size needed to obtain a desired conversion given the reactor feed flow rate and urea concentration.

For the simulation procedure, a 0.01 M (approximately 0.1% by weight) urea concentration was chosen as characteristic of a 20:1 dilution of pure human urine. Three reactor feed flow rates--25, 75, and 5,000 gallons per day--were chosen as a good cross section of the probable treatment rates. The curves produced are shown in Figures 27-29.

These curves were obtained by calculating the reactor diameter necessary to produce a given reactor fluid velocity provided the reactor feed flow rate is known. From the fluid velocity and urea concentration as input data, the reactor length necessary to produce a desired conversion may be obtained from the numerical model

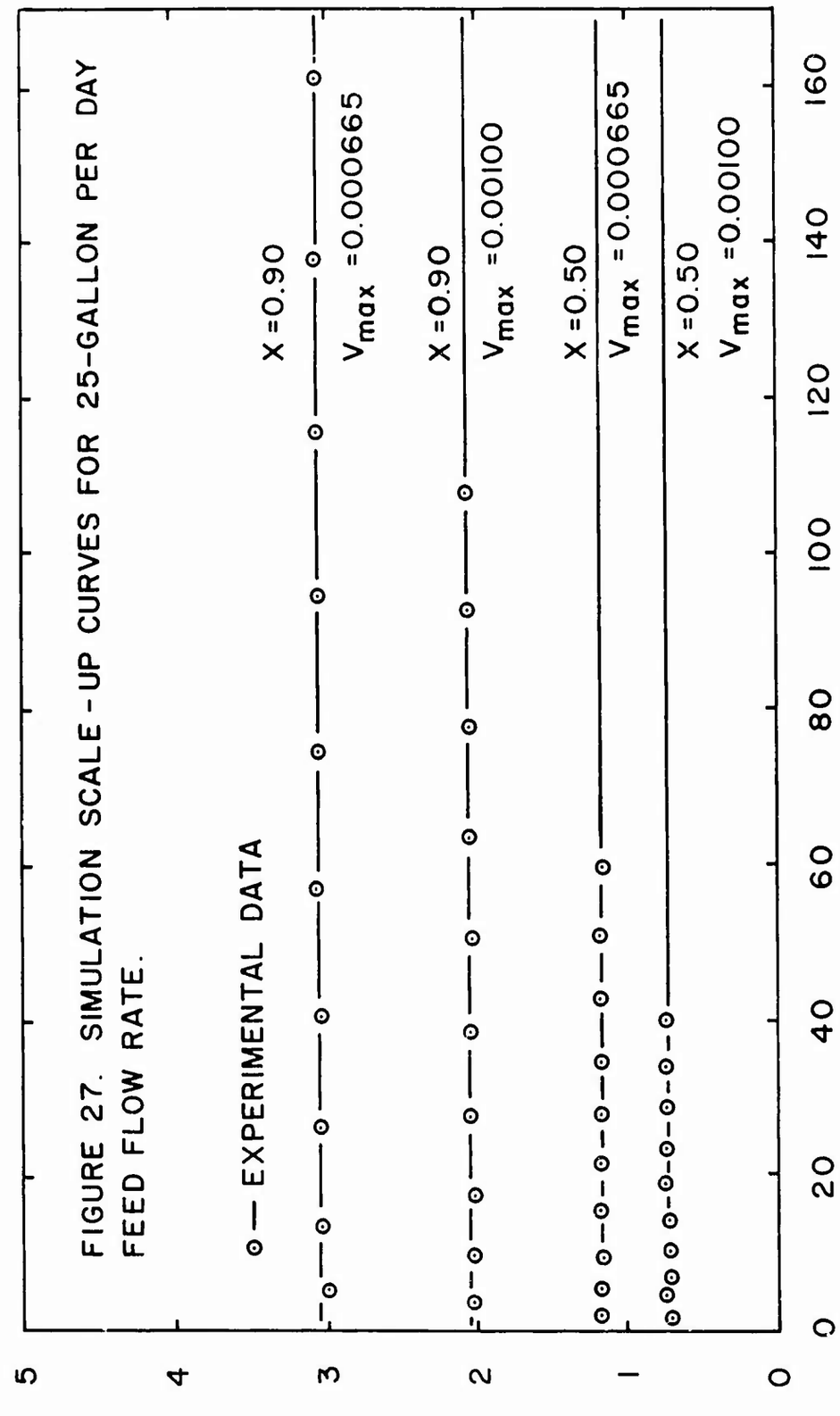
FIGURE 27. SIMULATION SCALE-UP CURVES FOR 25-GALLON PER DAY FEED FLOW RATE.
⊙— EXPERIMENTAL DATA
X =0.90
V_{max} =0.000665
X =0.90
V_{max} =0.00100
X =0.50
V_{max} =0.000665
X =0.50
V_{max} =0.00100
REACTOR VOLUME × 10^3 (cc)
L/D (DIMENSIONLESS)
0
1
2
3
4
5
0
20
40
60
80
100
120
140
160

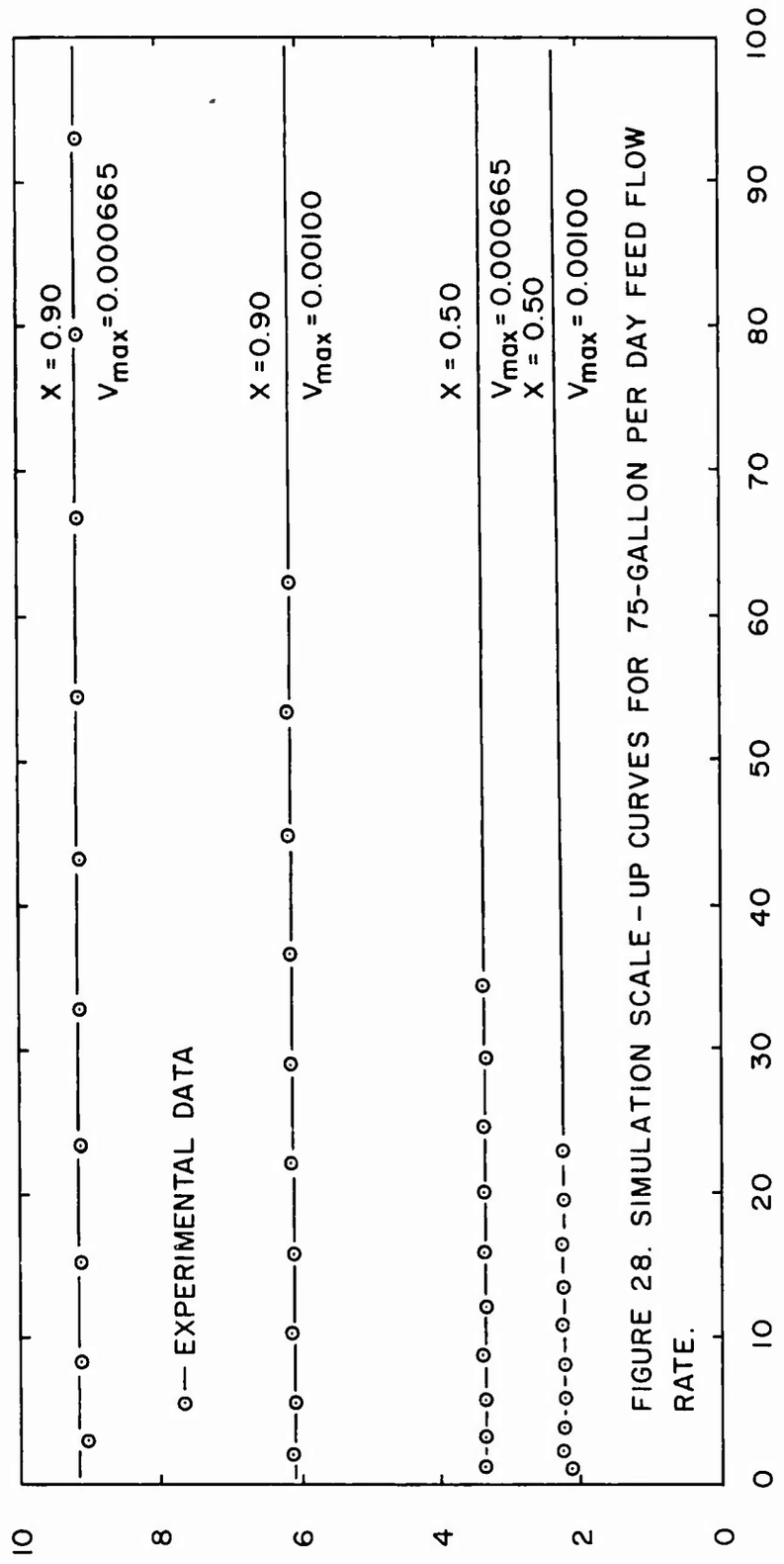

FIGURE 28. SIMULATION SCALE-UP CURVES FOR 75-GALLON PER DAY FEED FLOW RATE.

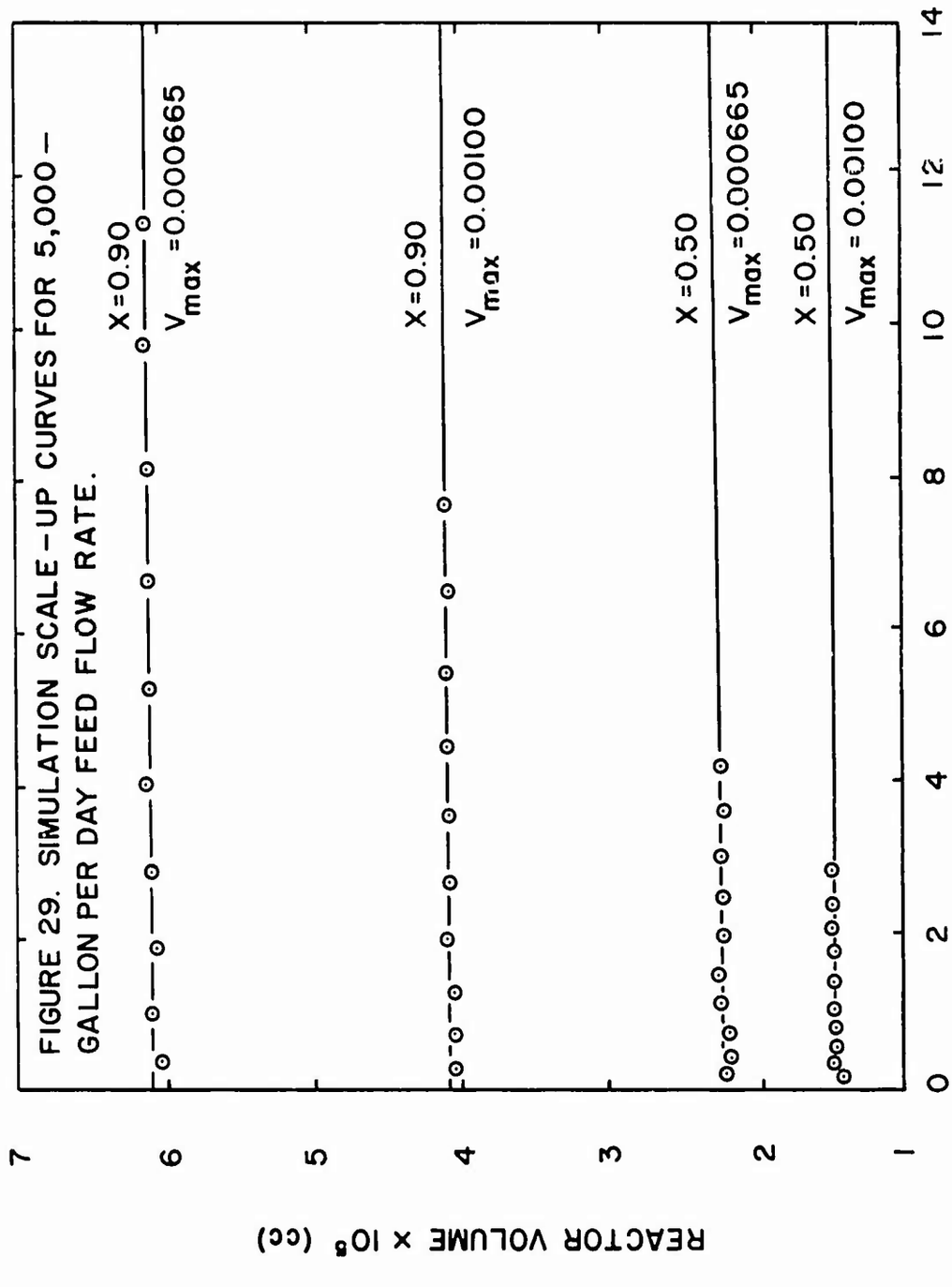
FIGURE 29. SIMULATION SCALE-UP CURVES FOR 5,000-GALLON PER DAY FEED FLOW RATE.
X=0.90
V_{max}=0.000665
X=0.90
V_{max}=0.00100
X=0.50
V_{max}=0.000665
X=0.50
V_{max}=0.00100
REACTOR VOLUME x 10^5 (cc)
L/D (DIMENSIONLESS)
1
2
3
4
5
6
7
0
2
4
6
8
10
12
14

described previously. The curves show the obvious intuitive result. In order to increase the desired conversion, the reactor volume must be increased. In addition, for a constant conversion, a variety of L/D ratios exist. This indicates that the reactor may either be long and thin or short and fat. The only stipulation for a constant conversion is that the volume remain constant. As a comparison to these simulation curves, under real operating conditions, the biocatalytic reactor module in our system (volume = 2,800 cc) gave an experimental conversion of 0.650 for a reactor feed flow rate of 28 gallons per day and a urea concentration of 0.01 M. The L/D ratio for this reactor is 3.1. This experimental conversion for the given size parameters compares well with the simulation curves.

As an addition to Figures 27-29, the same curves were reproduced using a V_{max} equal to 1.5 times the optimum V_{max} obtained in this study. This was done to show the effect of an increased enzyme loading factor for the collagen membrane. Since the V_{max} parameter is intrinsically related to the total amount of active enzyme present in the complex (see Section 4.5), by increasing the amount of enzyme per gram of the collagen-urease complex a higher conversion could be obtained with the same reactor volume which previously gave a certain fixed conversion. As is illustrated by the figures, a 50% increase in the V_{max} or total active enzyme concentration produces a 30% decrease in the reactor volume necessary to obtain comparable

conversion levels.

The ability to increase the V_{max} value is by no means a fantasy. The recommendations cited previously allude to the fact that the enzyme loading capacity may be increased by an alternative method of immobilization. Also, the use of an initially more active enzyme preparation may increase the unit enzymatic activity of the membrane complex.

APPENDIX 3

COMPLETE EQUIPMENT SPECIFICATIONS

The following is a complete listing of the equipment purchased for construction of the prototype system. The manufacturers' specifications as well as model numbers are given in order to facilitate the duplication of equipment where desired.

1. High Pressure Pump:

   Manufacturer: Milton Roy Company
   1300 East Mermaid Lane
   Philadelphia, Pennsylvania 19118

   Pump Specifications: 322-5705-983

   Solution: Water

   Model: FR-241-144 Duplex Mroy Pump

   Material: 316 Stainless Steel

   Plunger Size: 19/32

   Speed: 144 strokes per minute

   Str. Adjustment: Micrometer

   Suction Connection: 3/8 NPTF

   Discharge Connection: 1/4 NPTF

   Capacity: 14 gph at 100 psig or 12 gph at 1,500 psig. Note--capacity rating is per side on duplex pump

   Motor: Manufacturer's Stock, hp 3/4, rpm 1,750, phase/cycles 3/60, voltage 230/460, enclosure TE SXT NEMA 56C flange mtd

2. Accumulator:

   Manufacturer: Greer-Olaer Products
   5930 West Jefferson Boulevard
   Los Angeles, California 90016

   Model: 30A-1/8-WS

   Part: A1052-200

   Nominal Size: 1 pint

   Pressure Rating: 3,000 psi

   Gas Volume: 30.8 cu in

   Dry Weight: 5.25 lbs

3. Pressure Indicators:

   Manufacturer: J. Arthur Moore Company, Inc.
   342 Madison Avenue
   New York, New York 10017

   Model: USG Fig. 1870 and USG Fig. 1974

   Size: 4.5 in

   Pressure Rating: 0-1,500 psi

   Material: Stainless Steel-Nylon and Stainless Steel-Permaton Movements with 316 Stainless Steel connections and tubes

4. Flow Indicator:

   Manufacturer: Fischer and Porter Company
   Warminster, Pennsylvania 18974

   Model: 222751A

   Maximum Flow: 100% = 25 gph (water)

5. Pressure Vessel Assembly:

   Manufacturer: Gulf Energy and Environmental Systems
   10955 John Jay Hopkins Drive
   San Diego, California 92121

   Model: 5008-VD-13

Nominal Size: 2-in inside diameter

Material: 316 Stainless Steel

6. Reverse Osmosis Module:

   Manufacturer: Same as above

   Model: 4100

7. Mixing Equipment:

   Manufacturer: Mixing Equipment Company, Inc.
   135 Mt. Read Boulevard
   Rochester, New York 14611

   Model: 10

   Motor: Manufacturer's stock, hp 1/20, rpm 3 speed, phases/cycles 1/60, voltage 110

   Shaft Size and Material: 3/8 in x 30 in 316 Stainless Steel

   Propeller: 1 3.1 in and 1 2.0 in adjustable position

In addition to the above materials, all valves and piping were purchased according to a 3,000 psi pressure rating and type 316 stainless steel material specification. All tubing fittings are Swaglok fittings adjoined to 1/4 in schedule 40 pipe.

APPENDIX 4

RAW DATA FORMAT AND SAMPLE CALCULATIONS

Perhaps one of the most important parts of any research work is the clear and accurate recording of the raw data to be used for future analysis and calculation. The format of the data sheet (Table 6) used in this study was devised to show the data in a concise manner and to aid in direct comparison of such data on a day-to-day basis.

From the data collection, the following sample calculations have been performed:

$$\text{Percent salt rejection} = \frac{0.00052-0.000032}{0.00052} \times 100$$

$$= 93.8\%$$

$$\text{Percent urea rejection} = \frac{0.0078-0.0071}{0.0078} \times 100$$

$$= 9.6\%$$

$$\text{Percent urea conversion} = \frac{0.0095}{0.0141} \times 100$$

$$= 67.4\%$$

TABLE 6

RAW DATA SHEET

Time	11:25	12:30	1:30	2:30	3:30	
0.1 M NaCl (cation)	+159.2	-	-	-	-	
0.1 M NH_4Cl(cation)	+181.0	-	-	-	-	
0.1 M NH_4Cl (ammonia)	-198.3	-	-	-	-	
Pre-1 (cation)	+77.1	+10.0	+3.2	-10.3	-11.2	Start time
Pre-1 (NaCl)	0.0020	0.000085	0.000061	0.000032	0.000031	10:55 a.m.
Pre-1 (ammonia)	-161.8	-161.5	-161.0	-161.4	-162.0	on 6/9/74
Pre-1 (NH_3)	0.0144	0.0142	0.0138	0.0141	0.0146	
Pre-1 (urea)	0.0072	0.0071	0.0069	0.0071	0.0073	
Post-1 (ammonia)	-155.0	-142.7	-148.8	-153.9	-154.2	
Post-1 (NH_3)	0.0101	0.0052	0.0073	0.0095	0.0097	
Prod. (cation)	-	+91.2	+77.1	+80.8	+78.0	
Prod. (ammonia)	-	-13.0	-15.8	-16.4	-9.7	
Prod. (NH_3)	-	0.000005	0.000006	0.000007	0.000005	

Feed (cation)	+48.5	Ret. (cation)	+51.0
Feed (NaCl)	0.00052	Ret. (NaCl)	0.00059
Feed (ammonia)	-163.2	Ret. (ammonia)	-165.1
Feed (NH_3)	0.0156	Ret. (NH_3)	0.0172
Feed (urea)	0.0078	Ret. (urea)	0.0086

P1 (psig) = 700
P2 (psig) = 200

Temp (°C) = 22
Prod. flow = 76 cc/min

Ret. flow = 520 cc/min

APPENDIX 5

COMPUTER PROGRAMS

The computer programs which are documented on the following pages were used in the mathematical modeling procedure and in simple calculations for the production of the objective function contour map (Figure 24). The first main program with its three subroutines (JSRKB, EVAL, and RITE) was used for the solution of the differential equations which simulate the performance of the biocatalytic reactor module. The second program was used in conjunction with a contour mapping subroutine to produce a contour map of the objective function versus the kinetic parameters. The final program was used to calculate the data for the simulation scale-up curves. In all cases, Fortran was the chosen program language. The larger program was written for an IBM System 370/158 while the two smaller programs required the use of an IBM System 1130.

```
      IMPLICIT REAL*8(A-H,O-Z)
C
C     FIRST MODELING OF A SPIRAL WOUND REACTOR
C     INTEGRATION OF ORDINARY DIFFERENTIAL EQUATIONS USING FOURTH ORDER
C     RUNGE-KUTTA METHOD.  INITIAL CONDITIONS MUST BE KNOWN
C
C     NEQ=NUMBER OF EQUATIONS TO BE INTEGRATED
C     LL=NUMBER OF INTEGRATION STEPS TO BE TAKEN
C     NROW=LL+1
C     NCOL=NEQ+1
C     A(NROW,NCOL)=MATRIX CONTAINING THE SOLUTION OF THE DIFFERENTIAL
C     EQUATIONS.  THE FIRST COLUMN CONTAINS THE INDEPENDENT VARIABLE
C     THE DIMENSIONS OF MATRIX A MUST ALWAYS BE (NROW, NCOL)
C     XZR=INITIAL VALUE OF INDEPENDENT VARIABLE
C     XF=FINAL VALUE OF INDEPENDENT VARIABLE
C     YZR(50 )=INITIAL VALUES OF DEPENDENT VARIABLES(MAXIMUM OF 50)
C     DX=INCREMENT OF INDEPENDENT VARIABLE
      EXTERNAL EVAL
      DIMENSION YZR(50)
      DIMENSION CO(50)
C     ITEMS ENCLOSED BY XXXXXXXXXXXXXX MUST BE SPECIFIED BY USER
C     XXXXXXXXXXXXXXXXXXXXXXXXXXXXXXXXXXXXXXXXXXXXXXXXXXXXXXXXXXXXXXXXX
      DIMENSION A(101,5), YF(51)
      DIMENSION X(101),E(101)
    1 READ(5,110, END=190)CBULK,U,HS
      WRITE(6,122) CBULK, U, HS
      SKM=10.00000
      VM=0.000665
      DP=0.059
      EP=0.5
      AMU=0.01
      D=0.00001
      ALPHA=5.7
      BETA=0.78
      TRCOE=U*ALPHA*(DP*U/(60.0*AMU*(1.0-EP)))**(-BETA)*(AMU/D)**(-0.667
     Z)
      WRITE(6,121)          SKM, VM, TRCOE
      RO=0.0203
      EPSIL=0.46
      U=U/EPSIL
      DICOE=0.000300
      WRITE(6,123) RO, EPSIL, DICOE
  110 FORMAT(3E20.3)
  121 FORMAT( ' THE MICHAELIS CONSTANT  KM  IS',E12.3,'  MOLE/L,,   THE
     1MAXIMUM REACTION RATE  VM  IS',E12.3,'  MOLE PRODUCT/MIN-L ,',/,'
     1 THE MASS TRANSFER  COEFF.     AT THE MEMBRANE SURFACE IS',E12.3,'
     1 CM/MIN', / )
  122 FORMAT( ' THE INITIAL SUBSTRATE CONCENTRATION IS ',E10.4,'  MOLE/L
     2,      THE AXIAL FLUID VELOCITY IN THE REACTOR IS',F10.3,'  CM/MIN,
     2',/,' THE PARTITION COEFFICIENT FOR MEMBRANES IS', F10.2, /)
  123 FORMAT( ' THE MEMBRANE THICKNESS IS', E12.3,'  CM,     THE RATIO
     3OF VOID VOLUME TO THE TOTAL VOLUME OF THE REACTOR IS', F10.2,
     3 /,       ' THE DIFFUSIVITY OF SUBSTRATE IN THE MEMBRANE IS',E12.3,
     3'  CM2/MIN,'  , ///    )
      CO(1)=RO**2*VM/DICOE/SKM
      CO(2)= SKM/CBULK
```

```
      ALFA =THCOF*RO/DICOE
      NEQ=4
      XZR=1.
      XF=0.
      DX=-0.01
      LL=(XF-XZR)/DX
      NROW=LL+1
      NCOL=NEQ+1
      NPLOT=LL/50
      BC=0.001
      DZ=DICOE/RO**2/U*1.
      YF(1)=1.
      Z=0.
      YFIN2=1.
      X(1)=XZR
      DO 56 K=1,100,2
   56 X(K+2)=X(K)+2.*DX
      THIEL=DSQRT(CO(1))
      EK1=DEXP(THIEL)
      EK2=DEXP(-THIEL)
      A1=ALFA/(THIEL*(EK1-EK2)/2.+ALFA*(EK1+EK2)/2.*HS)
      A2=ALFA/(1.+HS*ALFA/(THIEL*DTANH(THIEL)))
      A3=(1.-EPSIL)/1./EPSIL*A2
      DO 60 I=1,30
      YZR(1)=1.
      YZR(2)=ALFA*(YF(I)-HS*YZR(1))
      YZR(3)=C.
      YZR(4)=1.
   50 CALL JSRKB(NEQ,NROW,NCOL,NROW,A,DX,XZR,YZR,EVAL,CO )
      DFAI=-A(101,3)/A(101,5)
      YZR(2)=YZR(2)+DFAI
      YZR(1)=(YF(I)-YZR(2)/ALFA)/HS
      IF(DABS(DFAI)-BC        ) 55,55,50
   55 DYF=-(1.-EPSIL)/1./EPSIL*ALFA*(YF(I)-HS*YZR(1))
      Z=Z+DZ
      DO 57 K=1,101,2
      EK3=THIEL*X(K)
   57 E(K)=A1*YFIN2*(DEXP(EK3)+DEXP(-EK3))/2.
      YFIN3=A2*YFIN2
      YF(I+1)=YF(I)+DYF*DZ
      YFIN=YF(I+1)
      CONVE=1.-YFIN
      CALL RITE(NROW,NCOL,A,NPLOT )
      WRITE(6,151) Z, CONVE
      WRITE(6,152)(E(K), K=1,101,2)
  152 FORMAT(5E20.4)
      YFIN2=DEXP(-A3*Z)
      CONV2=1.-YFIN2
      WRITE(6,110)YFIN3
      WRITE(6,151)Z,CONV2
  151 FORMAT( ' AT Z=', F12.4, ' THE CONVERSION IS', F20.6,  /,  '1  ')
   60 CONTINUE
      GO TO 1
  100 CONTINUE
      CALL EXIT
      END
```

```
      SUBROUTINE JSRKD(NEQ,NROW,NCOL,LL,A,DX,XZR,YZR,EVAL,CO)
      IMPLICIT REAL*8(A-H,O-Z)
C     JSRKD USES STANDARD FOURTH ORDER RUNGE-KUTTA METHOD TO INTEGRATE
C     SUBROUTINE MUST BE DECLARED EXTERNAL.
C        NEQ SIMULTANEOUS DIFFERENTIAL EQUATIONS.
C       NCOL IS THE NUMBER OF COLUMNS IN ARRAY A AND MUST
C    BE GREATER THAN NEQ.
C        NEQ= NUMBER OF DIFFERENTIAL EQUATIONS ,LL = NUMBER OF VALUES
C        OF THE INDEPENDENT VARIABLE X  ,  A = ARRAY  WITH COLUMNS
C        INDEPENDENT VARIABLE , FIRST DEPENDENT VARIABLE , SECOND
C        DEPENDENT VARIABLE , .....,NEQTH DEPENDENT VARIABLE
C        DX = INCREMENT IN X , XZR = INITIAL VALUE OF X , YZR =
C        VECTOR OF NEQ INITIAL VALUES OF THE DEPENDENT VARIABLES
C        SUBROUTINE JSRK CALLS ON SUBROUTINE EVAL(NEQ,X,Y,G)
C        WHERE NEQ = NUMBER OF EQUATIONS, X = VALUE OF THE INDEPENDENT
C        VARIABLE, Y= AN NEQ LONG VECTOR OF VALUES OF THE INDEPENDENT
C        VARIABLES, G = AN NEQ LONG VECTOR OF VALUES OF THE RIGHT HAND
C        SIDE OF THE GIVEN DIFFERENTIAL EQUATIONS.   EVAL MUST BE
C    SUPPLIED BY THE USER.
C        EVAL MUST DIMENSION Y(50),G(50)
      DIMENSION CO(50)
      DIMENSION YZR(50)
      DIMENSION A(NROW,NCOL)
      DIMENSION AK1(50),AK2(50),AK3(50),AK4(50),YM(50),YMP(50)
      NEQP=NEQ+1
      IF(LL.GT.NROW.OR.NEQP.GT.NCOL)WRITE(6,5)LL,NEQ
    5 FORMAT(25H ERROR SUB JSRK LL,NEQ   2I4)
      DO 80 L=1,LL
      DO 80 K=1,NEQP
      A(L,K)=0.0
   80 CONTINUE
      DXD=DX/2.0
      DXDD=DX/6.0
      A(1,1)=XZR
      DO 50 K=1,NEQ
      KD=K+1
      A(1,KD)=YZR(K)
   50 CONTINUE
      DO 100 L=2,LL
      LD=L-1
      XM=A(LD,1)
      DO 2 K=1,NEQ
      KD=K+1
      YM(K)=A(LD,KD)
    2 CONTINUE
      CALL EVAL(NEQ,XM,YM,AK1,CO)
      XMP=XM+DXD
      DO 4 K=1,NEQ
      YMP(K)=YM(K)+DXD*AK1(K)
    4 CONTINUE
      CALL EVAL(NEQ,XMP,YMP,AK2,CO)
      DO 6 K=1,NEQ
      YMP(K)=YM(K)+DXD*AK2(K)
    6 CONTINUE
      CALL EVAL(NEQ,XMP,YMP,AK3,CO)
      XMP=XM+DX
```

```
      DO 8 K=1,NEQ
      YMP(K)=YM(K)+DX*AK3(K)
    8 CONTINUE
      CALL EVAL(NEQ,XMP,YMP,AK4,CO)
      A(L,1)=XMP
      DO 10 K=1,NEQ
      KD=K+1
      A(L,KD)=A(LD,KD)+DXDD*(AK1(K)+AK4(K)+2.0*(AK2(K)+AK3(K)))
   10 CONTINUE
  100 CONTINUE
      RETURN
      END
```

```
      SUBROUTINE EVAL(NEQ,X,Y,G,CO)
      IMPLICIT REAL*8(A-H,O-Z)
C
C     CONTAINS DIFFERENTIAL EQUATIONS
C
      DIMENSION Y(50), G(50)
      DIMENSION CO(50)
C     X=INDEPENDENT VARIABLE
C     Y( )=VECTOR OF DEPENDENT VARIABLES
C     G( )=VECTOR OF DERIVATIVES(LEFT SIDE OF DIFFERENTIAL EQUATIONS)
C     ITEMS ENCLOSED BY XXXXXXXXXXXXXX MUST BE SPECIFIED BY USER
C     XXXXXXXXXXXXXXXXXXXXXXXXXXXXXXXXXXXXXXXXXXXXXXXXXXXXXXXXXXXXXXXXXXXXXX
      G(1)=Y(2)
      G(2)=CO(1)*CO(2)*Y(1)/(CO(2)+Y(1))
      G(3)=Y(4)
      G(4)=CO(1)*CO(2)**2/(CO(2)+Y(1))**2*Y(3)
C     XXXXXXXXXXXXXXXXXXXXXXXXXXXXXXXXXXXXXXXXXXXXXXXXXXXXXXXXXXXXXXXXXXXXXX
      RETURN
      END
```

```
      SUBROUTINE RITE(NROW,NCOL,A,NPLOT)
      IMPLICIT REAL*8(A-H,O-Z)
        DIMENSION  A(NROW,NCOL)
        DO 30 K=1,NROW , NPLOT
        WRITE (6,5)K,( A(K,L),L=1,NCOL)
   30   CONTINUE
    5   FORMAT (1X,I6,10E12.4/(7X,10E12.4))
        RETURN
        END
```

```
      DEFINE FILE 12(10000,2,U,NEXT)
      DIMENSION XE(11),XM(11),VM(10),SKM(13),AJ(11)
      READ(2,1)(XE(I),I=1,11)
1     FORMAT(F10.0)
      READ(2,2)(VM(K),K=1,10)
2     FORMAT(F10.0)
      DO 100 J=1,11
      READ(2,3)SKM(J)
3     FORMAT(F10.0)
      DO 100 K=1,10
      WRITE(5,5)
5     FORMAT(1H1)
      ASUM=0.0
      DO 200 I=1,11
      READ(2,6)XM(I)
6     FORMAT(F10.0)
      AJ(I)=(XM(I)-XE(I))**2.0
      ASUM=ASUM+AJ(I)
      KNEXT=(J-1)*10+K
      WRITE(12'KNEXT)  ASUM
      WRITE(5,7)XM(I),XE(I),AJ(I)
7     FORMAT(1H0,F10.8,5X,F10.8,5X,F10.8)
200   CONTINUE
      WRITE(5,8)SKM(J),VM(K),ASUM
8     FORMAT(1H0,F10.8,5X,F10.8,5X,F10.8)
100   CONTINUE
      CALL EXIT
      END
```

```
      DIMENSION CONV(20),D(20),AL(20),FUNC(20),VOL(20)
      PIE=3.14159
      READ(2,1)(CONV(I),I=1,3)
1     FORMAT(F10.0)
      DO 100 J=1,10
      READ(2,2)D(J)
2     FORMAT(F10.0)
      DO 200 I=1,3
      READ(2,3)AL(I)
3     FORMAT(F10.0)
      FUNC(I)=AL(I)/D(J)
      VOL(I)=(PIE*(AL(I))**3.0)/(4.0*(FUNC(I))**2.0)
      WRITE(5,4)CONV(I),FUNC(I),VOL(I)
4     FORMAT(1H0,3F20.4)
200   CONTINUE
100   CONTINUE
      CALL EXIT
      END
```